Dissertation zur Erlangung des
Doktorgrades der Fakultät für
Chemie und Pharmazie
der Ludwig-Maximilians-Universität München

Active Modes of the Translocon:

Snapshots of Sec61 Interactions with Different Substrates and Co-factors

Marko Gogala

aus

Zagreb, Kroatien

2015.

Erklärung

Diese Dissertation wurde im Sinne von § 7 der Promotionsordnung vom 28. November 2011 von Herrn Roland Beckmann betreut.

Eidesstattliche Versicherung

Diese Dissertation wurde eigenständig und ohne unerlaubte Hilfe erarbeitet.

München, 19.01.2015.

.....

Dissertation eingereicht am 22.01.2015

1. Gutachterin / 1. Gutachter: Prof. Dr. Roland Beckmann

2. Gutachterin / 2. Gutachter: Dr. Daniel N. Wilson

Mündliche Prüfung am 13.03.2015

Table of Contents

Summary

All proteins are synthesized in the cytoplasm. However some proteins function outside of cells, in the cell membrane, in the endoplasmic reticulum or one of the connected vesicular systems and need to be sorted and accordingly transported. Consequently, the secretory pathway, a highly conserved protein targeting, translocation and membrane insertion system has evolved to cope with this task. The central actor in the secretory pathway is the heterotrimeric Sec61αβγ protein complex also known as the translocon. This protein complex has been shown to act as a transmembrane channel facilitating protein translocation into the lumen of the endoplasmic reticulum, a starting point in protein secretion. The complex also contains a lateral opening, termed 'lateral gate' through which proteins have been suggested to insert into the membrane of the endoplasmic reticulum. The mechanics of translocon opening for protein secretion or membrane insertion has been a matter of debate.

The results presented here show secondary structure level resolution cryo-electron microscopic structures of the translocon in complex with stalled ribosome-nascent chain complexes carrying substrates with propensity for either secretion or membrane insertion as well as ribosome-bound inactive translocon molecules. The observed differences in secondary structure suggest a model for translocon activity in protein sorting.

Introduction

A short overview of protein transport

All proteins are synthesized in the cytoplasm but different proteins perform their functions in different cellular compartments as well as outside of the cell. Consequently they need to be transported to their intended location. Furthermore, some proteins require post-translational modifications in order to function properly. These processes can happen after release of the peptide (i.e. post-translationally) or during translation (i.e. co-translationally). Additionally, peptides may be transported in an unfolded state or as fully folded proteins (Fig1.) Most pathways of protein transport require an energy source to ensure unidirectionality. In a majority of cases this is an external energy source such as hydrolysis of GTP or ATP or an ion gradient but can also involve protein folding in making the translocation step irreversible (Berg et al. 2002; Stojanovski et al. 2008).

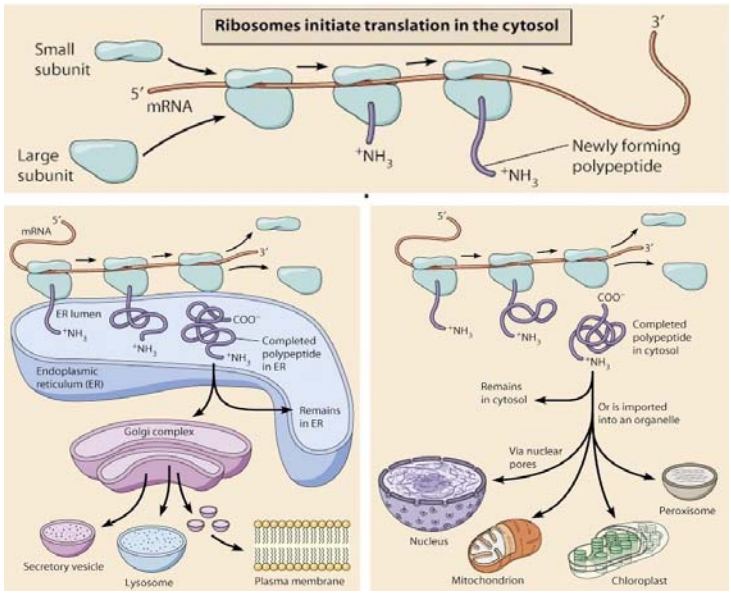

Figure 1: Possible routes for protein sorting into different organelles.
Top: all proteins are synthesized in the cytoplasm. Bottom left: co-translational sorting of proteins into the ER and further on into the GA, lysosomes, cellular membrane or secretion into the extracellular space. Bottom right: post-translational sorting of folded proteins into the nucleus, peroxisomes, mitochondria and, in plants, also into the chloroplast (Cooper & Hausman 2007).

In order to ensure targeting of correct proteins to appropriate cellular locations, complex targeting and translocation systems have evolved. These systems are evolutionarily, mechanistically and structurally diverse but have a shared trait: they all recognize some signal sequence, located either amino-terminally (N-terminally) or carboxyl-terminally (C-terminally) on the substrate peptide. This signal sequence is then recognized by a targeting or adapter molecule and transferred to the appropriate transport machinery.

The secretory pathway is an essential sorting pathway in all living cells

Roughly a third of proteins synthesized in an average cell is destined to become transmembrane proteins or to be secreted out of the cell. Prior to their localization these proteins must pass through the secretory pathway.

As for most other protein localization pathways, the targeted proteins carry a signal sequence that gets recognized by cytosolic factors that target the protein to a translocation channel. In the case of the secretory pathway, this process can occur both co- and post-translationally.

In the co-translational pathway, the signal sequence is recognized by the signal recognition particle (SRP) that binds the SRP receptor (SR) located on the membrane and transfers the substrate to the Sec61 complex that facilitates the actual translocation or membrane insertion and is thus termed the ‘translocon’.

This complex is located in the endoplasmic reticulum (ER) membrane of eukaryotes and in the plasma membrane of prokaryotes. Once the proteins are localized in the ER, they can be modified and sub-sorted in various ways.

The post-translational targeting steps of the secretory pathway involve different proteins than those in co-translational targeting as well as external sources of energy that replace the ribosome. Furthermore, these proteins are not conserved between the three domains of life, at least partially due to differences in cellular organization and availability of energy sources in different cell compartments. The central element of most post-translational pathways, however, remains the translocon complex which functions in much the same way in these pathways as it does in the co-translational pathway.

The signal sequence

In case of proteins destined for the secretory pathway, the signal sequence is placed N-terminally and consists of three distinct areas: the N-terminus of the sequence usually consists of several basic amino-acids followed by a central region of 8-12 hydrophobic amino-acids in a sequence with high helical propensity and a C-terminal sequence rich in hydrophilic amino-acids. These regions are termed n, h and c regions respectively (von Heijne 1985). Despite conforming to these general rules signal sequences are highly variable in their exact amino-acid composition, overall hydrophobicity and charge as well as sequence length (von Heijne 1985; Nyathi et al. 2013).

Co-translational protein targeting

In co-translational protein transport, when a signal sequence appears in the exit tunnel of the translating ribosome, the signal recognition particle (SRP) is recruited to the complex. In eukaryotes and archaea the particle consists of a 7S RNA molecule which is divided into two structural and functional domains: central the S-domain and the 5' and 3'-terminal Alu-domain. The S-domain is responsible for signal sequence binding and carries four proteins: SRP54, SRP19, SRP68 and SRP72. SRP54 in particular plays a central role containing the C-terminal, peptide-binding, methionine rich M-domain. The M domain of SRP54 contains a hydrophobic groove that binds hydrophobic signal sequences of nascent secretory proteins. SRP54 also contains the N and G domains that are tightly associated and referred to as the NG domain which functions in targeting the SRP to the membrane. SRP54, together with SRP RNA helix 8 forms an essential and highly conserved core of the SRP molecule.

The Alu-domain which contains the SRP9/14 heterodimer binds the ribosome in the factor binding site and is responsible for translational arrest.

Upon SRP binding, the arrested ribosome-nascent chain-SRP (RNC-SRP) complex is targeted to the SRP receptor molecule (SR) on the ER membrane.

SR is a heterodimer: SRα contains a C-terminal NG domain which dimerizes with the SRP54 NG-domain enabling GTP hydrolysis and substrate transfer and an N-terminal

X domain which binds SRβ a single spanning helical transmembrane domain that serves as a membrane anchor (Helmers et al. 2003).

Upon peptide release from the M-domain of SRP54 and corresponding transfer to the Sec61/SecYEG channel, two NG-domains act as mutual GTPase activators (GAPs) and hydrolyze their GTP molecules, stimulating dissociation (Grudnik et al. 2009; Halic & Beckmann 2005; Kinch et al. 2002; Shan & Walter 2005), (Fig 2).

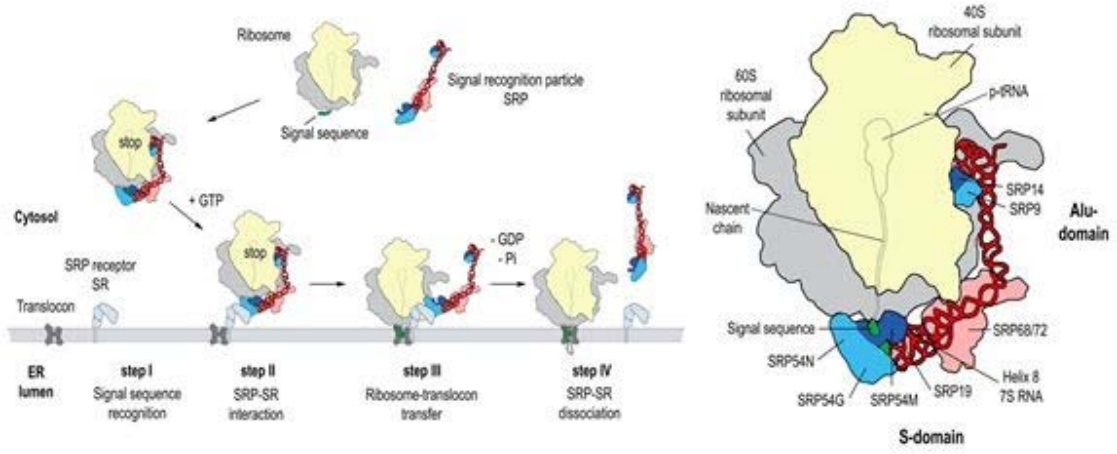

Figure 2: Protein targeting in eukaryotes.

When a signal sequence emerges from the ribosomal exit tunnel, the ribosome is bound by an SRP particle. The complex is then targeted to the ER membrane, where SRP binds the SRP-receptor (SR) molecule. This binding facilitates the transfer of the ribosome-nascent chain complex (RNC) to the translocon. The proces is very similar in bacteria and archaea. The only significant differences are that most prokaryotic SRPs and SRs are simpler and that the complexes are targeted to the plasma-membrane in the absence of the ER.

The translocon complex is a universally conserved protein conducting channel

The translocon complex is a universally conserved channel for protein insertion into and translocation across the ER membrane of eukaryotes and inner membrane of prokaryotes. Due to its dual role this complex is sometimes referred to as the protein conducting channel (PCC). The PCC has been the subject of extensive biochemical, crystallographic and cryo-EM studies both alone and in complex with substrates (Frauenfeld et al. 2011; Park et al. 2014; Gogala et al. 2014; Becker et al. 2009), substrate-mimics (Egea & Stroud 2010), binding partners (Becker et al. 2009) and mimics of binding partners (Tsukazaki et al. 2008). This wealth of data has brought important insights into this molecule. It consists of three transmembrane proteins, Sec61α, Sec61γ and Sec61β forming a heterotrimer. The first two subunits are necessary and sufficient for channel activity while the third subunit is dispensable (Görlich & Rapoport 1993). The higher oligomeric state of this complex has been a matter of some controversy but the basic active unit is now widely believed to be a single trimeric unit.

The organization of the translocon subunits Sec61α, Sec61γ and Sec61β as well as an overview of their homologues in different organisms is shown in Figure 3.

Sec61α	Sec61β	Sec61γ
Sec61p	Sbh1p	Sss1p
Ssh1	Sbh2p	Sss1p
SecY	SecG	SecE
SecY	Secβ	SecE

Figure 3: Overview of translocon subunits.

Translocon subunits in mammals (top row), two types of fungal translocon (second and third row), bacteria (fourth row) and archaea (bottom row). The color codes for the subunits fit those in the structure on the right (Van den Berg et al. 2004).

Sec61α

Sec61α (or SecY in prokaryotes) is a transmembrane channel. It is this protein that is responsible for the main functions of the translocon: ligand binding, substrate binding, protein secretion and membrane insertion. Although conserved across all domains of life, this channel is highly malleable and adaptable to different substrates and conditions. Indeed, significant segments of Sec61α can be deleted or replaced with heterologous amino acid sequences without abolishing function (Junne et al. 2006; Li et al. 2007; Shimokawa et al. 2003).

A crystal structure of the archaeal *Methanococcus jannaschii* SecYEβ molecule has revealed important insights into the structure of the Sec61α/SecY subunit at the same time suggesting its functional mechanisms (Van den Berg et al. 2004). The channel consists of ten membrane spanning helices with both termini facing the cytosol (Fig. 4). The second helix, TM2, is structurally split into the N-terminal, shorter, hydrophilic TM2a and the C-terminal, longer, hydrophobic TM2b. The ten transmembrane helices are arranged in two pseudosymmetric, similarly folded halves, containing five TM-segments each. The N-terminal half, consisting of TM1-5 is connected by a hinge-like loop between TM5 and TM6 (loop L5) to the C-terminal half that contacts the ribosome via its cytosolic loops between TM6-7 (loop L6) and TM8-9 (L8). Each of the two halves has three outer and two inner TM helices.

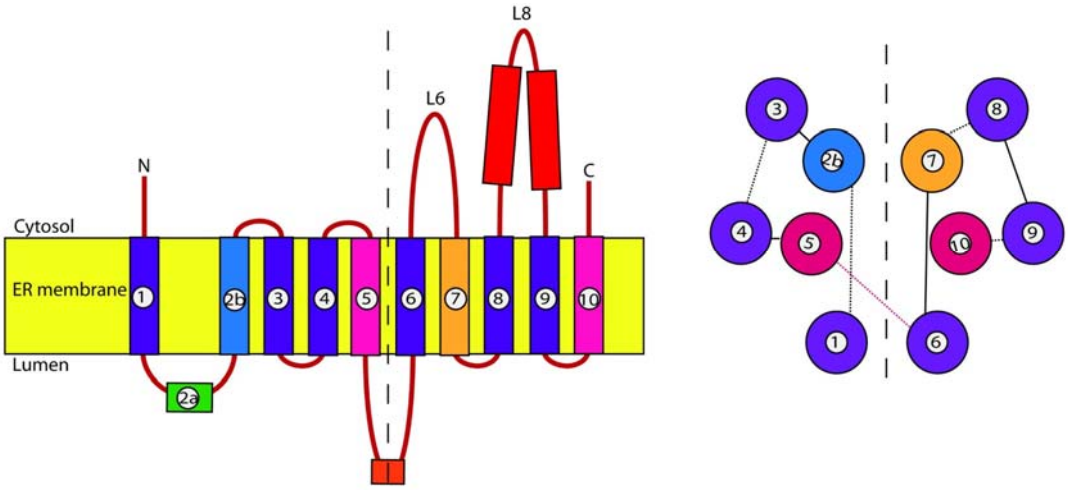

Figure 4: Overview of Sec61/SecY topology.

On the left, side view of the scheme. The dashed line represents the plane dividing the two pseudo-symmetric halves of the molecule. TM2b and TM7 are blue and yellow respectively. Other centrally located TM helices (TM5 and TM10) are colored pink. Helices which are located peripherally to the central channel are colored magenta. Plug helix 2a is colored green. Ribosome contacting loops L6 and L8 are indicated. On the right: top view of the molecule. Color scheme is the same.

The two halves come into contact dorsally via the hinge-like L5 loop and frontally via TM2b and TM7 that form a vertical fissure through which protein segments have been conceived to laterally insert into the membrane. This opening has hence been named the lateral gate. In the inactive state of the molecule the gap between TM2b and TM7 is too narrow to allow passage of molecules so the helices have been expected to move away from each other during TM insertion. Due to the role of the C-terminal half of the molecule in binding the ribosome and the post-translational factor SecA, the flexibility of the L5 hinge and relative rigidity of each pseudo-symmetric half, it has been suggested that most of this movement is due to a shift in the N-terminal half of Sec61α/SecY with the C-terminal half acting as a pivot (Fig. 5).

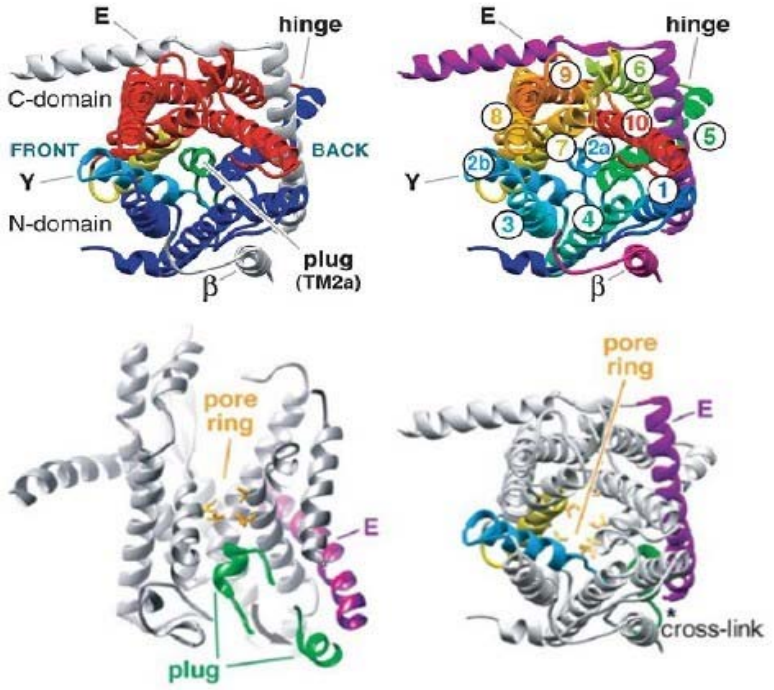

Figure 5: Model of the idle, archaeal SecYEβ.

Top left: Top view of the translocon. The main features of SecY are indicated. The molecule consists of two pseudo-symmetric halves (N- and C-terminal) that come together at the front. The center of the molecule is obstructed by the so called plug helix. Top right: Different helices are indicated in the top view. Helices 2b and 7 come together to form the lateral gate while 2a is the plug. Subunits SecE and Secβ are bound to the molecule peripherally. Lower left: side view of the translocon. The plug helix has to slide out in order for protein secretion to occur. The pore ring consists of aliphatic amino-acid side chains that maintain a seal for ion flow during translocation. Lower left: a top view of the translocon. Helices 2 and 7 are indicated in blue and yellow respectively. The pore ring is indicated as yellow side chains. In this image, the plug is removed to the side to show the position where it has been cross-linked experimentally (Van den Berg et al. 2004).

Most of the TM helices are not positioned perpendicularly in the membrane with the inner four helices enclosing an hour-glass shaped hydrophilic channel obstructed in its luminal/periplasmic side by the small TM2a helix. Based on its position, this helix has been termed the 'plug'. The hydrophilic channel can be envisaged as a conduit for extended chains passing through the membrane if the plug helix would dis-attach from the central constriction and slide further out towards the luminal side of the hourglass channel. This

movement is plausible based on the available structural data as well as cross-linking studies showing that TM2a can contact SecE (bacterial homologue of Sec61γ) which lies more than 20 Å away (Harris & Silhavy 1999).

The central constriction of the hour-glass hydrophilic channel is lined by six aliphatic amino-acid side chains forming the 'pore ring', a hydrophobic filter preventing free diffusion of ions while still flexible enough to allow for passage of a wide variety of peptide substrates. The pore ring, which was first observed in the crystal structure of the archaeal *Methanococcus jannaschii* PCC is highly conserved and also present in eukaryotic and bacterial Sec61α/SecY.

Sec61γ

The Sec61γ subunit (SecE in prokaryotes) is a highly conserved protein. Although Sec61γ homologues from some organisms have additional segments, the conserved core of the molecule consists of two helices: a cytoplasmic, N-terminal amphipathic helix in contact with the C-terminal half of the α-subunit and a C-terminal transmembrane helix, crossing the membrane under a 35° angle and contacting both the C- and the N- terminal halves of the α-subunit. The two helices are connected by a hinge region containing several conserved amino-acids (Lycklama a Nijeholt et al. 2013).

There have been several suggestions for the role of this protein. Based on the position of its C-terminal transmembrane segment, the γ-subunit has been proposed to act as a clamp on the α-subunit.

Deletion of the conserved hinge region of Sec61γ abolishes the activity of the translocon but replacing the deleted region with a heterologous sequence of same length restores the function, implying that the sequence conservation in this segment is not of functional importance (Kontinen et al. 1996; Murphy & Beckwith 1994).

Of the two helices, the C-terminal transmembrane helix seems to be important as a membrane anchor of the molecule but its exact sequence can be varied with little effect upon translocation activity of the PCC while the amphipathic helix appears to be functionally dispensable (Lycklama a Nijeholt et al. 2013; Pohlschröder et al. 1996). Large

portions of both C- and N-terminal sides of the sequence can be deleted without significantly impairing activity of PCC (Schatz et al. 1991).

Another potential role of the γ-subunit could be to act as a stabilizing factor for the α-subunit. Indeed, in bacteria, SecY expressed without SecE is readily degraded through a quality control mechanism by the membrane protease FtsH (Kihara et al. 1995).

In support of the structural stabilization hypothesis, when *E. coli* SecY is cleaved into two halves at its hinge site, the PCC remains translocation-competent as long as the SecE subunit is unperturbed. Upon additional cleavage of SecE activity is abolished completely. In addition, cleavage of the hinge region of SecE, but not its N-terminal amphipathic helix significantly reduces translocation activity of the SecYEG translocon. Covalent cross-linking of SecE to SecY simultaneously at contact points in the N-terminal and C-terminal helices of SecE has no significant effect on SecYEG function, further implying that the helical regions of SecE remain in contact with the two halves of SecY while the hinge area accommodates the movement of SecY (Lycklama a Nijeholt et al. 2013).

All these data together imply a role of Sec61γ/SecE in providing structural stability of the α-subunit without playing a role in the protein conducting activity of the complex.

Sec61β

Although a majority of protein conducting channels have a third components termed Sec61β in eukaryotes, Secβ in archaea and SecG in prokaryotes, sequences of these proteins do not seem to be conserved across domains of life. Indeed, this component is dispensable for translocation and insertion functions of the PCC.

The Sec61β/SecG protein typically consists of a single TM helix with a cytoplasmic N-terminus, and a cytoplasmic domain. The TM segment is almost perpendicular to the plane of the membrane has little contact with α and γ subunits.

Due to its dispensability for the core functions of the Sec61 complex, little is known about its functions. This subunit seems to be involved in targeted secretion of some metazoan developmental factors, in particular the EGF receptor ligand Gurken (Kelkar & Dobberstein 2009) and is essential in embryonic development of *Drosophila melanogaster* (Valcárcel et al. 1999) Interestingly, even in *D. melanogaster* cells depleted of Sec61β

Gurken is successfully translocated across the ER membrane and delivered to the *cis*-Golgi. Further progression of Gurken through the secretory pathway of such cells is impeded, suggesting a posttranslocational role for Sec61β (Valcárcel et al. 1999) This role may come through interactions with members of the exocyst complex which plays a role in late protein secretion (Lipschutz et al. 2003)

There is also biochemical data indicating that, in eukaryotes, the Sec61β functions as a GEF for the β subunit of SR there by facilitating SRαβ heterodimer formation and efficient ribosome-SRP targeting to the membrane (Helmers et al. 2003; Kinch et al. 2002; Schwartz & Blobel 2003; Jiang et al. 2008).

Cold sensitive mutants of the fungal Sec61β homologue, Sbh1 in *S. cerevisiae* have a non-lethal but observable phenotype that can be complemented by the transmembrane section of human Sec61β, indicating that any function is probably localized in that segment (Leroux & Rokeach 2008).

Likewise, the prokaryotic analogue of Sec61β, SecG seems to play a highly specialized role in secretion of specific substrates (Sibbald et al. 2010).

Gating the translocon

After signal sequence recognition by SRP and transfer from the SR to the Sec61 complex i.e. targeting, a final act of substrate recognition occurs, for which the translocon itself is necessary and sufficient. Indeed, the Sec61 complex together with SR forms a minimal unit needed for translocation of many proteins while some need an additional factor (translocating chain-associating membrane protein, TRAM) with SRP being dispensable for translocation in absence of additional cytosolic factors (Jungnickel & Rapoport 1995).

Substrate binding strengthens the ribosome interaction with the membrane (Adelman et al. 1973) in relation to salt concentration and EDTA treatment (Wolin & Walter 1993). This gating property of the translocon is also involved in post-translational translocation in both eukaryotes (Plath et al. 1998) and prokaryotes (Brundage et al. 1990). The gating causes the substrate to become protease resistant and simultaneously exposed to the luminal side of the translocon (Jungnickel & Rapoport 1995).

Mutations in the signal sequence that do not disrupt SRP binding and targeting of the substrate to the Sec61 complex can still prevent membrane insertion of substrates through disruption of translocon gating (Kim et al. 2002; Jungnickel & Rapoport 1995) further stressing the importance of the gating step in addition to targeting.

Important insights into the mechanism of translocon gating have come from mutants in the Sec-genes suppressing these mutations in the signal sequences. Indeed, the core components of the bacterial secretion machinery were first identified through an assay for suppressor mutants of the mutated signal sequence from the outer membrane λ-receptor protein (*lamB*) in *E. coli* (Emr et al. 1981). These suppressors that restore the localization of LamB to the outer membrane were termed *prl*-mutants (PRotein Localization). Most of the mutants, with the least specificity in signal sequence discrimination targeted to a locus termed *prlA* (Emr et al. 1981; Emr & Bassford 1982). Some of these mutants lose all proofreading activity and enable posttranslational translocation of proteins lacking the signal sequence entirely (Derman et al. 1993). Additional *prl* loci were later discovered and found to co-localize with *sec*-genes, specifically with *E* and *secA*, a gene coding for a protein involved in bacterial post-translational protein secretion. The strongest suppressor, *prlA* was found to correspond with the gene for the protein SecY (Bieker et al. 1990). The *prlA* mutants cluster within three distinct domains of SecY: TM7, TM2a, and TM10 (Osborne & Silhavy 1993).

The main hot spot for *prl* mutants seems to be the DNA sequence coding for TM7, indicating its primary role in signal sequence recognition. Mutant SecY channels missing 11 amino acids from TM7 can translocate substrates missing the 12 amino acids from the hydrophobic parts of their signal sequences. Interestingly, strains carrying such large deletions in TM7 are viable and their SecY molecules are translocation competent, indicating that TM7 plays a key role in signal sequence recognition but is otherwise dispensable (Osborne & Silhavy 1993). The functional mechanism of these mutations is quite clear when taking into account the known models of SecYEG/Sec61. The role of TM7 as a primary site of translocon gating is in accordance with its position as part of the lateral gate, which is a proposed binding site for signal sequences of translocon substrates.

The second hotspot for *prl*-mutants in *secY* is the sequence coding for the TM2a plug helix (Smith et al. 2005; Osborne & Silhavy 1993). The amino-acid sequence of this

helix is not vital for the function of the translocon and deletion mutants have been obtained that show the *prl*-phenotype but are otherwise active. It has been shown that in these deletion mutants, areas adjacent to the plug fold into a helix that can partially compensate for lack of TM2a. If, however, TM2a is cross-linked to SecE, thereby creating a constitutively active conformation, the cells carrying the construct die, probably due to ion leakage. The construct itself shows increased translocon activity *in vitro* (Tam et al. 2005). Hence, the plug plays an important role in translocon gating and a vital one in preventing ion leakage in the resting state of the channel (Harris & Silhavy 1999; Maillard et al. 2007; Li et al. 2007).

The plug helix and the pore ring are proposed to stabilize the closed conformation of the translocon and need to be displaced in order for protein secretion and insertion to take place (Smith et al. 2005). The importance of the pore ring might explain why another transmembrane segment that appears to be important in signal sequence recognition is TM10, specifically its residue I401 which in *E. coli* forms part of the pore ring. Some of the *prl*-mutations in this helix exhibit synthetic lethality with *prl*-mutations in the transmembrane helix of SecE (*prlG* mutations). The mutated subunits seem to form a stable complex whose presence is lethal to the cell (Osborne & Silhavy 1993). These double mutants are recessive, indicating that the resulting complex is inactive (Flower et al. 1995). Individually, the mutants strengthen SecY-SecE interaction and result in a translocon that lacks gating discrimination but is otherwise active. The exact mechanism of this phenotype is not known (Osborne & Silhavy 1993). Mutants in TM10 also exhibit synthetic lethality with mutants in TM7, further indicating the importance of pore ring residues in translocon function (Smith et al. 2005).

From the mutational and structural analysis it can be concluded that the resting state of the translocon, stabilized by the contacts between the plug and the pore ring residues, is disrupted by lateral gate opening upon signal sequence binding to the lateral gate. Mutations that partially destabilize the resting state enable translocon opening even with defective signal sequences. Mutations which lock the translocon in a permanently active state through cross-linking of the plug to SecE are dominantly lethal due to ion leakage (Van den Berg et al. 2004; Smith et al. 2005).

Opening of the lateral gate for signal sequence binding and peptide membrane insertion

In addition to its role in recognition of signal sequences and its partial opening for vertical translocation of secretory peptides, the lateral gate of the translocon can open to facilitate membrane insertion of hydrophobic helices (Van den Berg et al. 2004), (Fig. 6).

The first crystal structure of the inactive translocon from *M. jannaschii* was suggestive of the role of TM2b and TM7 in both membrane insertion and signal sequence binding (Van den Berg et al. 2004). Further information was obtained from another crystal structure of SecYEβ from *Pyrococcus furiosus*. Here, crystal packing interactions led to formation of a unit cell in which two SecYE complexes were interacting via their long TM10 helices. The C-terminal helix of each molecule was inserted into the vestibule and bound to the C-terminal helix of the other. This led to a state claimed to be analogous to physiological signal sequence binding (Egea & Stroud 2010).

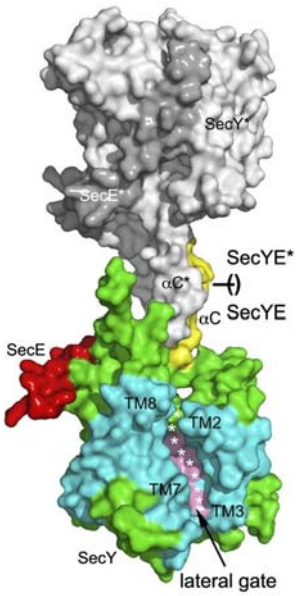

Figure 6: Opening of the lateral gate in *P. furiosus* SecY due to crystal packing interactions.

In the lower half of the image, SecE is indicated in red while SecY is indicated in green, with the lateral gate colored cyan, central channel pink and TM10 in yellow. The opposing SecY molecule is gray. As can be seen, insertions of the opposing extended TM10s induces opening of the lateral gate and exposure of the central channel to the lipid environment. The position that the substrate peptide is proposed to occupy is indicated by white stars.

In these molecules, helices TM2b and TM7 have moved away from each other, creating an 11 Å wide opening in the lateral gate, large enough to bind a signal sequence or a transmembrane helix. In this structure the hydrophobic pore ring is dismantled through structural rearrangement that creates 13.6 Å wide gap in the central channel but the plug helix remains in roughly the same position as in the inactive *M. jannaschii* structure, thereby occluding the passage for protein secretion (Egea & Stroud 2010).

Additional insight has come from a cryo-EM structure of an *E. coli* RNC-SecYEG complex translating a signal anchor sequence where the SecYEG molecule was embedded into a Nanodisc particle that created an environment analogue to that in a membrane, namely a lipid bilayer. In this structure a model of an open the lateral gate was built with an extra helix bound between TM2b and TM7. Unfortunately, the low resolution of this structure obscured any additional detail e.g. movement of the plug (Frauenfeld et al. 2011), (Fig. 7).

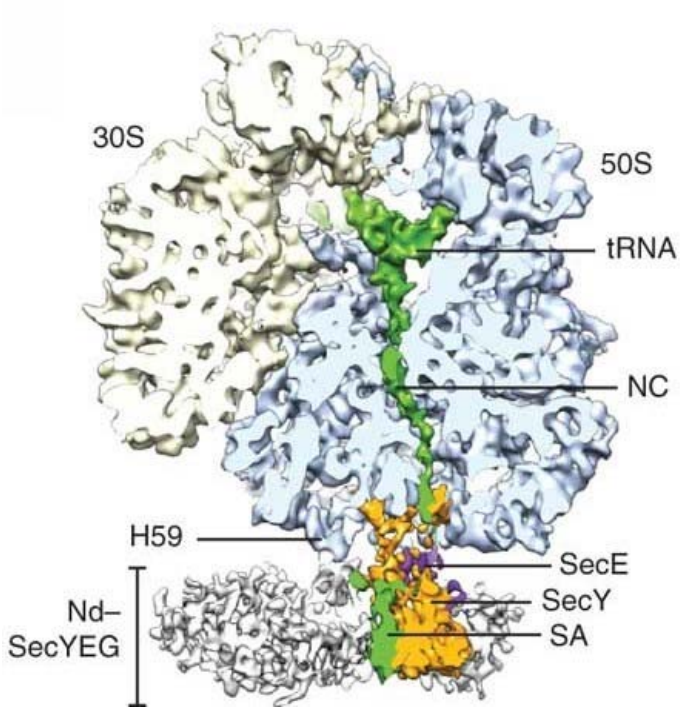

Figure 7: Structure of RNC-bound SecY embedded into the Nanodisc lipid bilayer.
The ribosome subunits are indicated in yellow and blue, SecY in orange, SecE in magenta, Nanodisc in gray and the peptidyl-tRNA in green.

Opening of the translocon central channel for protein secretion

Protein translocation through the Sec61/SecYEG translocon has been extensively probed through various biochemical methods. Based on this data, translocation has been suggested to take place through the hydrophilic central channel. Due to the small size and hour-glass shape of the channel, it is expected that the substrate would have to transverse the membrane in an unfolded state (Park & Rapoport 2011; Bonardi et al. 2011; Lycklama A Nijeholt et al. 2010; Lycklama a Nijeholt et al. 2011).

Upon translocon gating, the plug helix is expected to slide away from the central constriction, though to what extent is a matter of debate (Lycklama a Nijeholt et al. 2011; Van den Berg et al. 2004). The lateral gate is also expected to at least partially open (du Plessis et al. 2009) but the pore ring is expected to remain largely in place, providing a barrier for ion flow. Important insights into how exactly these movements happen have been provided by several X-ray and Cryo-EM structures of the Sec61/SecYEG complex in various states of activation.

A model based on a crystal structure of eubacterial, *Thermus thermophilus* SecYE in complex with an anti-SecY antibody Fab fragment shows an opening in the cytoplasmic part of the lateral gate (Fig. 8), but an otherwise similar morphology to the inactive *M. jannaschii* structure (Tsukazaki et al. 2008).

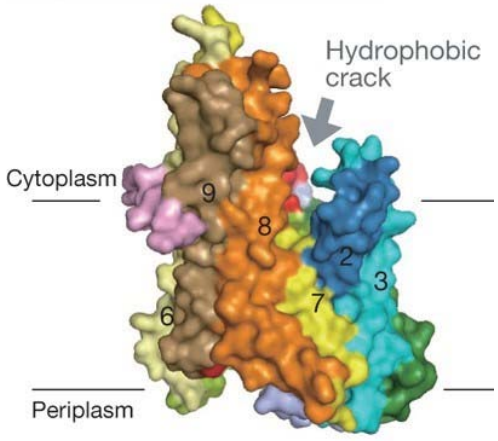

Figure 8: Structure of *Thermus thermophilus* SecYE in complex with an anti-SecY antibody Fab fragment.

SecE is indicated in pink. Other colors represent different helices of SecY. The cytoplasmic and periplasmic sides of the membrane are labeled. The hydrophobic opening of the lateral gate is indicated between TM2 and TM7.

A structure of a bacterial SecYEG complex, from *Thermotoga maritima* in complex with the post-translational factor SecA depicts a further step in translocon activation (Fig. 9). Here, a two-helix finger domain of SecA is inserted into the cytosolic vestibule of SecY. This interaction pries the lateral gate of SecY open and causes a significant outward shift in the plug (Zimmer et al. 2008).

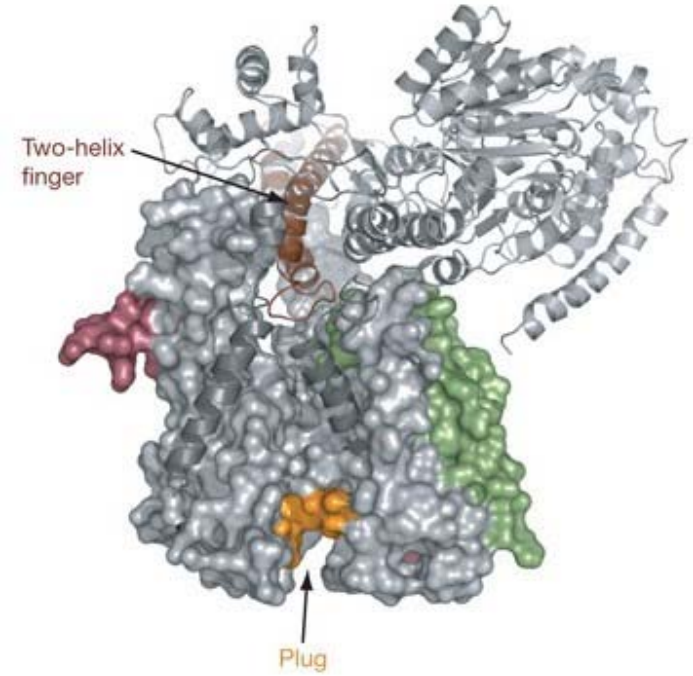

Figure 9: Opening of SecY in complex with SecA.

SecE and SecG are indicated in purple and green respectively. The shifted plug is shown in yellow. The two helix finger domain of SecA that pries the lateral gate of SecY open is colored brown and additionally labeled.

These two structures suggest that in addition to the gating step through signal sequence recognition, translocon binding to a translocation motor may play a significant role in initiating peptide secretion.

A snapshot of translocon activation in co-translational translocation came from a Cryo-EM structure of a mammalian Sec61 complex bound to an RNC carrying a nascent chain with a signal sequence. The lateral gate is slightly open in this structure, mostly due to movement in TM2b suggesting that binding to the ribosome can also prime the translocon for further activation (Fig. 10). Due to comparatively high resolution, this study was also the first one to unambiguously demonstrate that the translocon in its activated, ribosome bound state is a monomer (Becker et al. 2009). Preceding Cryo-EM studies were suggestive of a higher oligomeric state of the translocon due to the large size of the density observed in the electron-density maps (Mitra et al. 2005; Ménétret et al. 2005; Morgan et al. 2002; Menetret et al. 2000; Beckmann et al. 1997; Hanein et al. 1996). The work by Becker et al. demonstrated that this apparent large size of the translocon was in fact an

artifact due to the presence of a detergent-lipid micelle around the heterotrimeric molecule. Another important aspect of this work was determining the exact nature of translocon-ribosome interactions through loops L6 and L8 of Sec61α (Becker et al. 2009). Although some previous data suggested that the Sec61 complex was a single trimer interacting with the ribosome through cytosolic loops of the α-subunit, this data was produced at a lower resolution with non-translating ribosomes thus leaving the nature of the active state of Sec61 ambiguous (Ménétret et al. 2008; Ménétret et al. 2007).

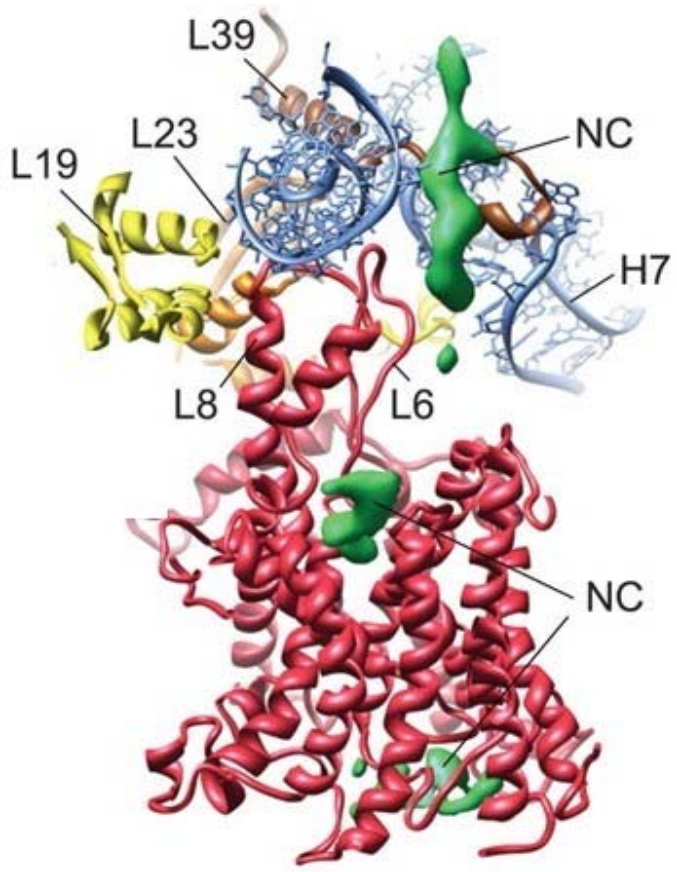

Figure 10: The pre-activated, RNC-bound translocon.

The Sec61-complex is indicated in red, the additional density, attributed to the nascent chain, in green. Contacts of translocon loops 6 and 8 with ribosomal proteins and RNA are shown.

Unanswered questions about translocon function

Despite the amount of structural, biophysical, biochemical and genetic research of translocon structure and function, important questions remain unanswered.

Prior to this work, the translocon has never been observed bound to a substrate in a physiological way at a high enough resolution to allow determination of secondary structure changes. While the roles of the lateral gate, the plug helix and the pore ring can be deduced from the structure of the inactive translocon and have been confirmed biochemically, the roles of other helices as well as the extent to which the lateral gate and the pore ring have to open to facilitate secretion or insertion of different substrates have not been unambiguously determined.

The extent to which the plug helix has to shift to allow substrate conductance has been particularly disputed. Different approaches have produced results ranging from small shifts to a 20 Å movement out of the channel (Lycklama a Nijeholt et al. 2011; Van den Berg et al. 2004).

To answer these questions it was necessary to solve structures of the translocon engaging both secretory and transmembrane substrates in as similar way as possible to the *in vivo* situation.

Accessory factors of the translocon

Aside from the main components, SRP, SR, Sec61αβγ/SecYEG and translocation motors (i.e. ribosome, Bip or SecA), secretion and membrane insertion of proteins often require accessory factors.

In eukaryotic cells additional factors are required for co-translational translocation of certain substrates.

In mammals, the translocating chain -associating membrane protein (TRAM), an eight time membrane spanning glycoprotein, has been shown to be in proximity to nascent chains early in the process of translocation. The exact role of TRAM is not known but it has been shown to be necessary for translocation of certain substrates and to have an enhancing effect for others (Görlich et al. 1992; Görlich & Rapoport 1993).

Another factor shown to contact nascent chains in the early stages of translocation in metazoans is the tetrameric translocon-associated protein (TRAP). All four subunits of TRAP are transmembrane proteins with α, β and δ-subunits being single-spanning and the four times spanning γ-subunit (Fig. 11). The peptide-binding subunit is TRAPα which also interacts with TRAPβ and, more weakly, TRAPγ and TRAPδ (Hartmann et al. 1993).

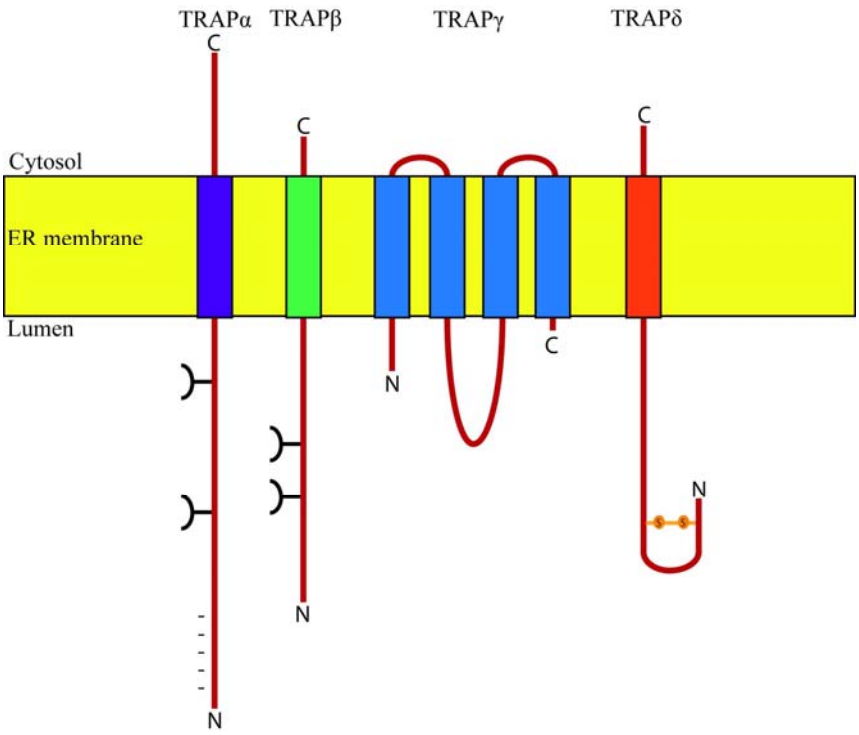

Figure 11: Scheme of the TRAP-complex topology.

TRAP is a heterotetramer consisting of seven transmembrane helices. All subunits have their N-termini in the lumen of the ER and all of them, except the gamma subunit, have luminal C-termini. TRAP alpha and beta have two glycosylation sites each and TRAP delta also has a disulphide bridge on its N-terminus. The N-terminus of TRAP alpha is strongly negatively charged. Image modeled after (Hartmann et al. 1993).

Cryo-EM studies of mammalian ribosome-translocon complexes have shown TRAP complex to interact stably with the Sec61 complex in a 1:1 stoichiometry even in the absence of nascent chains.

These studies revealed TRAP is physically located closely to the γ-subunit of the Sec61 trimer but is separated from it by a sheet of phospholipids (Fig. 12). Further a large,

luminal segment of TRAP has been observed and termed as the 'TRAP-hook'. The resolution of these structures was, however, too low to elucidate the exact mechanism of TRAP-Sec61 interaction (Menetret et al. 2000; Ménétret et al. 2008).

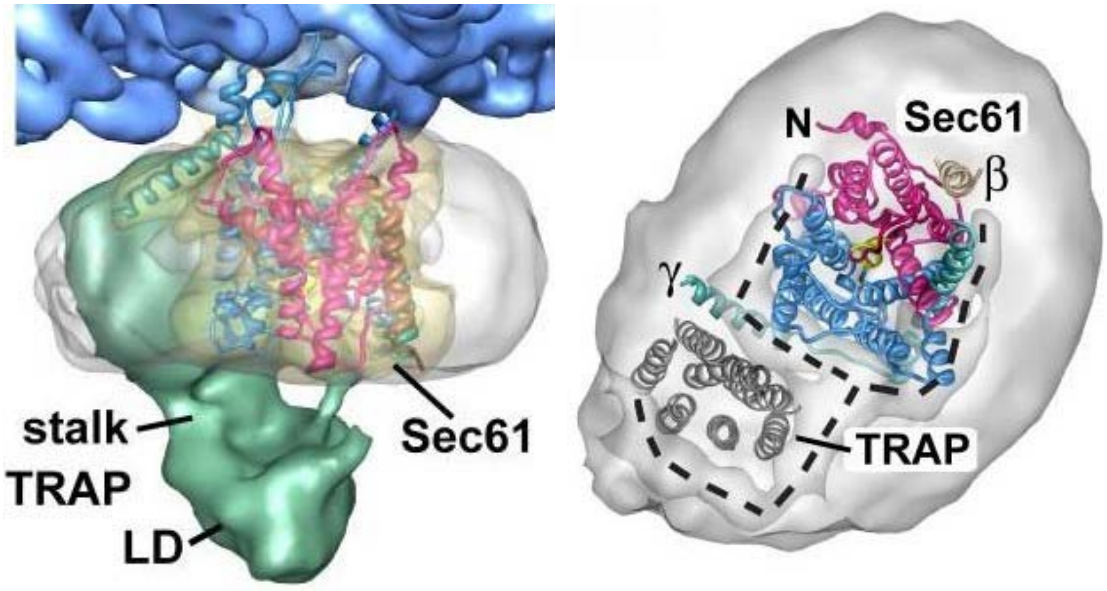

Figure 12: A low resolution Cryo-EM image showing the localization of the TRAP complex with respect to the Sec61 complex and the ribosome.

On the left, a side view of the TRAP-Sec61 density. The Sec61 has been modeled into the electron density while the density corresponding to TRAP is shown as a cyan-colored opaque surface. On the right is a luminal view of the same complex. Here, a putative model of TRAP has been suggested. The dashed area indicates the part of the micelle probably consisting of phospholipids (Ménétret et al. 2008).

As with TRAM, the exact role that TRAP plays in protein secretion is not yet clear but important indications are emerging. TRAP seems to be necessary for secretion of some substrates and to enhance secretion of others *in vitro*, but not *in vivo*. Recent *in vivo* data points to a potential role for the TRAP complex as an auxiliary determinant of transmembrane helix topology, promoting the N^{inside} orientation of helices with charge distribution that would otherwise favor C^{inside} orientation. This effect is limited to countering charge distribution and does not extend to highly hydrophobic helices that preferentially insert with their N-terminus facing the lumen of the ER (Sommer et al. 2013).

Altogether, knowledge about the roles and structures of eukaryotic translocon accessory proteins is lacking. In particular, a high resolution structure of the translocon in

complex with TRAP or TRAM could determine where on the translocon these proteins bind and how they might interact with the substrate. This data might then point to their exact function.

Further down the secretory pathway

Glycosylation

In eukaryotes, many proteins are post-translationally modified after entering the secretory pathway. The most common post-translational modification occurring in the ER is N-linked glycosylation. N-linked glycans play important roles in folding, quality control, compartmentalization and function of secretory and transmembrane proteins (Mohorko et al. 2011).

In the process of glycosylation the multi-subunit oligosaccharyl-transferase complex (OST) (Fig. 13) catalyzes the transfer of a pre-assembled oligosaccharide from a dolichol pyrophosphate lipid carrier to thee side chain amide group of the asparagine residue in the glycosylation sequence motif N-X-S/T (where X is any amino acid except proline). The stretch of amino-acids contacting the OST is in an unfolded state during the process.

The catalytic subunit of OST, Stt3, is conserved in all three domains of life while other subunits are specific to eukaryotes. In mammals, the OST is composed of seven highly conserved subunits.

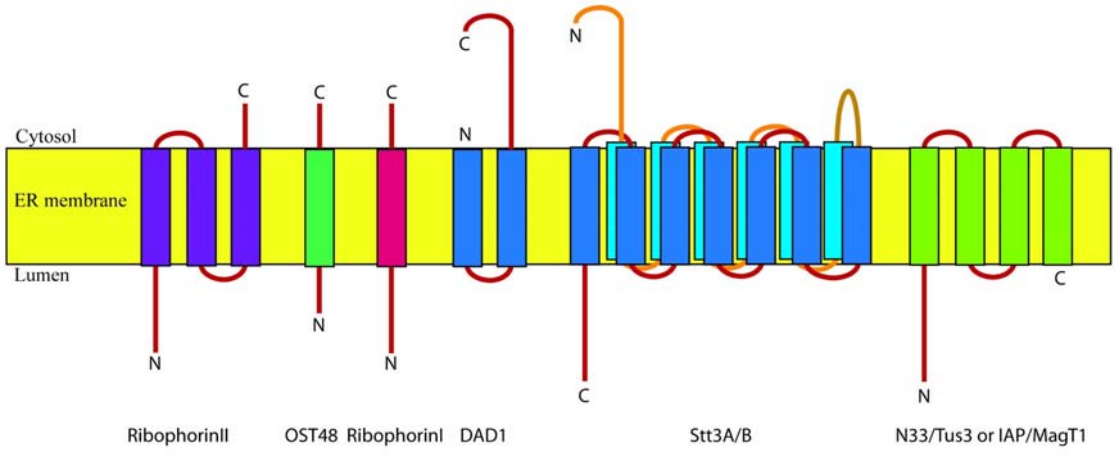

Figure 13: Conserved eukaryotic components of the OST complex.
Image according to Mohorko et al. (Mohorko et al. 2014)

All these subunits are conserved in yeast, with five being essential for cell viability (Table 1).

Mammalian subunit	Yeast homologue	Suggested function
Stt3A, Stt3B	Stt3p	Transfer of the glycosyl-moiety
ribophorin I	OST1p	Ribosome/Sec61 binding
ribophorin II	Swp1p	Ribosome/Sec61 binding
OST48	Wbp1p	Scaffold
DAD1	OST2p	Stabilization of the complex
N33/Tusc3	OST3p	Thioreductase
IAP	OST6p	Thioreductase
OST4	OST4	Recruitment of subunits, stabilization of the complex

Table 1: Subunits of the eukaryotic OST from mammals and yeast.

Essential subunits are highlighted in blue. Mutually exclusive thioreductase paralogues are highlighted in red (Dumax-Vorzet et al. 2013).

Aside from subunits directly and indirectly involved in the core function of OST, the complex contains two mutually exclusive, paralogous subunits involved in a thioreductase function. This reaction is believed to enhance glycosylation of certain substrates by keeping them in an unfolded state for an extended period (Mohorko et al. 2014).

Crystal structure of a bacterial homologue of Stt3, PglB and an archaeal homologue, AglB, have been solved (Lizak et al. 2011; Matsumoto et al. 2013). The core enzyme of OST consists of 11 to 13 transmembrane amino-acids, depending on the species, with a cytoplasmic N-terminus and a large, globular C-terminal periplasmic domain. The catalytic site is located in the periplasmic side of the membrane, at the membrane-aqueous interface, precisely in position to interact with dolichol-pyrophosphate. The site is formed by a group of conserved, acidic residues coordinating a divalent metal cation (Maita et al. 2010) and simultaneously binding the substrate peptide asparagine side chain in a conformation

suitable for nucleophilic attack. The Ser/Thr of the glycosylation site is bound to a separate binding site. It does not participate in the reaction itself but serves to maintain the substrate in an extended state during the reaction (Lizak et al. 2011).

Since the OST also contains ribophorin subunits that co-localize with the ribosomes and were, in fact, discovered as ribosome binding factors before their role as subunits of OST was known, (Kelleher et al. 1992) and since OST is known to catalyze both post- and cotranslational glycosylation, (Ruiz-Canada et al. 2009) it is expected that the OST complexes might co-localize with RNC-bound Sec61-complexes.

Unanswered questions on OST structure and function

While there have been attempts to determine the arrangement of the subunits within the eukaryotic OST complex, (Chavan et al. 2005; Li et al. 2008) the methods used so far were of rather limited resolution and have not produced unambiguous results. The functional roles of different subunits, while tentatively assigned are also far from certain. Architecture of OST and biochemical roles of its subunits thus still pose an unanswered and important question.

Furthermore, although there are strong biochemical indications that OST colocalizes with the RNC bound translocon, prior to this work this complex has never been visualized by Cryo-EM (Wang & Dobberstein 1999).

Also, data on the interaction of OST-subunits with the translocon has so far been sketchy (Chavan et al. 2005). It would be very interesting to find out how transmembrane parts of OST are positioned with respect to the lateral gate of the translocon and how the luminal parts are positioned with respect to the luminal vestibule of the translocon.

Since glycosylation is a very common modification of proteins that pass through the secretory pathway and in fact plays roles in folding and quality control in the ER, it is a very attractive target for research within the field of protein secretion.

Materials and Methods

Polymerase chain reaction and *E. coli* transformation

Polymerase chain reaction (PCR) was used to amplify specific double-stranded DNA fragments for *in vitro* transcription as well as for site-directed mutagenesis.

Amplification of substrate DNA for *in vitro* transcription was performed using the self-made Taq polymerase (Charlotte Ungewickell, AG Beckmann) with a 10× Taq buffer (100 mM Tris pH 8.8, 500mM KCl, 0.8% Triton X-100, 15 mM $MgCl_2$) and a dNTP mix (Roth). A primer complementary to the T7 polymerase site was used as the forward primer while two different primers were used as reverse primers for LepT and LepM based substrates. Primer sequences are given in Table 2.

Primer name	Sequence
LepT-R	TCA GGG AGG GAT ATA CTT GC
LepM-R	TCA GGG AGG GAT GTA TTT GC

Table 2: Reverse primers used for amplifying LepT and LepM DNA

Site-directed mutagenesis was performed using the Phusion Flash High Fidelity Master Mix (Finnzymes) according to the manufacturer's protocol, followed by digestion with restriction enzyme DpnI (NEB) (50 µL of unpurified PCR product, 5.7 µL NEB-buffer4 (10×), 1.3 µL DpnI) for 1h at 37°C followed by trasfornation into *E. coli* cells.

All primers were ordered from Metabion.

Cell transformation and stocks

Transformation into *E. coli* DH5α cells was performed using the heat-shock method. The linear vector (5 µL of DpnI digested PCR product) was mixed with 50 µL of competent cells (kindly donated by J. Musial and A. Gilmozzi), incubated on ice for 20 min, exposed to 42°C in a water bath for 2 min, incubated on ice for 5 min and recovered at 37°C with shaking for 45 min. After recovery the cells were inoculated onto ampicillin (100 µg/ml) containing LB plates and left to grow over night at 37°C. The colonies were transferred into 5 mL of ampicillin containing (100 µg/ml) LB medium and left overnight at 37°C with shaking.

On the following day, 0.5 mL of the culture was mixed with 0.5 mL of sterile 50% glycerol and shock-frozen in N_2(l). The rest of the culture (~4.5 mL) was used for DNA purification.

Plasmid purification and sequencing

Plasmids were purified using the QIAprep®Spin Miniprep Kit (Qiagen) according to the manufacturer's protocol. The resulting DNA was stored at -20°C or used directly as template for PCR. Aliquots of the purified plasmids were sent for sequencing to Eurofins MWG.

In vitro transcription

In vitro transcription was performed using the self-made recombinant T7 RNA polymerase (kindly prepared by S. Ungewickell), nucleotides and 10× transcription buffer (400 mM Tris/HCl, pH 7.9; 25 mM Spermidin, 200 mM $MgCl_2$, 0.1 % Triton X-100). Exact composition for a typical reaction is given in Table 3.

Component	Final concentration
10× Transcrition buffer	1 ×
1 M DTT	0.5 mM
ATP (130 mM)	8.06 mM
GTP (106 mM)	8.06 mM
CTP (112 mM)	8.06 mM
UTP (127 mM)	8.06 mM
Taq PCR DNA(purified)	~2.5 µg/100 µL

Table 3: Components for in vitro transcription.

When all components were added, 4µL of the T7 RNA polymerase were pippeted into the mix and a transcription was performed for 1h at 37°C. After addition of 4µL of polymerase, the reaction was performed for another hour a 37°C.

After assaying the result of transcription with agarose gel electrophoresis, the RNA was precipitated with LiCl and purified.

Precipitation and purification of RNA

After transcription 125 µL of saturated LiCl solution (Ambion) was added to 100 µL of reaction. After addition of 150 µL of Rnase-free H_2O (Ambion) the mixes were incubated at -80°C for 1h and pelleted in a cooled table-top centrifuge (25 min, 20000 g at 4°C). The pellets were washed in 70% ethanol (-20°C) and pelleted again as before. The pellets from the second centrifugation were dried for 5 min and resuspended into Rnase-free H_2O to a mass concentration of ~800 ng/ µL.

Agarose gel electrophoresis

For visualization, DNA and RNA samples were analysed by agarose gel electrophoresis. Gels were prepared with 1.0-1.2% agarose in 1× TAE buffer (40 mM Tris/HCl pH 8.0, 20 mM acetic acid, 1 mM EDTA). DNA and RNA samples were mixed with 6x Gel Loading Dye (NEB) and 2x Loading Dye (NEB) respectively and mixed with GelRed™ (Biotum) according to the manufacturer's recommendations. The 100 bp and 1 kb DNA ladder Plus from NEB were used for size comparison. Gels were run at 120 V for 20 min using the PerfectBlue Gel system Mini (Peqlab).

Purification of canine SRP

Canine SRP used in glycosylation assays was purified from canine pancreatic rough ER membranes by a high salt wash followed by gel filtration chromatography and ion exchange chromatography. Canine SRP used for sample preparation was additionally purified by gradient ultracentrifugation.

First, canine pancreatic rough ER membranes (roughly 40,000 Eq in 9 mL, 4.3Eq/ µL) were thawed in a cold water bath. These membranes were decanted into a beaker and the volume was adjusted to 50 mL with 41 mL of RM buffer (50 mM Hepes/KOH 7.5, 50 mM KOAc/HAc 7.5, 2 mM Mg(OAc)2, 1 mM DTT, 250 mM Sucrose). To increase salt concentration, 25 mL of HS buffer (1.5 M KOAc/HAc 7.5, 1 M $Mg(OAc)_2$) were added slowly, with swirling. After a 20 min incubation on ice with occasional swirling, the membranes were removed from the solution by ultracentrifugation (1 h, 32.000 rpm, at 4°C in a Ti 45 rotor) over a sucrose cushion (SC) (50 mM Hepes/KOH 7.5, 500 mM KOAc/HAc 7.5, 5 mM Mg(OAc)2, 1 mM DTT, 500 mM Sucrose). The supernatant, now enriched in SRP was subjected to another ultracentrifugation step (75 min, 65.000 rpm at 4°C in a Ti70 rotor) over SC in order to remove ribosomes. The supernatant of this step was concentrated in UltraCell 100k protein concentrators (Amicon) according to the manucfacturer's instructions to a volume of 2 mL.

SRP was purified from this sample on the Äkta system over a 26/60 S200 Sepharose gel filtration column (GE Healthcare) in a gel filtration buffer (GF buffer) (50 mM Hepes/KOH 7.5, 250 mM KOAc/HAc 7.5, 2.5 mM Mg(OAc)2, 2 mM DTT, 0.01% Nikkol). The fractions enriched for SRP were identified by a large peak in A260 absorption indicating presence of RNA. These fractions were further analysed by SDS-PAGE and fractions where protein bands characteristic of SRP could be identified were pooled. For further purification as well as enrichment the pooled fractions were bound to a 5 mL HF DEAE column (GE Healthcare), washed in 25 mL GF buffer followed by 25 mL of washing buffer (WB) (50 mM Hepes/KOH 7.5, 350 mM KOAc/HAc 7.5, 3.5 mM Mg(OAc)2, 1 mM DTT, 0.01% Nikkol) and eluted with 25 mL of elution buffer (50 mM Hepes/KOH 7.5, 750 mM KOAc/HAc 7.5, 6 mM Mg(OAc)2, 1 mM DTT, 0.01% Nikkol). Absorbtion at the 260 nm wavelength was monitored and peak fractions were collected and

tested for substrate targeting activity as observed by an increase in glycosylation efficiency. The active fraction was aliquoted, frozen in N_2(l) and stored at -80°C for further use.

Purification of canine PKRM

Puromycin and high salt treated rough ER membranes (PKRM) were prepared from canine pancreatic rough ER membranes (B. Dobberstein). The rough ER membranes were thawed in a water bath (RT) and diluted with RM-buffer (50 mM Hepes/KOH pH 7.5, 250 mM Sucrose, 1 mM DTT, 1 Pill/µL) to a concentration of 1 Eq/µL. KOAc/HAc (pH 7.5) was than added with stirring to a concentration of 150 mM. After that $Mg(OAc)_2$, DTT, Pill protease inhibitor mix (Roche) and GTP were added to concentrations of 5 mM, 1 mM, 10 pill/mL and 1 mM respectively. The mix was then homogenized by mixing 3× in a 7 mL dounce homogenizer with a loose pestle. Following homogenization, puromycin was added to a final concentration of 1 mM with stirring. The mix was incubated for 1 h at 4°C followed by 15 min at 37°C and 15 min at room temperature. Following incubation the mix was transferred into a TLA 110 tube and spun for 30 min at 100000 rpm in a Beckman TLA110 rotor at 2°C to remove the puromycin.

Following pelleting the membranes were re-suspended into buffer 1 (50 mM Hepes/KOH pH 7.6, 15 mM $Mg(OAc)_2$, 2 mM DTT, 500 mM Sucrose, Pill/µL, 800 mM $CsCl_2$) to a volume of 550 µL and mixed with buffer 2 (50 mM Hepes/KOH pH 7.6, 15 mM $Mg(OAc)_2$, 2 mM DTT, 2M Sucrose, Pill/µL, 800 mM $CsCl_2$) to a final volume of 950 µL. This mix was then underlayed with 1 mL of buffer 3 (50 mM Hepes/KOH pH 7.6, 15 mM $Mg(OAc)_2$, 2 mM DTT, 800 mM Sucrose, Pill/µL, 700 mM $CsCl_2$), overlayed with 800 µL of buffer 6 (50 mM Hepes/KOH pH 7.6, 2 mM DTT, 250 mM Sucrose, Pill/µL) and subjected to centrifugation for 1h at 100000 rpm in a Beckman TLA110 rotor at 20°C. The membranes appeared as a white layer in the upper third of the tube, which was collected by a pippete, diluted with three volumes of buffer 4 (50 mM Hepes/KOH pH 7.6, 3 mM $Mg(OAc)_2$, 2 mM DTT, 1 Pill/iL, 1 mM EDTA) and pelleted for 20 min at 100000 rpm in a TLA110 rotor at 2°C. The membrane pellet was resuspended in 4 mL of buffer 5 (50 mM Hepes/KOH pH 7.6, 3 mM $Mg(OAc)_2$, 250 mM sucrose 2 mM DTT, 1 Pill/iL, 1 mM EDTA) and pelleted again using the same centrifugation parameters. The membranes were resuspended in 4 mL of buffer 6 and pelleted again under the same conditions. The

step was repeated once more. The membranes were finally resuspended in buffer 6 to a final concentration of 1.8 Eq/iL, aliquoted into 20 iL aliquots, shock-frozen in N_2(l) and stored at -80°C.

Preparation of the wheat germ extract

The wheat germ extract for the eukaryotic translation system was prepared from wheat embryos (kindly donated by Rosenmühle). The embryos were first washed in a 100:6 mix of chloroform with cyclohexane. The embryos that floated in this mix were collected and dried for 2h. The wheat germs were grinded in a N_2(l) cooled mortar. Each batch of 2.5 g of ground wheat germ was mixed with 2×homogenization buffer (40 mM Hepes pH 7.6, 100 mM KOAc, 5 mM $(MgOAc)_2$, 2 mM $CaCl_2$, 4 mM DTT, 0.15 Pill/mL, 0.4 U/mL RNasin) and centrifuged for 20 min at 4°C at 20000 rpm in an SS34 rotor followed by a second centrifugation step in a TLA110 rotor for 30 min at 30000 rpm at 4°C. The supernatant was then purified over a PD10 column (GE Healthcare) in 1×homogenization buffer. Fractions were collected, aliquoted, shock-frozen in N_2(l) and stored at -80°C.

Translation in the wheat germ extract *in vitro* translation system

In vitro translation was carried out in the self-made wheat germ translation system. In a typical reaction 450 µL of the wheat germ extract was mixed with 90 µL of 10× buffer A (140 mM Hepes pH7.6, 750 mM KOAc pH7.6, 12.5 $Mg(OAc)_2$, 20 mM DTT), 90 µL of 10× buffer B (12.5 mM ATP, 2.5 mM GTP, 160 mM creatine phosphate, 4.5 mg/mL creatine kinase), 90 µL of complete AA mix (Promega) and 36 µL of Rnasin (Promega) Rnase inhibitor. After addition of the inhibitor, 100-150 µg of mRNA was added. To the appropriate reactions, 72 eq of PKRM and 90 pmol of dog pancreas SRP were added and reactions were incubated for 5 min at 30 °C followed by 90 min at 25 °C.

Purification of ribosome-nascent chain (RNC) complexes

Following translation the concentration of KOAc in the reaction mix was increased to 650 mM and incubated for 30 min 25 °C. Membranes were isolated by pelleting through a sucrose cushion (0.5 M sucrose, 30 mM Hepes/KOH pH 7.6, 10 mM $Mg(OAc)_2$, 500 mM KOAC/HAc pH 7.6, 1 mM DTT, protease inhibitors) in a TLA 110 rotor for 10 min at 4172*g* at 4°C and dissolved in binding buffer (10 mM $Mg(OAc)_2$, 100 mM KOAC/HAc 7.6, 30 mM Hepes/KOH 7.6, 0.5 % Digitonin, 1 mM DTT, protease inhibitors) for 45 min at 25 °C. The mix was then applied to streptavidin-coated beads (GE Healthcare) and bound for 20 minutes at 25 °C followed by 1h at 4 °C. During purification of LepM the beads were washed two times for 10 min in 1 ml washing buffer (30 mM Hepes/KOH pH 7.6, 10 m_M Mg(OAc)2, 100 mM KOAC/HAc pH 7.6, 0.3 % Digitonin, 1 mM DTT, protease inhibitors) , followed by a 10 min wash in high salt buffer (30 mM Hepes/KOH pH 7.6, 10 m_M Mg(OAc)2, 500 mM KOAC/HAc pH 7.6, 0.3 % Digitonin, 1 mM DTT, protease inhibitors) and again two times for 10 min in 1 ml washing buffer. For purification of LepT the beads were washed five times for 10 min in 1 ml washing buffer. Elution was done by washing the beads in elution buffer (30 mM Hepes/KOH pH 7.6, 10 m_M Mg(OAc)2, 100 mM KOAC/HAc pH 7.6, 0.3 % Digitonin, 1 mM DTT, 5 mM desthiobiotin) for 20 min at 25°C. The eluted ribosomes were pelleted through a sucrose cushion (1 M sucrose, 30 mM Hepes/KOH pH 7.6, 10 m_M Mg(OAc)2, 500 mM KOAC/HAc pH 7.6, 0.5 % Digitonin, 1 mM DTT,) in a TLA 110 rotor for 1h *at* 417200g at 4°C. The purified PCC-RNC complexes were resuspended in grid buffer (30 mM Hepes/KOH 7.6, 10 m_M $Mg(OAc)_2$, 180 mM KOAC/HAc pH 7.6, 0.3 % Digitonin, 1 mM DTT).

Precipitation of proteins

Some protein samples were precipitated for SDS-PAGE by trichloroacetic acid (TCA). The samples were adjusted to a volume of 1 mL by the addition of cold, autoclaved, deionized water. To facilitate protein denaturation, 100 µL of 15% sodiumdeoxycholate was added to the sample. For precipitation of proteins, 100 µL of 72% TCA was added to the sample. The samples were thoroughly mixed using the vortex stirrer and left to incubate on ice for 20 min. The precipitated proteins were collected by centrifugation in a cooled table-top centrifuge (20 min, 20000 g at 4°C), washed by vortexing in 1 mL of acetone (-20°C) and again collected by centrifugation (10 min, 20000 g at 4°C). The pellets were then air-dried for 10 min and resuspended in 1× SDS PAGE sample buffer.

Endoglycosydase H treatment

To confirm that the observed shift in protein size was indeed due to N-linked glycosylation, samples were treated with endoglycosydase H (NEB) following instructions by the manufacturer.

Overexpression and purification of Amb-suppressor tRNA charged with pBpA

Fresh BL21 cells were transformed with plasmid. Overnight precultures were directly inoculated with the recovered bacteria (for cca 5 mL of preculture 4 mL of LB and 1mL of recovered cells). A short growth curve was performed to get the cells at mid log-phase (OD_{600} = 0.4-0.5). Cultures were induced with 2g arabinose for 1L of culture for 2h (200 mg/ 100 ml) then p-benzoylphenylalanine (pBpA) was added. pBpA was dissolved in 1M NaOH and diluted with H_2O and further added to the LB-medium to a final concentration in of 0.2-1 mM after induction with arabinose. The cultures were incubated at 30 ºC for 2h. After that time, 5 mL post-induction tRNA samples were collected into 15 mL falcon tubes, spun down (rotanta, 20 min, 20000 rcf) and stored at -20 ºC.

Frozen pellets from 5mL of culture were re-suspended in 5ml cold sodium acetate (0.3M, pH 4.5), 10 mM EDTA 7.5 mL mL phenol: chloroform (roti-aqua-phenol: chloroform 50:50) was added to the resuspension. The falcon tubes were stirred for 30 min with the cold-room vortex-machine on max. Samples were centrifuged 4500 rpm, 30 min, 4ºC in rotanta. The top layer (aqueous phase) was transfered to new tubes and the phenol extraction was repeated by adding 1.5 vol roti-aqua-phenol:chloroform and spinning for 30 minutes, 4ºC, 4500rpm (rotanta) and collecting the aqueous phase to a fresh falcon. LiCl precipitation was performed (½ volume of LiCl solution, incubation at -80ºC for 1h, spin 25 min 14 krpm in cooled table top at 4 ºC); The supernatant (~5 mL) was transferred to another tube. Addition of Vol. of IPA and cca. 30 min at -80 ºC caused another fraction of tRNA to precipitate. The pellets were washed with ice cold 70% EtOH, spun again and resuspended in H_2O.

Cross-linking experiments

For cross-linking experiments, the purified suppressor tRNA was tritrated into the in vitro translation mix before start of translation. After ribosome pelleting, purified RNCs were exposed to UVC for 30 min on ice.

SDS-polyacrylamide gel electrophoresis

For protein separation by size the method of sodiumdodecylsulphate-polyacrylamide gel electrophoresis (SDS-PAGE) was used. Protein samples were first mixed with 4× SDS-PAGE sample buffer (200 mM Tris pH 6.8, 8% (w/v) SDS, 0.4% (w/v) bromphenol blue, 40% (v/v) glycerol, 400 mM DTT). The final size of the sample was ~10 µL The samples were then heated to 50°C for 10 min and loaded onto a polyacrylamide gel.

NuPAGE® gradient gels (4-12% acrylamide) supplied by Life Technologies were used for electrophoresis. The gels were run according to instructions by the manufacturer, at 45 mA for 15 min and at 60 mA for 1h 20 min. Gels were either stained for protein using the SimplyBlue^{TM} SafeStain (Invitrogen) according to the manufacturer's protocol or used for western blot analysis.

Western blot analysis

Different components of the RNC-Sec61 complex were identified by western blot analysis. For this purpose, proteins that were separated by size were transferred onto a PVDF (Millipore) membrane for HA-tag detection or onto a nitrocellulose membrane for detection of Sec61α. Prior to use, PVDF membranes had to be activated by incubation in 100% methanol. Both nitrocellulose and activated PVDF membranes have a strong and unspecific affinity for binding proteins. In both cases transfer was performed in the wet blot apparatus (Life Technologies) according to the instructions of the manufacturer.

Blotted membranes were stained by a solution containing amido-black (7.5% HOAc, 20% EtOH, 0.1 % amido-black) and destained by the same solution without amido-black. Stained membranes were washed in water and the acidic pH of the stain/destain solutions was neutralized by a wash in 1× TBS buffer (50 mM Tris-Cl, pH 7.5, 150 mM NaCl). Membranes were then incubated for 1h in 5% milk dissolved in TBS to reduce the unspecific affinities for binding protein.

For detection of HA-tagged substrates, PVDF membranes were incubated in a 1:500 solution of goat anti-HA antibody (Santa Cruz) in 1× TBS containing 2% bovine serum albumin (BSA) at 4°C over night. The membranes were then washed in 1× TBS, 1× TBS-T (50 mM Tris-Cl, pH 7.5, 150 mM NaCl, 0.05% Tween 20) and, again 1× TBS, for 10 min each time. For detection, the decorated membranes were incubated in a 5% solution of milk in TBS containing a rabbit-anti goat horseradish peroxidase (HRP) conjugated antibody diluted 1:5000 for 1h at room temperature. Thus decorated membranes were again washed in 1× TBS, 1× TBS-T and 1× TBS for 10 min each time. The proteins were detected using the ECL solution (Thermo Scientific) and exposure to LucentBlue X-ray film (Advansta)

For detection of Sec61, nitrocellulose membranes were incubated in a 5% solution of milk in TBS-T containing rabbit anti-sec61antibody (provided by R. Gilmore and E. Mandon) dissolved 1:2000 at 4°C over night. The membranes were then washed three times in 1× TBS-T for 10 min each time. For detection, the decorated membranes were incubated in a 5% solution of milk in TBS-T containing a goat-anti rabbit horseradish

peroxidase (HRP) conjugated antibody diluted 1:4000 for 1h at room temperature. The protein was detected using ECL as described.

Mass spectrometry

Mass spectrometry was performed by S. Pfeffer and F. Förster on the LepT sample in order to characterize its protein content.

Single particle Cryo-electron microscopy and initial processing

For Cryo-electron microscopy, freshly prepared samples were applied to Quantifoil grids pre-coated with 2 nm carbon on top. The grids were prepared using a Vitrobot Mark IV (FEI Company). Data were collected on a Titan Krios TEM (FEI Company) under low-dose conditions at 200 keV and magnification of ×148,721 at the plane of the CCD using a TemCam-F416 CMOS camera (TVIPS GmbH) resulting in an image pixel size of 1.049 Å/pixel on the object scale. For automated data collection the EM-TOOLS software was used and data were collected in a defocus range of 1.3 - 4.0 µm. Following defocus determination and generation of power spectra (SPIDER), selection of micrographs was performed by manual inspection for drift, astigmatism and particle density in WEB (Frank et al. 1996). Based on these criteria 9805 micrographs (6119 for LepT, 3686 for LepM) were selected for Single Particle Analysis and 3D reconstruction. Automated particle selection was performed using the program Signature which was followed by a second automated particle classification step using the MAPPOS software.

Initial alignment and refinement

Datasets for LepT (487470 particles) and LepM (298491 particles) were processed individually. In both datasets sets of three pixels in images were initially summated into one (3×decimated) to facilitate computational processing. Initial alignment was performed using a *Triticum aestivum* ribosome volume solved to 5.5 Å resolution (Armache et al. 2010). Following initial alignment and back projection, refinement was performed until no more improvement in resolution and map quality was observed. Alignment could be further improved by sorting. This was done in two phases. In the first phase, termed 'Supervised sorting', performed on 3×decimated datasets, several different references were offered and the particles were allowed to align to any of them for several refinement rounds. After additional refinement of datasets sorted in this way, the datasets were converted into 2×decimated datasets i.e. two pixels were summated into one. After a few more rounds of refinement, very similar references were offered for sorting allowing differences to emerge through a stochastic process. This was termed 'Unsupervised sorting' (*For a detailed description of the two sorting methods, check the next paragraph*).

Volumes that were created by sorting were used in a repeated step of initial alignment and refinement followed by repeated sorting. After no more differences could be sorted out, the homogenous datasets were further refined, converted to the undecimated state and subjected to several additional rounds of refinement.

Dataset sorting and electron density map refinement

Processing included computational sorting of collected particles. The sorting process was performed after initial alignment and refinement steps in two phases: an iterative supervised sorting step was followed by several steps of unsupervised sorting. In the supervised sorting step the datasets were sorted for the presence of Sec61-complex, P-site tRNA and 'non-particles'. In both datasets, 3D maps were obtained which showed the enriched Sec61 complex but lacked any peptidyl-tRNA density. These datasets were merged and further refined as a single 'Idle' dataset. After several rounds of refinement the datasets were changed from 3×decimated to 2×decimated (two pixels summated into one). These datasets were then subjected to unsupervised sorting: for each dataset volumes from two refinement rounds were selected as references and sorted against each other. After several rounds of sorting (5-10) differences in the reference volumes became apparent and different conformational states of the ribosome could be separated. The process was performed until no more states could be sorted out. During this step, a sub-dataset of the LepT dataset was sorted out. This sub-dataset contained large patches of extra electron density on the part of the volume assigned to Sec61. This extra density was shown to belong OST and TRAP by mass spectrometry and the dataset was correspondingly names 'OST'. Each of these four datasets: LepM (30455 particles), LepT (53248 particles), Idle (162655 particles) and OST (15705 particles) was subjected to further rounds of refinement until no more improvements in resolution and map quality could be observed. Finally, decimation was changed to 'undecimated' (each pixel treated individually) and refinement continued until final resolutions of 6.9 Å (Idle), 7.4 Å (LepT), 7.8 Å (LepM) and 9.3 Å (OST) were reached.

Modelling

Electron densities obtained by single particle Cryo-EM were used for building molecular models. For that purpose a homology model of the canine Sec61-complex was built based on the structure of *M. jannaschii* SecYEβ (PDB entry 1rhz) using the programs HHPRED and MODELLER (Sali & Blundell 1993). For the wheat germ (*T. Aestivum*) 80S ribosome, an existing molecular model (PDB entries 3iz6, 3iz7, 3iz9 and 3izr)(Armache) based on the crystal structures of the *S. cerevisiae* 80S ribosome (PDB entries 3u5b, 3u5c, 3u5d and 3u5e) and the *Tetrahymena thermophila* small 40S ribosomal subunit (PDB entries 2xzm, 2xzn).was used for model building.

These initial models were placed into density using UCSF Chimera (Pettersen et al. 2004). Positions of α-helices and loops were manually adjusted in Coot (Emsley et al. 2010). Further correction of clashes and minimization of potential energy was performed in VMD (Humphrey et al. 1996) and MDFF (Trabuco et al. 2008).

Results

Lep-based constructs can be efficiently translated and targeted in a wheat germ expression system supplemented with canine SRP and PKRMs

The goal of this work was to obtain structures of the translocon engaging a hydrophilic peptide segment and a membrane inserting helix. To this end, a substrate was chosen which has previously been biochemically well characterized.

The leader peptidase (Lep) is a membrane protein from *E. coli* which contains two transmembrane domains followed by a long periplasmic domain (P2). A part of this domain had been chosen as a site for extensive mutagenesis experiments in previous research and will thus be referred to as the variable region. In these experiments, two glycosylation sites were engineered in the P2 domain: one before and one after the variable region (Fig. 14). Upon expression in eukaryotic translation systems and in presence of canine pancreatic membranes, the site preceding the variable region was exposed to the glycosylation machinery of the ER. Glycosylation of the second site depended on the propensity of the variable region for secretion. If the variable region was efficiently secreted, the second site would be exposed to the OST and glycosylated. In the case of membrane insertion, the site would remain outside of the ER and remain unmodified.

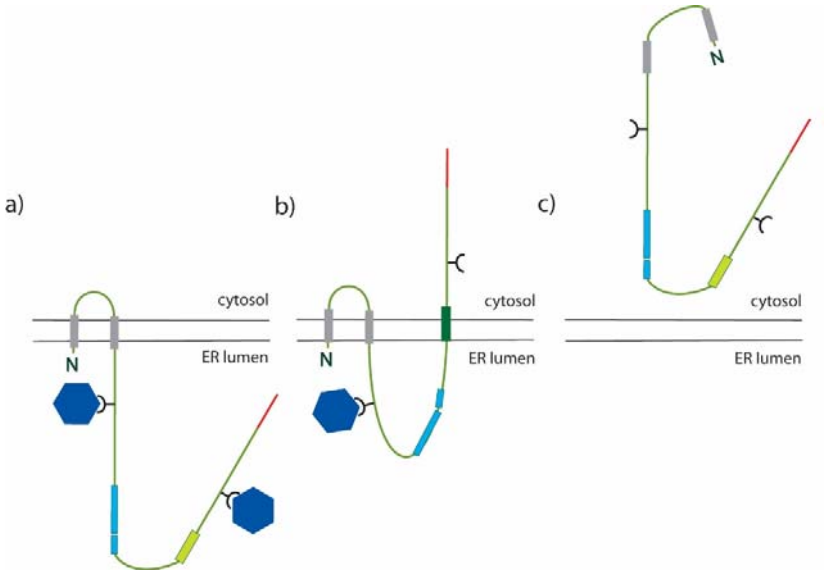

Figure 14: Scheme for Lep-based substrate glycosylation.

Depending on the properties of the variable segment, it is either a) secreted or b) inserted into the membrane. In the former case, the upstream glycosylation site is accessible to the OST resulting in an additional glycosylation while in the latter the site remains unmodified. c) In case of improper targeting, neither glycosylation site will be modified.

For this work two variations of Lep were chosen, one with a secretion prone and one with an inserting variable region. In the original publication these clones were named Lep93 and Lep62 respectively. In this work they were renamed into LepT (translocating) and LepM (membrane inserting). At the 3'-end of each clone, a CMV stalling sequence was engineered to obtain efficient stalling. A hemagglutinin (HA) tag for detection by western blot and a streptavidin (Strep) tag for affinity purification were also engineered into the unstructured loop between the second transmembrane helix and the variable region (Fig. 15).

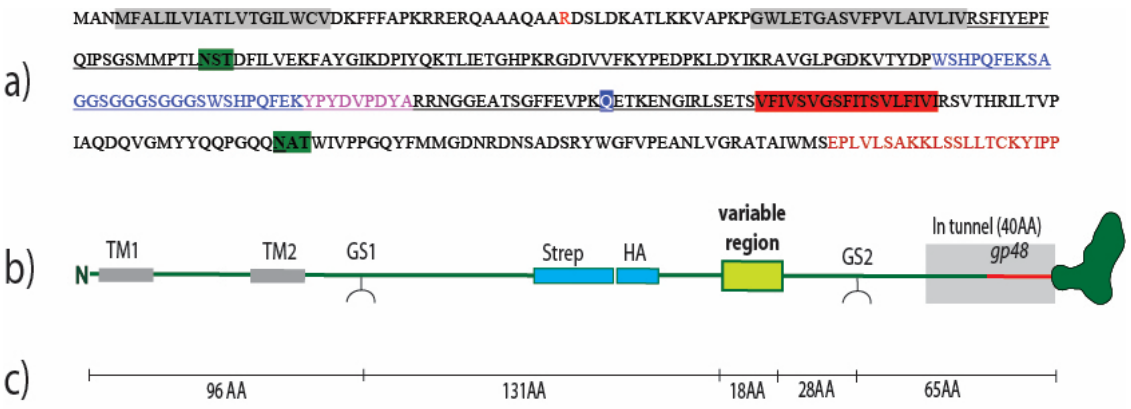

Figure 15: Overview of the Lep-constructs.

a) Annotated sequence and b) scheme of the Lep-substrate. Lengths of different segments in terms of amino acid numbers are given c).

The protein was then expressed in the wheat germ *in vitro* expression system in the presence of purified canine SRP and puromycin and high salt treated canine pancreatic membranes (PKRMs). This system which has been discovered several decades ago (Goldman & Blobel 1981; Walter & Blobel 1983; Erickson & Blobel 1983; Schechter et al. 1979; Audigier et al. 1987; Roberts & Paterson 1973) shows high efficiency (high ratio of glycosylated to non–glycosylated peptides) as well as high specificity; in the absence of SRP, practically no substrate was glycosylated (Fig. 16).

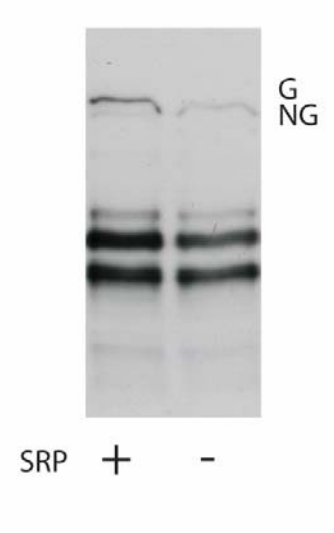

Figure 16: Dependence of glycosylation on the presence of SRP.
Size shift in the peptidyl-tRNA band for LepM between glycosylated (left) and unglycosylated (right) samples. Both samples contain PKRM. The only difference is addition of SRP to the left sample. Lower bands are different degradation stages of the free peptyde.

Aside from targeting itself, proper recognition of translocated and inserted domains as well as proper orientation of transmembrane helices in the lipid bilayer are necessary for a functioning secretory pathway. To check for proper orientation of the variable region of Lep, two N–linked glycosylation sites were introduced: one in the loop N–terminal of the helix and the second one C–terminal to the helix. If a helix is inserted into the membrane in a N^{in} C^{out} conformation as happens in case of the LepM construct, a shift due to a single glycosylation event should be observed irrespective of stalling. In the case of the variable region of LepT which is an unfolded, secretory substrate a shift due to a single glycosylation should be observed in a stalled substrate while a larger shift corresponding to two glycosyl moieties should be observed in the released peptide. This was confirmed in translation reactions treated with puromycin in order to release the substrate.

That the observed shift in size was indeed due to glycosylation was confirmed by treatment of the glycosylated substrate with endoglycosidase H (EndoH). A downward shift in the apparent size of the peptide on SDS–PAGE showed loss of glycosylation upon EndoH treatment of the samples (Fig. 17).

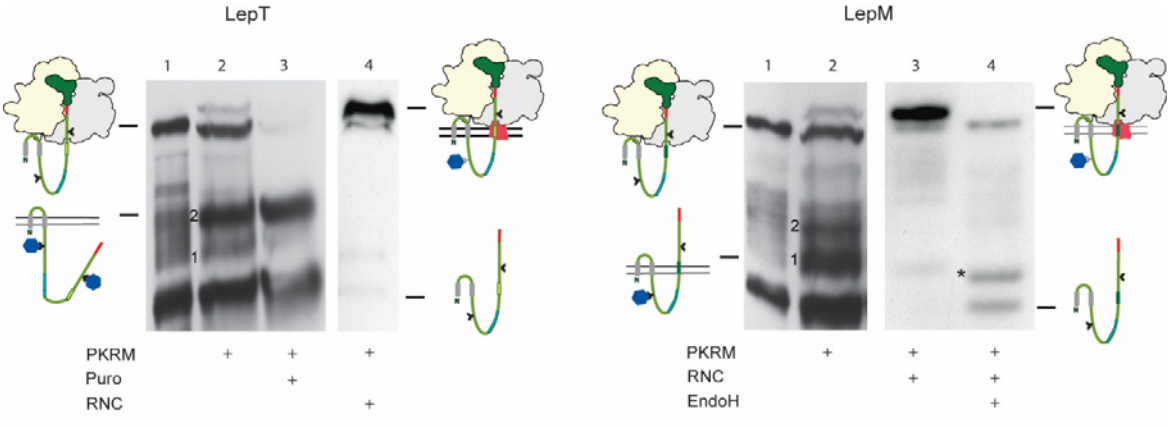

Figure 17: Analysis and purification of LepT and LepM intermediates.

Western blots probing for the haemagglutinin tag indicate (glycosylated) peptidyl-tRNA, unglycosylated as well as mono- and bi-glycosylated free peptides as illustrated in schematic drawings. The extra glycosylation bands disappear upon EndoH treatment. An EndoH background band is indicated by an asterisk.

The co–translationally produced RNC–Sec61 complex can be purified in a functionally locked state

For structural analysis the Lep–RNCs were co–purified with the Sec61 complex from translation reactions. Behavior of the complex during purification was tracked by western blotting using antibodies specific for the HA–tag introduced into the Lep–substrates and for Sec61α.

It can be seen in Fig. 18 that the two components appeared in the same fractions during the affinity purification step.

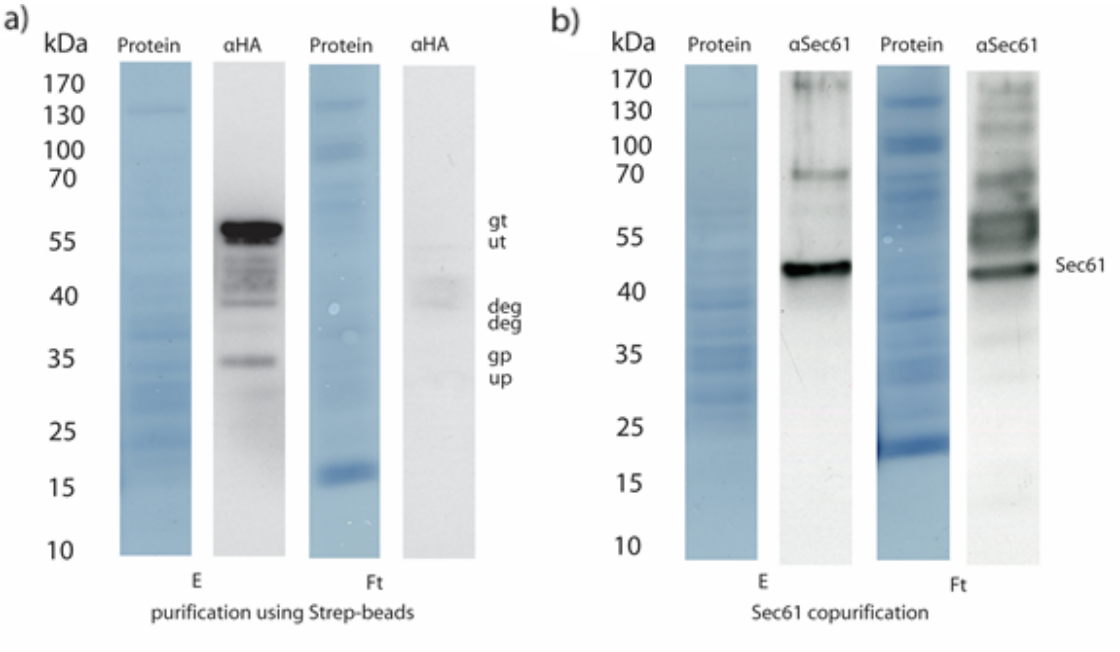

Figure 18: Western blot analysis for co-purification of HA-tagged Lep and Sec61.
Showing western blots (black and white lanes) and corresponding membranes (blue lanes) for elution (E) and flow through (Ft) fractions during RNC-Sec61 purification. a) shows western blots for HA tag while b) shows western blots for Sec61. While some Sec61 washes out with idle ribosomes in the flow-through fraction, a large part co-elutes with the RNC-s.

The ribosome was kept in a translationally stalled state by the cytomegalovirus stalling sequence. This mechanism of stalling is very strong and insures a high yield of stable RNCs.

Three homogenous states of the ribosome were separated by sorting of the LepT sample

Despite best efforts, biochemical preparations of samples for Cryo–EM are a heterogeneous mix of ribosomes in different states (Fig. 19). In order to provide a sensible structure, the LepT containing dataset had to be sorted for the presence or absence of tRNA in the P-site, for presence or absence of the translocon as well as the ratcheted state.

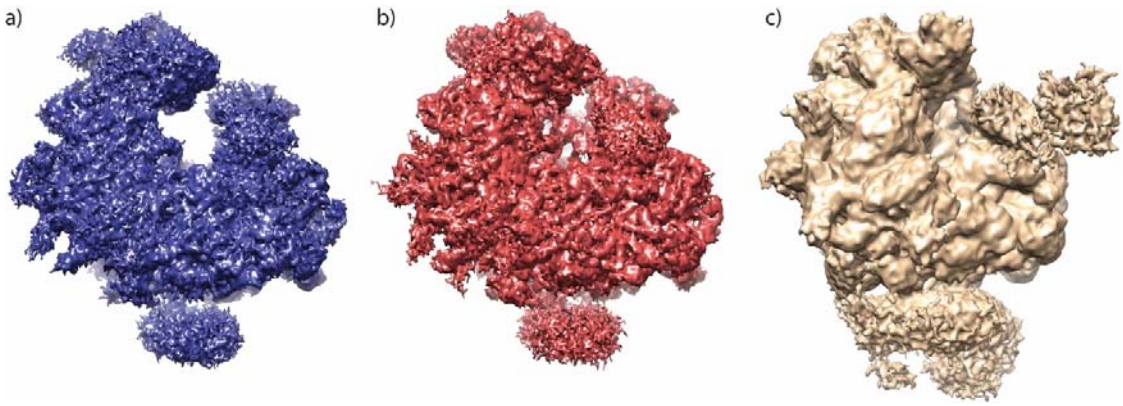

Figure 19: The three sub-datasets that could be sorted from the LepT containing dataset.
a) Idle ribosome b) programmed ribosome c) programmed ribosome with additional densities in around the translocon micelle

The sorting for presence and absence of different factors is performed using references resembling the desired state, so called supervised sorting. To sort for different states of the ribosome, so called unsupervised sorting was performed.

During the supervised sorting step, out of a total number of 487,470 particles a large sub–population of 78187 non-programmed ribosomes was obtained. These ribosomes were subjected to additional steps of unsupervised sorting and the homogenous dataset was merged with a similarly obtained dataset from the LepM sample and further refined.

In the course of unsupervised sorting, a sub–dataset with additional density was sorted out. This dataset consisted of 15705 particles and was later refined to reveal the structure of OST and TRAP bound to Sec61.

A highly homogenous dataset of 53,248 particles was used in the LepT-RNC reconstruction.

Two homogeneous states of the ribosome separated by sorting of the LepM sample

Similarly to the LepT sample, the dataset obtained from the LepM preparation was subjected to several steps of supervised and unsupervised sorting. Out of an initial dataset consisting of 298,491 particles, supervised sorting produced a large sub–population of 84,468 non programmed ribosomes (Fig. 20 a). After additional steps of unsupervised sorting the dataset was merged with an analogous dataset obtained from LepT and further refined to obtain the idle dataset.

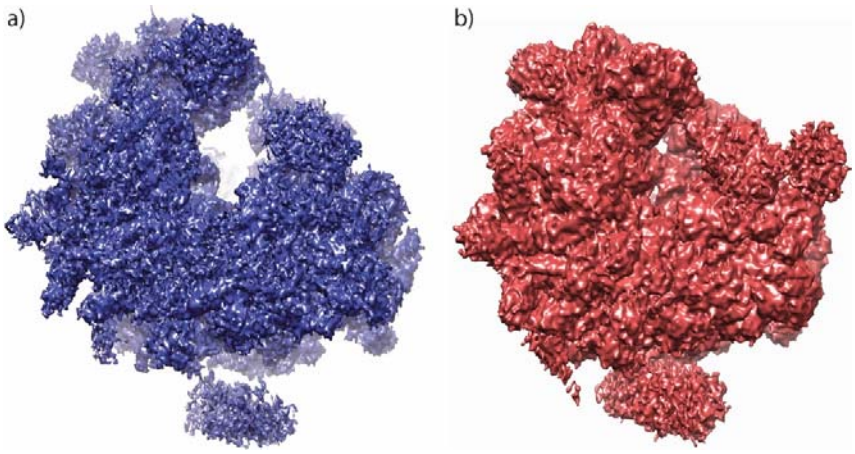

Figure 20: The two sub-datasets that could be sorted from the LepM containing dataset.
a) idle ribosome b) programmed ribosome

The population of programmed ribosomes was also subjected to unsupervised refinement. In this way, several ratcheted states of the ribosome were sorted out and a homogenous dataset of 30,455 particles programmed with LepM was obtained (Fig. 19 b) that could be further refined.

During the unsupervised sorting, no indication was observed that the population contains any particles with additional proteins bound to Sec61 complex. This is in contrast to the presence of OST and TRAP complexes in the LepT sample. It is not clear whether this difference is intrinsic to the substrate or comes from the difference in sample preparation procedures.

The Cryo–EM–structure of the idle ribosome–translocon complex

Sub–datasets of non–programmed ribosomes were sorted out from datasets for ribosomes translating sequences for either LepT or LepM. These sub–datasets were later sorted again for structural heterogeneity and presence of the translocon. This process generated homogenous sub–datasets that could be merged to produce a dataset of 162,655 particles that was further refined to a resolution of 6.9 Å (Fig. 21).

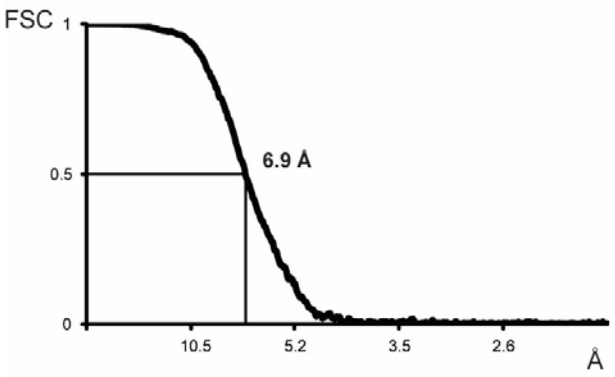

Figure 21: Resolution curve for the idle dataset

In the volume densities for the ribosome and the translocon can be clearly discerned. Within the translocon density two areas can be distinguished: a central area displaying tubular densities was assigned to protein while the surrounding area showed no identifiable elements. This area of very low density was surrounded by a shell–like mantle of higher density (Fig. 22).

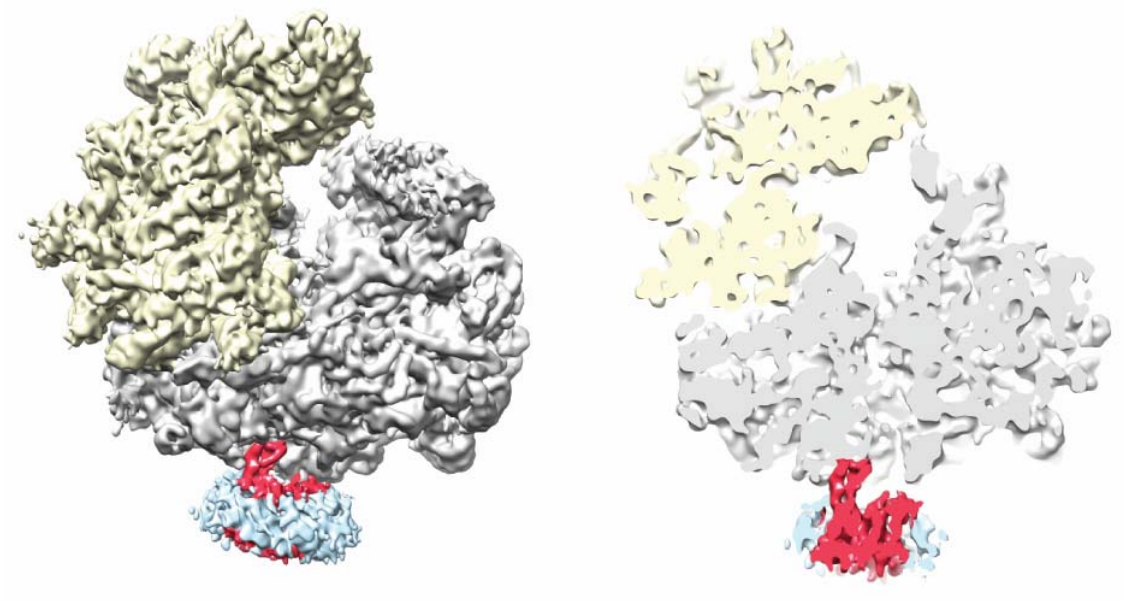

Figure 22: The density for the idle ribosome-Sec61 complex.

The small ribosomal sub-unit is yellow, the large sub-unit is gray, translocon density is red while the surrounding micelle is in light blue. In the cut-through view on the right it is shown that in addition to the absence of P-site tRNA, no extra density for the nascent chain can be observed in the ribosomal exit tunnel.

This configuration is characteristic of detergent micelles and was assigned as such. This micelle density was observed in all structures analyzed in this work. The relatively large size of the micelle is probably due to use of digitonin, a mild detergent which leaves a large number of fatty acids bound to the molecule (Becker et al. 2009).

The idle ribosome bound translocon is structurally similar to the *Methanococcus jannaschii* SecYEβ crystal structure: the lateral gate is closed (Fig. 23) and the central channel is partially obstructed by the plug helix and TM10.

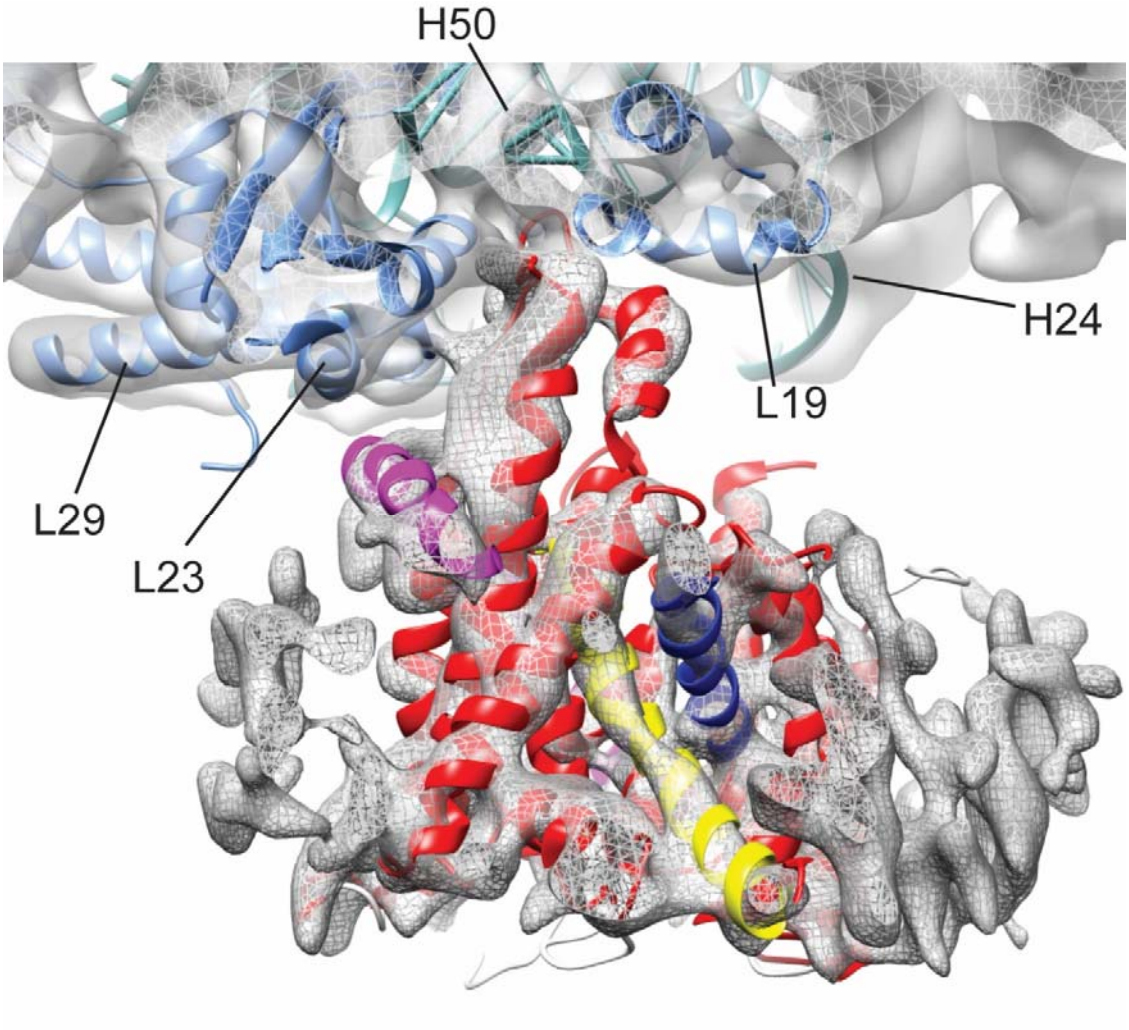

Figure 23: Model of the idle translocon is shown in the context of the electron density map and the model for the ribosome.
Surrounding micelle is visible.

The plug helix in the ribosome bound translocon is shifted by approximately 3.5E compared to the *M. jannaschii* translocon. This movement is somewhat compensated for by a shift and rotation in TM10. The physiological function of this movement is not clear but it might explain electrophysiological data indicating ion leakage of mammalian translocons upon binding of non–translating ribosomes (Simon & Blobel 1991). An alternative possibility would be that this conformation is intrinsic to the mammalian Sec61–complex and is not due to ribosome binding. As there is no crystal structure of a mammalian Sec61–complex available, this hypothesis cannot be dismissed. However, the

fact that no homology models take on this conformation as well as the aforementioned electrophysiological data would speak against it.

While the lateral gate of the translocon bound to an inactive ribosome is closed (Fig. 24), TM7 is shifted slightly toward the N–terminal half of the translocon. Although it is impossible to see movements of individual amino acid side–chains, these shifts in the plug, TM7 and TM10 do not seem to affect the area where these amino–acids are located and thus should not open the translocon significantly. It is possible however, that ribosome binding alone is partially responsible for priming the translocon for peptide secretion or insertion.

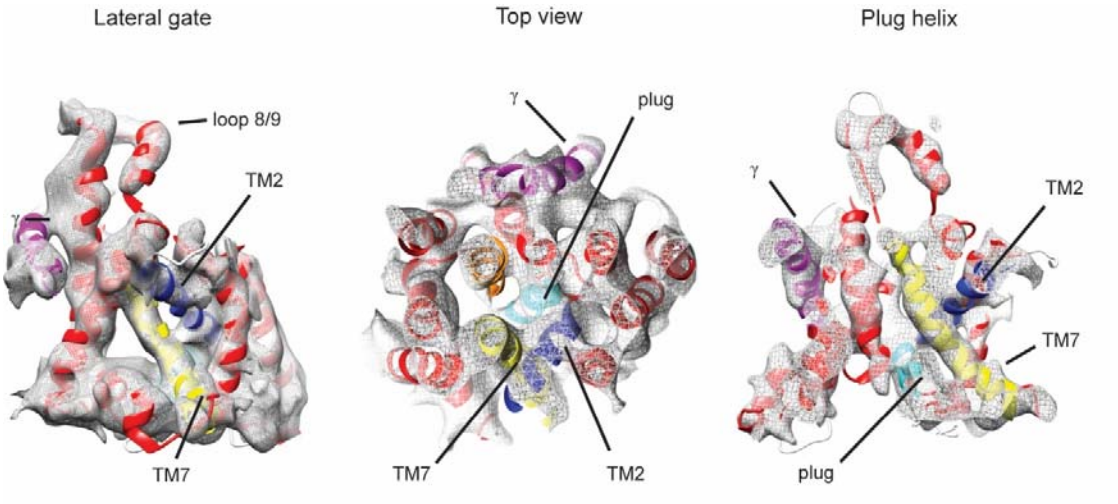

Figure 24: A close-up on the conformation of the idle translocon is shown.
The closed positions of the lateral gate (left) and of the central channel (center, right) are shown.

Validation of the model to density fit for the idle dataset

In order to examine to what extent the models that were built for the ribosome and the idle translocon fit the density, Fourier shell correlation analysis was performed between the expected densities generated from the models and the experimentally obtained densities (Fig. 25). Because of the usual difference in the quality of the density for the ribosome and its ligands, this procedure was performed for the translocon area separately from the rest of the ribosome. The measurements showed that the signal–to–noise ratio of 0.5 (i.e. 50%) was reached at 7.7 Å filtering for the model of the ribosome and 7.5 Å for the model of the translocon. Since a map at a resolution of 6.9 Å was used to build these models, this was judged to be an acceptable level of accuracy.

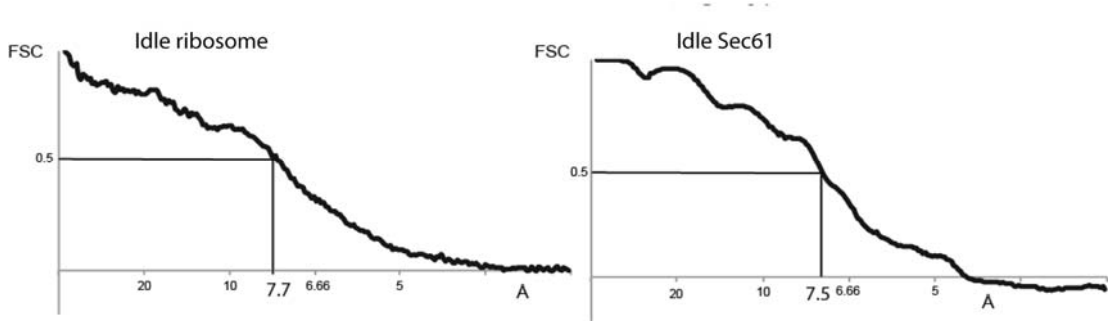

Figure 25: Model density fits for the models of the ribosome and the translocon for the idle dataset.

The Cryo–EM–structure of the translocon bound to a ribosome translating a secretory peptide

Structure of the translocon bound to a ribosome translating the secretory LepT sequence was refined to a resolution of 7.4 Å (Fig. 26).

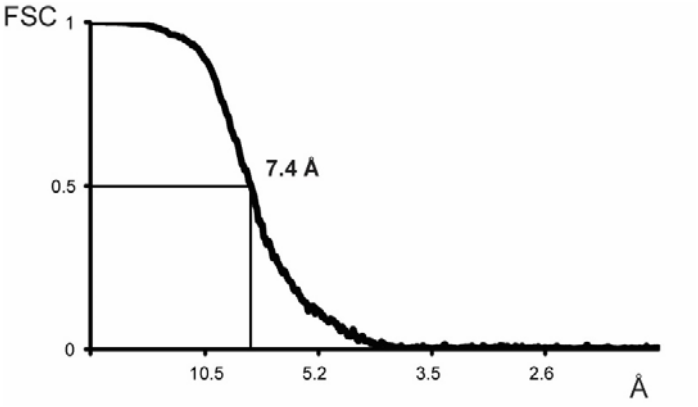

Figure 26: Resolution curve for the LepT dataset

The active state of the ribosome was obvious through the presence of a tRNA in the P–site. The characteristic density for the translocon complex surrounded by a thick lipid–detergent micelle was observed (Fig. 27).

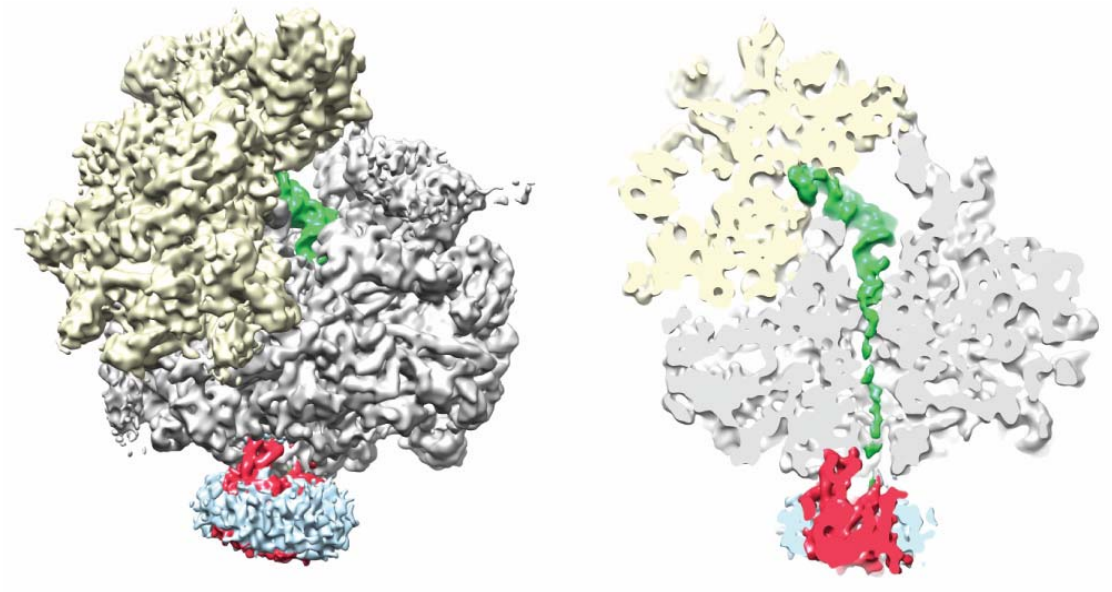

Figure 27: Density for the LepT Sec61-RNC.

The small ribosomal sub-unit is yellow, the large sub-unit is gray, the P-site tRNA is green, the translocon density is red while the surrounding micelle is in light blue. In the cut-through view on the right it is shown that in addition to the P-site tRNA, an extra density for the nascent chain can be observed in the ribosomal exit tunnel.

At this resolution it was impossible to detect the translocating peptide which was predicted to be unfolded but the conformational shifts in the translocon with respect to the idle molecule could be studied.

Conformation of the translocon in the act of peptide secretion mostly resembles the structure observed before by Becker et al. (Becker et al. 2009) The ribosomal contact sites in loops L6–7 and L8–9 remain in an unchanged conformation with respect to the idle structure. The lateral gate remains essentially closed with only a small movement in TM7 clearly visible (Fig. 28).

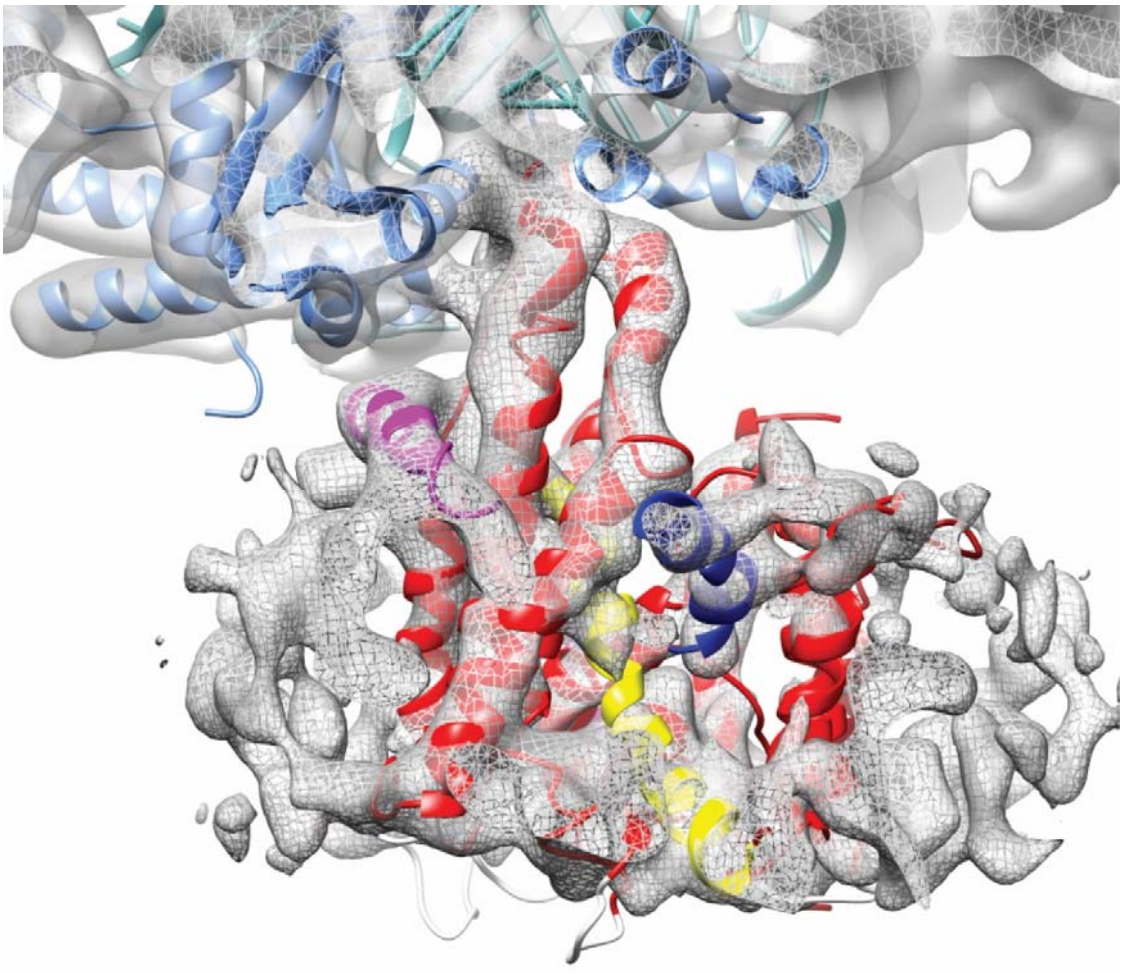

Figure 28: Model of the LepT-RNC translocon is shown in the context of the electron density map and the model for the ribosome.

Surrounding micelle is visible.

The plug helix has the same position as in the idle structure. The opening of the central channel is achieved through an outward movement of the lower part of TM10. This movement creates a central opening of sufficient diameter to allow for translocation of an extended peptide chain, even one with bulky side chains (Fig. 29).

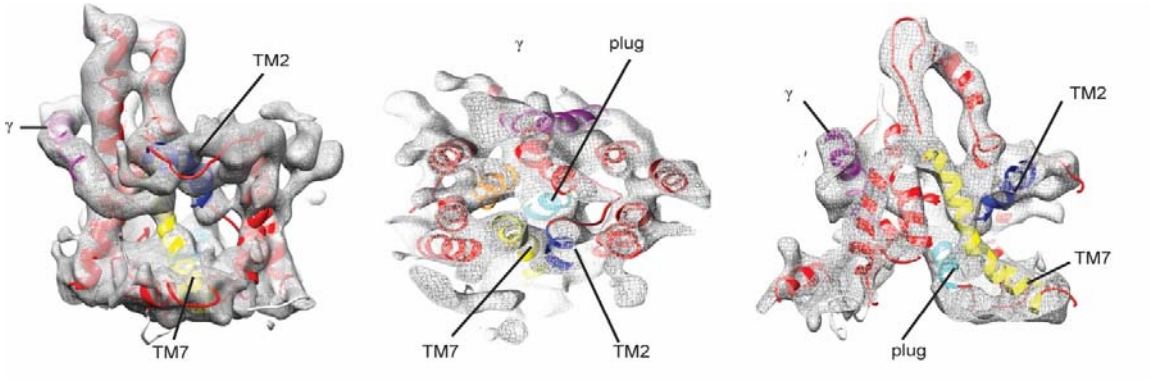

Figure 29: A close-up on the conformation of the LepT-RNC translocon is shown.
The closed position of the lateral gate (left) and the open position of the central channel (center, right) are shown.

A small but significant movement occurs by helices TM3 and TM4 accompanied by a much smaller movement of TM2. The role of this shift is not clear as it does not contribute to the opening of either the central channel or the lateral gate. The remaining helices of the N–terminal half of the molecule are not affected by this movement.

Based on the positions of pore ring residues on TM7 and TM10 seems likely that movements of these helices only partially affect the stability of the pore ring. This is in line with the proposed role of this ring to act as a barrier for ion leakage in protein secretion.

Altogether, the LepT engaged translocon is in a state where the lateral gate remains largely closed but a hydrophilic channel is opened in the center of the molecule. This general state was expected from the model suggested by previous crystal structures (Van den Berg et al. 2004). However, this structure shows this opening to originate mostly from a movement of TM10 and not the plug helix, as previously suggested.

Validation of the model to density fit for the LepT dataset

As for the idle dataset, it was examined to what extent the models that were built for the ribosome and the translocon fit the density by performing Fourier shell correlation analysis between the expected densities generated from the models and the experimentally obtained densities (Fig. 30). As in the case of the idle dataset this procedure was performed for the translocon area separately from the rest of the ribosome. The measurements showed that the signal–to–noise ratio of 0.5 (i.e. 50%) was reached at 7.6 Å filtering for the model of the ribosome and 7.5 Å for the model of the translocon. With a map at a resolution of 7.4 Å, this was judged to be an acceptable level of accuracy.

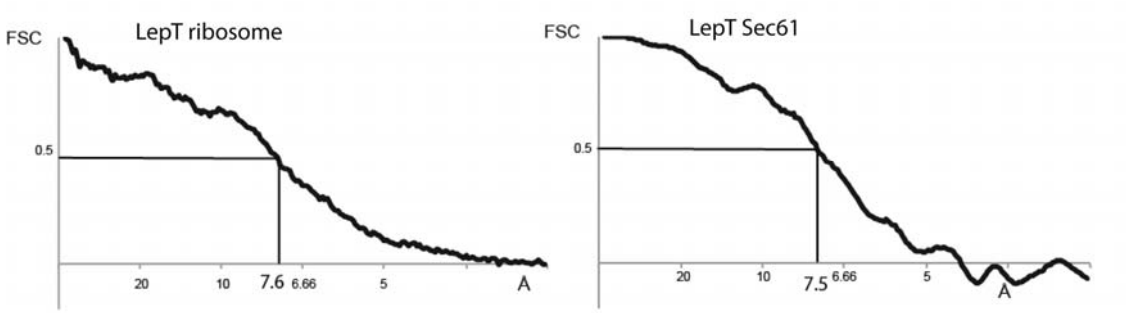

Figure 30: Model density fits for the models of the ribosome and the translocon for the LepT dataset.

The Cryo–EM–structure of the translocon engaging a transmembrane helix

Structure of the translocon bound to a ribosome translating the transmembrane LepM sequence was refined to a resolution of 7.8 Å (Fig. 31). This resolution, while lower than resolutions for the idle and LepT engaged molecules still allowed for determination of the secondary structure of the molecule.

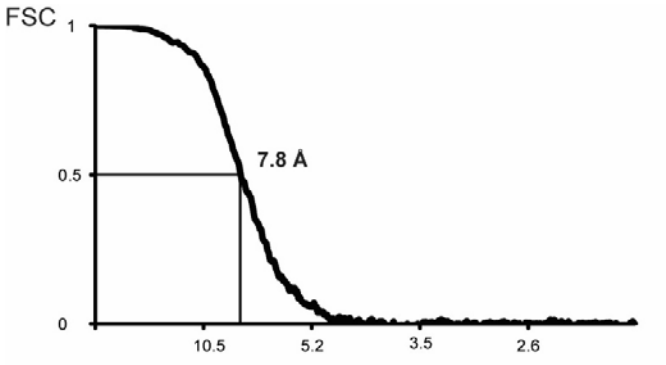

Figure 31: Resolution curve for the LepM dataset

The overall appearance of the volume was very similar to LepT: a density for the translocon was visible below the exit tunnel opening on the 60S subunit and the active site of the ribosome was indicated through a presence of a P–site tRNA (Fig. 32).

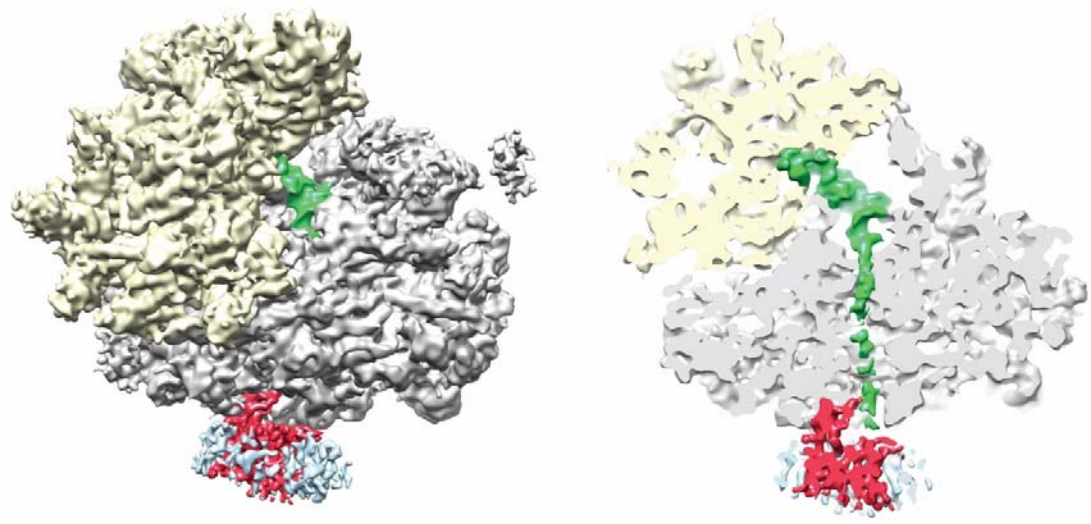

Figure 32: The density for the LepM Sec61-RNC.

The small ribosomal sub-unit is yellow, the large sub-unit is gray, the P-site tRNA is green and the translocon density is red while the surrounding micelle is in light blue. In the cut-through view on the right it is shown that in addition to the P-site tRNA, an extra density for the nascent chain can be observed in the ribosomal exit tunnel.

Different areas of the translocon show a different response to substrate binding. The ribosome contact loops L6–7 and L8–9 remain in a state that is unchanged with respect to the idle and LepT–engaged structures. On a broader level the entire C–terminal half of the Sec61α molecule (TM6–10) with the exception of TM7 remains in a practically identical position to the one in the idle Sec61α. In contrast, the N–terminal half of the molecule shows significant outward, rotational shifts for all helices except for TM5 which is positioned as a pivot for this rotation. This movement of the N–terminal half of the molecule is in contrast to the state of the LepT engaged translocon where helices TM2, 3 and 4 shift as a bundle but the N–terminal half as a whole remains largely in the same position as it is in the idle molecule (Fig. 33).

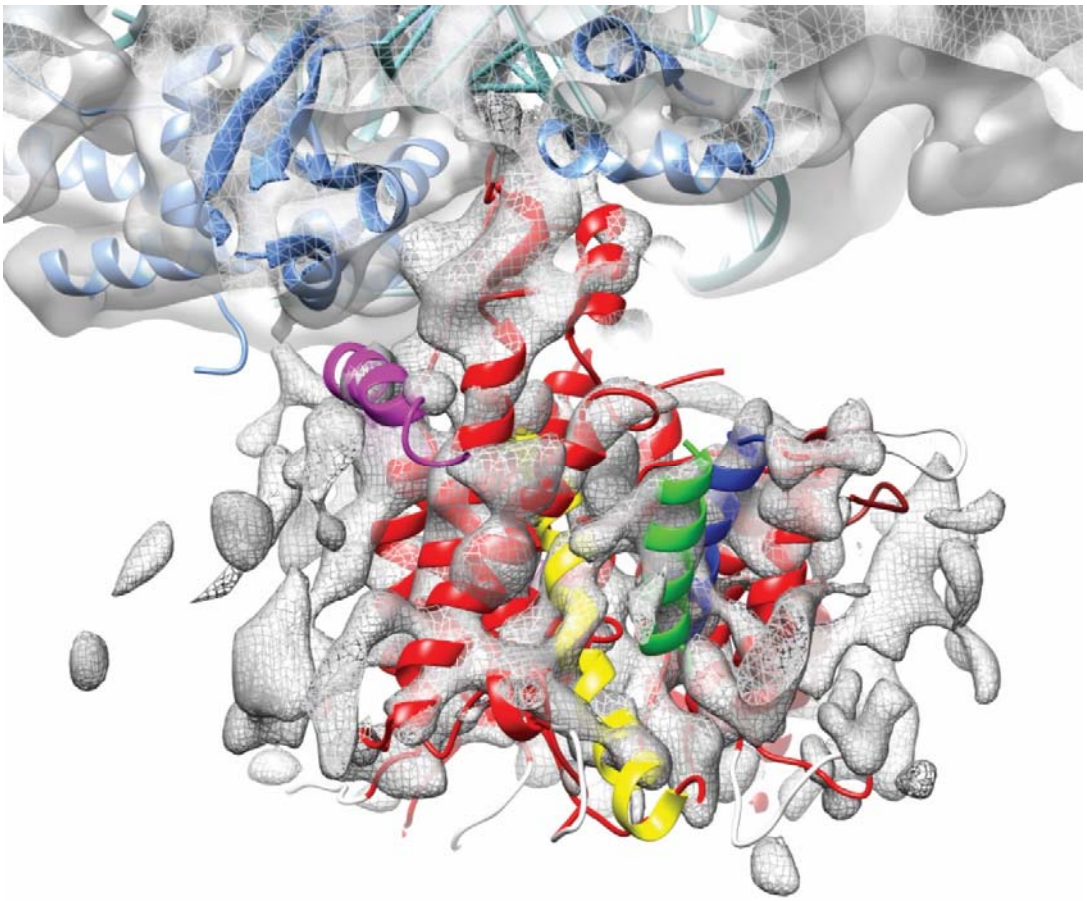

Figure 33: The model of the LepM-engaged translocon is shown in the context of the electron density map and the model for the ribosome.

Surrounding micelle is visible. A helically shaped extra density, explained as a substrate transmembrane helix is visible (green helix).

The most striking feature of the structure is the change in the lateral gate and the plug helix. Transmembrane helices that form the lateral gate (TM2 and TM7) are shifted away from their positions in the idle molecule. An additional electron density occupies a spot that partially overlaps with the idle position of TM2. This density was suggested to originate from the third transmembrane helix of LepM (Fig. 34). In addition, helix TM3 is also shifted outward, creating an even larger opening in the lateral gate area.

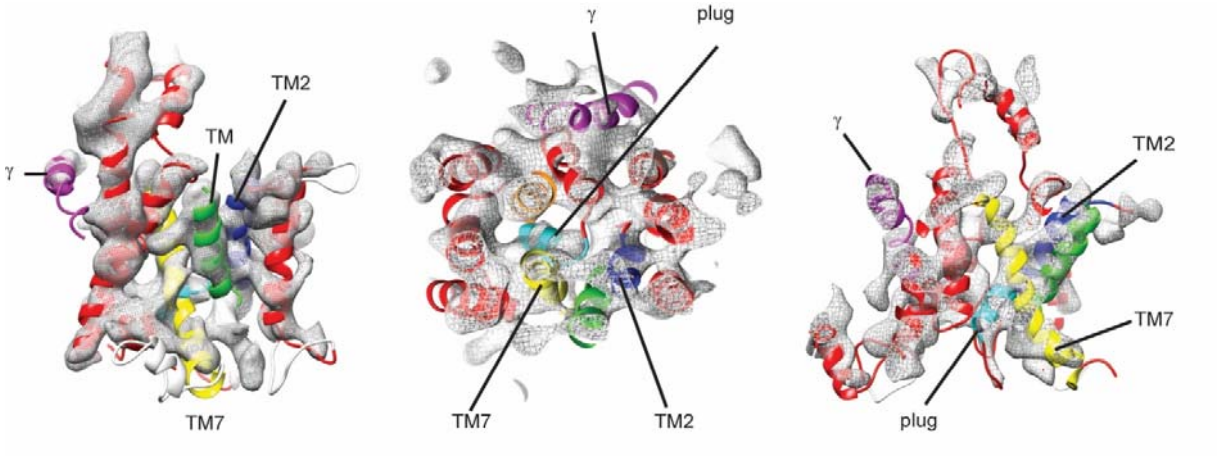

Figure 34: A close-up on the conformation of the translocon engaging a hydrophobic peptide.
The open position of the lateral gate (left) and the closed position of the central channel (center, right) are shown.

In summary, structure of the Sec61 engaging an insertion substrate shows that a nascent transmembrane helix is interacting with the lateral gate and not with the hydrophilic interior of Sec61. For this to happen, the lateral gate had to open to a large extent in a manner previously observed in a crystal structure where crystal packing interactions trapped the translocon in a pseudo-active state (Egea & Stroud 2010).

The role of TM2b and TM7 in transmembrane helix insertion has previously been suggested from crystal structures (Egea & Stroud 2010; Van den Berg et al. 2004) but in this work this interaction was for the first time unambiguously shown in a structure.

Validation of the model to density fit for the LepM dataset

As for the idle and LepT datasets, Fourier shell correlation analysis was performed between the expected densities generated from the models and the experimentally obtained densities to examine to what extent the models fit the experimentally obtained map. As in previous cases this procedure was performed for the translocon area separately from the rest of the ribosome (Fig. 35). The measurements showed that the signal–to–noise ratio of 0.5 (i.e. 50%) was reached at 7.8 Å filtering for the model of the ribosome and 7.5 Å for the model of the translocon. With a map at a resolution of 7.8 Å, this was judged to be an acceptable level of accuracy.

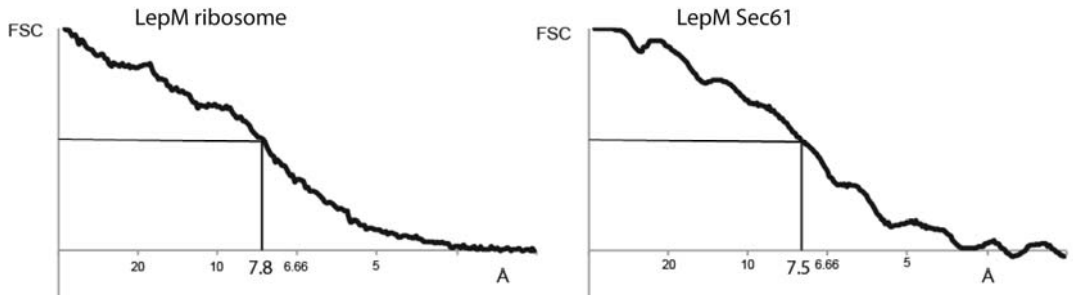

Figure 35: Model density fits for the models of the ribosome and the translocon for the LepM dataset.

Cross-linking of LepM to Sec61

In order to inspect the interaction of the variable region of LepM with the lateral gate of the translocon more closely, it was attempted to examine which amino-acids in the region can cross-link to Sec61. To this end constructs which carried amber STOP-codons in nine sites throughout the LepM TM3 were designed (Fig. 36).

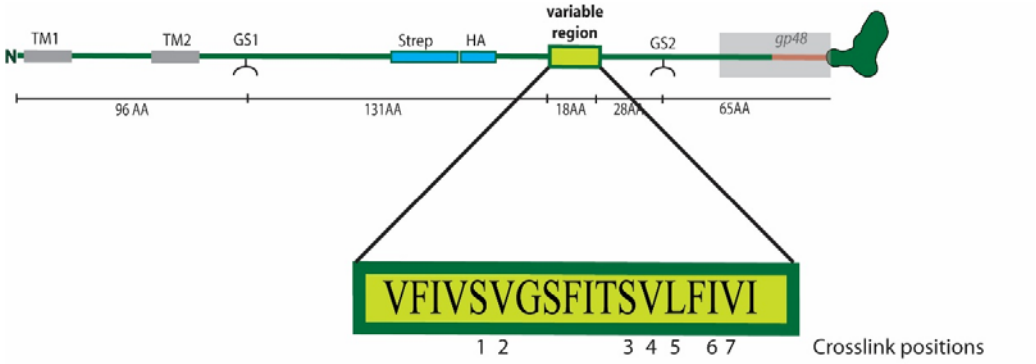

Figure 36: Scheme for selection of sites for incorporation of the artificial amino-acid pBpA.
Different cross-linking positions are indicated by numbers.

The translation mix was then supplemented with amber-suppressor tRNA carrying an unnatural amino acid, the UV activated cross-linker p-benzoyl-L-phenylalanine (pBpA). The suppressor tRNA was generated by co-expressing the tRNA and the appropriate amino-acyl-tRNA synthetase in BL21 *E. coli* cells in the presence of pBpA and subsequent extraction by phenol-chloroform (see materials and methods for more details).

In the absence of the suppressor tRNA, expression resulted in truncated peptides, as expected. Addition of the tRNA resulted in the appearance of the full length peptide as well as the stalled peptidyl-tRNA (Fig. 37).

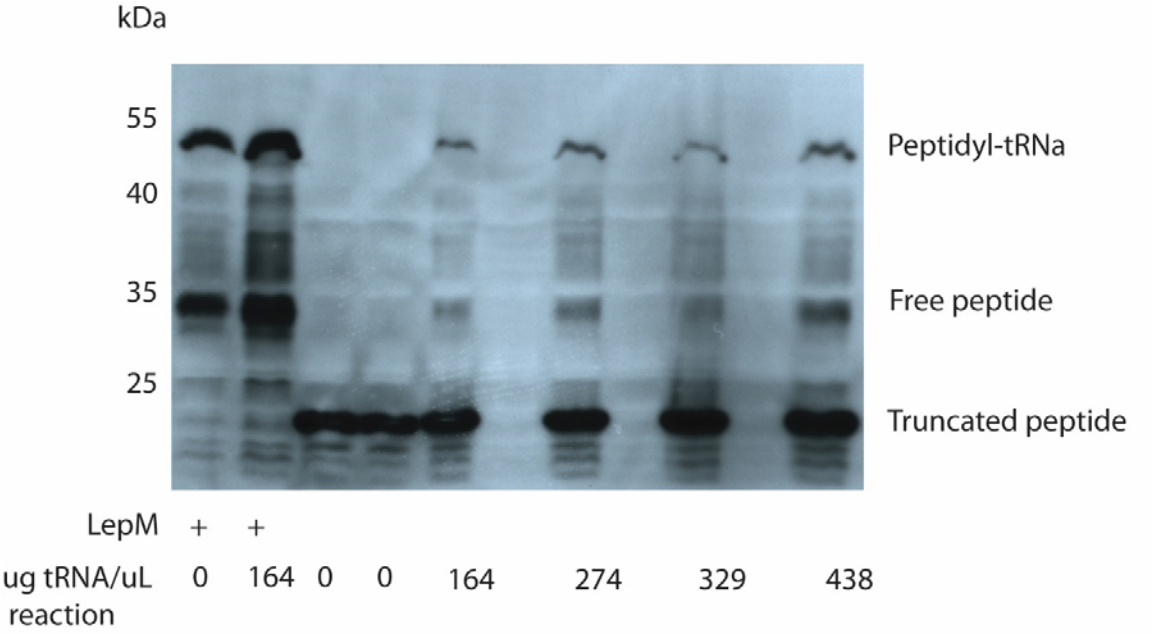

Figure 37: Testing of incorporation of tRNA^{pBpA} in different amounts.
First two lanes show the western blot for wild type LepM. Third and fourth lane show LepM-mutant 1 without any added tRNA while the following lanes show the effect of adding increasing amounts of tRNA^{pBpA}.

The peptide and the peptidyl-tRNA were glycosylated in the presence of PKRMs and SRP indicating that they could be efficiently targeted to the translocation machinery.

With a functioning system for incorporation of unnatural amino-acids into the substrate it was possible to obtain the cross-links by exposing pBpA-containing RNC-Sec61 complexes to UV radiation. Non-exposed pBpA RNC-Sec61 as well as UV-exposed wild type RNC-sec61 complexes were used as controls. For several of the probed sites additional bands of higher molecular weight could indeed be observed using a western blot against the HA-tag present in the Lep-substrate (Fig. 38).

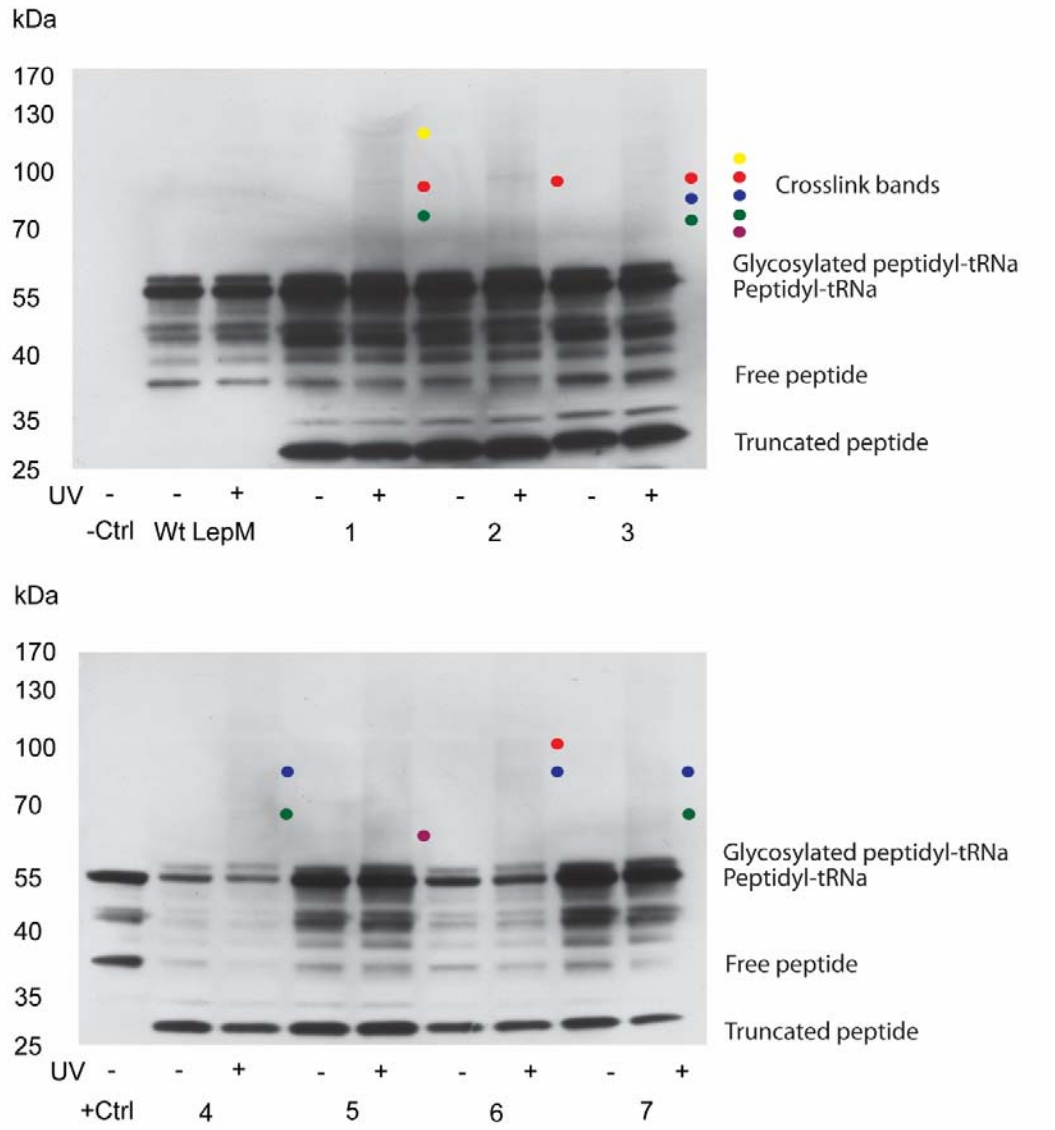

Figure 38: Effect of exposing RNC-Sec61 complexes of different mutants as well as the wild type LepM to UV radiation.

Appropriate negative controls are added. Several higher molecular weight bands that were observed are indicated. Unfortunately, none of these could be examined by anti-Sec61α western blot.

However, for final confirmation of LepM-Sec61 interaction, a blot against Sec61α was necessary. Due to issues with antibody specificity and cross-reactivity it was not possible to unambiguously characterize the TM-Sec61 interaction.

The Cryo–EM structure of the TRAP–OST–Sec61 complex bound to a translating ribosome

A small sub–dataset of the dataset for LepT translating ribosomes produced an electron density volume with a large amount of additional density observable. Based on results of Cryo–EM tomography by another group this density was assigned to the OST and TRAP complexes (Fig. 39).

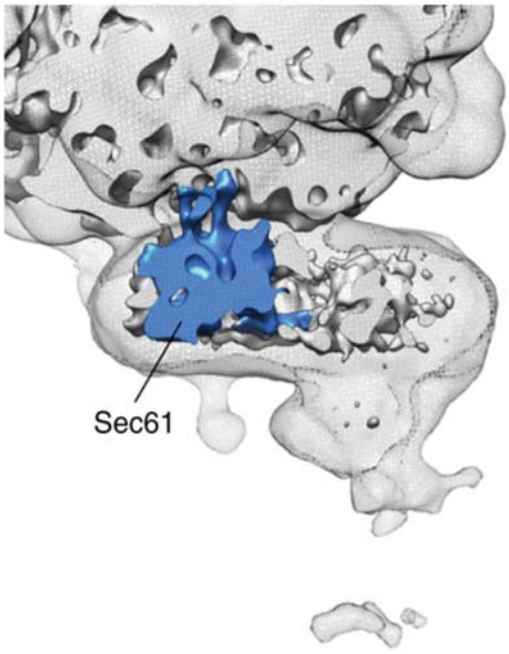

Figure 39: The density for the LepT Sec61-OST-TRAP-RNC.

The density for the ribosome, the micelle, TRAP and OST is gray while the density belonging to the translocon is highlighted in blue.

These assignations were confirmed with mass spectrometry results (Table 4).

Proteins	stoichiometries
TRAP alpha	0.073532208
TRAP gamma	0.117498962
TRAP delta	0.20746214
STT3A	0.011
Ribophorin 1	0.129338801
Ribophorin 2	0.064973766
OST48	0.109095905
OST3/OST6	0.102951248
DAD1	0.044350006
KCP2	0.013066878

Table 4: Subunits of TRAP (green) and OST (red) that could be identified by mass spectrometry.

Additional density belonging to a lipid–detergent micelle could be assigned based on the characteristic presence of an electron–dense mantle surrounding an electron–poor central area and a distinct lack of tubular areas of electron density characteristic of α–helical proteins.

This larger complex was refined to a resolution of 9.3 Å (Fig. 40) although the resolution of the distal parts of the extra density was significantly worse than the average resolution of the volume. This resolution allowed for placing a model of the LepT engaged translocon into density.

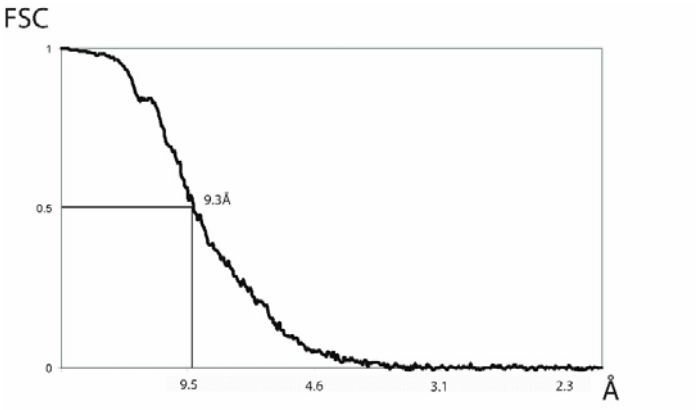

Figure 40: Resolution curve for the OST dataset.

Since there is no crystal structure available for the TRAP complex and the crystallized structure of archaeal (Lizak et al. 2011; Matsumoto et al. 2013) Stt3 accounts for only half the mass of canine OST, no models could be placed in these parts of the density. Due to qualitative differences in electron density for the micelle and protein, however, density could be assigned to the two protein complexes. This assignment was supported by siRNA experiments by Pfeffer et al. (Pfeffer et al. 2014), (Fig. 41).

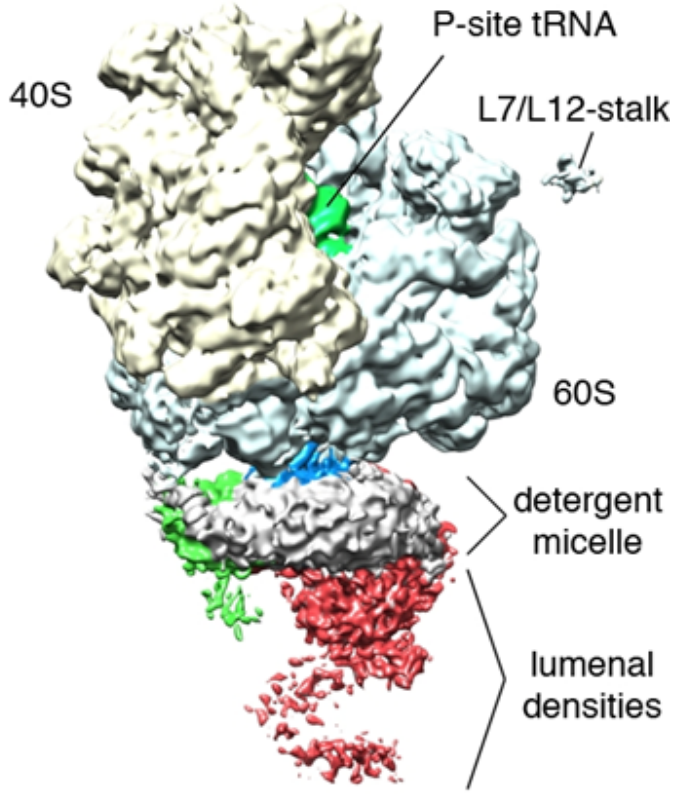

Figure 41: The density for the LepT Sec61-OST-TRAP-RNC.
The small ribosomal sub-unit is yellow, the large sub-unit is light blue, the P-site tRNA is green, as is the TRAP sub-unit; the translocon density is blue while the surrounding micelle is in gray. The density for OST is highlighted in red.

The density for OST was observed distally to the lateral gate of the translocon, near the transmembrane helix of Sec61γ and could be divided into three parts based on localization: the cytoplasmic projection, the transmembrane area and the luminal

projection. The density projecting into the lumen of the ER makes by far the largest part of the OST density. Based on the crystal structure of the bacterial Stt3 molecule, this is also the part of OST expected to be catalytically active (Lizak et al. 2011; Matsumoto et al. 2013).

The density for TRAP was located laterally to the lateral gate, near the amphipathic helix of Sec61γ and followed basically a similar pattern to the one for OST.

Discussion

As mentioned in the introduction, previous study of the translocon spans several decades and multiple research groups. Despite much data about its structure and function there are several key questions unanswered about the translocon.

In particular, the extent to which the lateral gate has to open and the plug helix has to move in peptide secretion and insertion has been a matter of some debate.

Furthermore, the state of an idle, ribosome bound Sec61 translocon has previously never been studied at a high enough resolution to observe changes at the secondary structure level with respect to the crystal structure of the prokaryotic SecY translocon without any binding partner or bound to SecA.

Also, substrate binding significantly strengthens Sec61-ribosome binding. It was therefore interesting to know whether the contacts between the ribosome and the translocon, in particular its loops 6/7 and 8/9, were different in the idle with respect to the active complex.

Finally, the structure of the holotranslocon, the Sec61-complex with OST, TRAP and other factors bound had not been studied at a high enough resolution to address questions on the position and arrangement of subunits in this complex.

In my work, I have tried to tackle these questions by visualizing the canine Sec61 translocon in complex with the wheat germ 80S ribosome. I analyzed three types of complexes: Sec61 in complex with the idle 80S ribosome, Sec61 in complex with an RNC translating a secretory substrate and finally, Sec61 in complex with an RNC containing an inserting transmembrane helix.

As my substrate molecule I chose Lep, a leader enteropeptydase-derived substrate containing two transmembrane helices followed by a long luminal loop containing a glycosylation site, a Strep-tag and an HA-tag. At the C-terminal end of the loop there is a segment which has in previous experiments been replaced by segments of various amino-acid composition and hence different secretion/membrane insertion propensity (Sääf et al. 1998). I chose two clones from this study: the Lep93 construct that displayed a high propensity for secretion and Lep62 that was shown to almost exclusively insert into the membrane. I renamed these substrates LepT (T for translocated) and LepM (M for membrane) respectively (Fig. 42). Aside from being well characterized biochemically in

previous studies, these substrates provided the additional benefit that they are identical except for the variable segment, ensuring that any difference in translocon conformation can be ascribed exclusively to the difference in interaction with the segment.

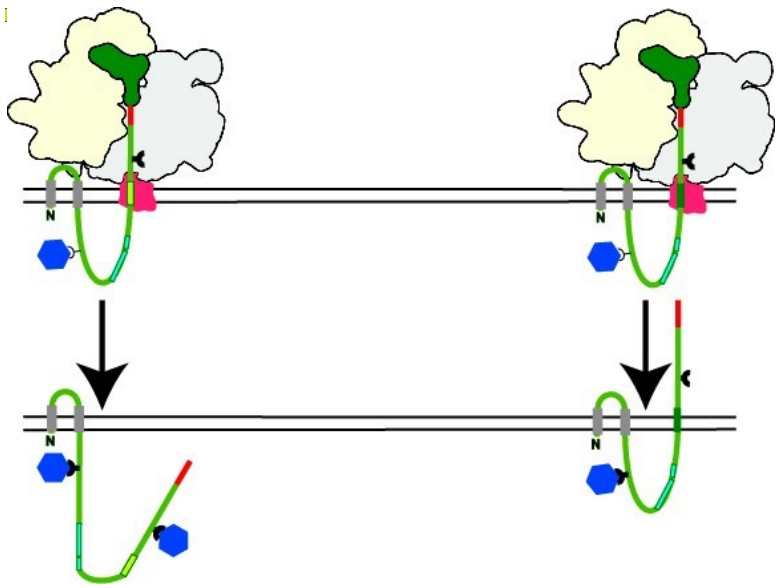

Figure 42: A display of LepT (left) and LepM (right) versions of Lep.
The top part of the image shows Lep-RNCs bound to the translocon in the membrane. The lower part shows the different topologies of free peptides of LepT and LepM.

Through *in vitro* translation of LepT and LepM, coupled with targeting to canine microsomes and followed by affinity purification I obtained Sec61-RNC complexes for both LepT and LepM engaged Sec61 samples. During cryo-EM analysis, I could sort out a subdataset of empty particles from both samples. By combining these subdatasets, I obtained a dataset of Sec61 translocon molecules bound to idle 80S ribosomes. I built models for all three structures, analyzed them and compared them to available structures and biochemical data.

Contacts between the ribosome and Sec61

At 150 mM salt concentration, the purified mammalian Sec61 binds the ribosome with an affinity of around 5 nM (Raden & Gilmore 1998; Kalies et al. 1994). This value falls to 50 nM for Sec61 in its physiological, membranous surroundings (Schaletzky & Rapoport 2006). This interaction is not resistant to treatment with high concentration of monovalent salts (>500 mM) but becomes resistant upon RNC-translocon binding (Jungnickel & Rapoport 1995). This ability of the translocon to sense a correct substrate as well the effect of the membrane on weakening translocon-ribosome binding roughly 10-fold makes translocon-ribosome interactions an interesting target for structural research.

The structures within the translocon that have been mostly implied in partner binding are the cytoplasmic loops 6/7 and 8/9 (Cheng et al. 2005; Raden et al. 2000; Song et al. 2000). The loop most responsible for ribosome binding seems to be loop 8/9 while loop 6/7 has been proposed to serve as a recognition site for initial complex formation. This has been corroborated by thermodynamic data showing only slight reduction in ribosome binding in 6/7 mutants and a larger reduction in 8/9 mutants. Interestingly, while several positively charged amino acid residues from loop 8/9 that contact the ribosome are important for ribosome binding and mutating them into negative residues is detrimental for ribosome binding, mutating them into glycine and therefore eliminating their side-chains only reduces the binding constant roughly two to three-fold, leaving it well within the lower nanomolar range. The question of how just a few amino acids in a single loop, that can be freely eliminated can be responsible for 5 nM binding affinity remains unanswered (Cheng et al. 2005).

Since I produced structures of the translocon, engaged with a secretory and a transmembrane substrate as well as a structure of the translocon engaging an empty 80S ribosome, this gave me the opportunity to analyze potential conformational changes in the cytoplasmic loops of the translocon as well as the nature of ribosome binding by loop 8/9.

Although the resolution of my electron densities precludes any comments of side-chain orientations, it is clear from the comparison of the idle translocon and the translocon bound to a secretory substrate that no change in the conformation of the loop 8/9 polypeptide chain occurs. In the model of the translocon bound to an inserting substrate, the segment of loop 8/9 that carries residues corresponding to the binding residues of yeast

(H404 and R405 corresponding to K405 and R406 in yeast) is slightly closer to the ribosome than in the other two models. The biological significance of this change is not clear but might contribute to the strengthening of the ribosome-Sec61-complex.

Since the publication of my work, another Cryo-EM study of the translocon-ribosome interaction has been published, showing the contact residues at high resolution. However, despite the fact that the residues implicated in complex stabilization do indeed seem to contact the rRNA; neither my work nor the more recent study explains how these residues can be mutated into completely different amino acids with only slight to moderate reductions in binding affinity (Voorhees et al. 2014).

The empty Sec61 opens slightly upon ribosome binding

The crystal structure of the archaeal SecYEβ complex has provided great insight into the architecture of different translocon homologues across the three domains of life. Due to the high sequence and function conservation, it is safe to assume that the mammalian Sec61-complex takes on a very similar conformation to its archaeal homologue (Van den Berg et al. 2004).

However, a series of crystal structures of different prokaryotic translocons bound to several artificial or physiological interacting partners demonstrate that complex formation is enough to induce significant changes in translocon conformation and possibly prime it for substrate binding (Zimmer et al. 2008; Tsukazaki et al. 2008). It was therefore of interest to examine the conformation of the eukaryotic Sec61 bound to an idle 80S ribosome and compare it to the crystal structures of both SecYEβ alone as well as different structures of SecYE(G) in complex with SecA and an anti-SecY antibody.

Overall, the similarity between the SecYEβ crystal structure and the idle, ribosome bound Sec61 is striking. With the exception TM1 and TM4, the positions of TM helices are largely unchanged. TM1 is moved by translational movement into a position parallel to its position in the crystal structure while TM4 stays in the same position but is tilted into the opposite direction of its crystal structure counterpart. Since neither of these helices has been implicated in protein translocation or insertion, this difference might be ascribed to difference in sequence.

Upon further inspection, subtle but important differences begin to emerge (Fig. 43). The plug helix of the mammalian Sec61 is shifted outwards compared to the crystal structure, with the opening filled by an elongation of TM10. At the same time, the lateral gate of the eukaryotic translocon is slightly more closed than the archaeal gate mostly due to shifts in TM2 the upper part of TM3.

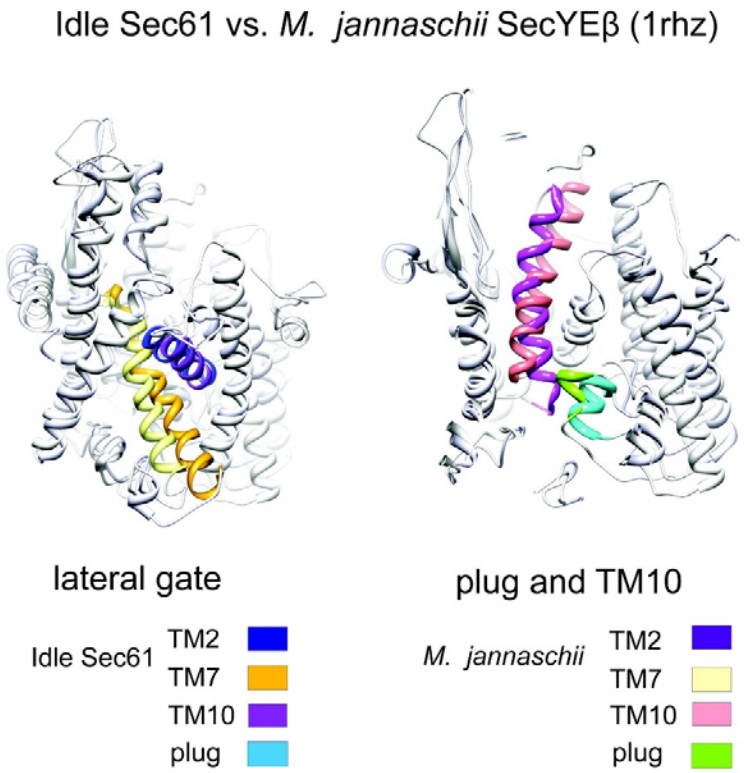

Figure 43: Idle mammalian Sec61 compared to *Methanococcus jannaschii* crystal structure of SecYEβ (van den Berg).

In the upper part are the comparisons of the lateral gate (left) and the positions of the plug and TM10 (left). The color codes are given in the lower part of the figure.

Finally, the positions of the cytoplasmic loops 6/7 and 8/9 are quite different between the two molecules. This difference is most likely due to the fact that these loops do not have any binding partner in the crystal structure and their positions in the crystal are therefore of no physiological value.

Altogether, the idle eukaryotic Sec61-complex is in a similar conformation to its archaeal homologue in the apo-form. A slight change in the position of the plug helix and a corresponding shift in TM10 is visible, possibly priming the structure for activation.

Structure of the secreting translocon

One of the main functions of Sec61 is translocation of secretory proteins or protein segments. From analyzing the structure of the archaeal SecYEβ it has been suggested that secretion occurs trough the central, hydrophilic channel of Sec61α with the aliphatic residues of the pore ring serving to prevent any ion leakage. In order for translocation to occur in this way, the TM2a plug helix has to move from its position to create a central opening large enough for a peptide chain to fit (Van den Berg et al. 2004).

The extent of this movement has been debated. Cross-linking experiments have shown that the plug helix of SecY can be cross-linked to amino acids more than 20 Å away, suggesting large freedom of movement (Harris & Silhavy 1999). On the other hand, fluorescence measurements of SecY plug helix have shown that it moves only slightly for protein translocation and remains in the periplasmic vestibule of SecY (Lycklama a Nijeholt et al. 2011). The argument for a limited shift of the plug in translocation has been strengthened by data indicating that immobilizing the plug within the SecY channel allows for unrestricted translocation (Lycklama A Nijeholt et al. 2010).

Another unresolved question is to what extent the lateral gate has to open for protein secretion. Cross-linking studies have demonstrated that the lateral gate of SecY has to open by about 5 Å for SecA mediated protein secretion (du Plessis et al. 2009). However, the opening was correlated with the catalytic cycle of SecA and it remains unclear if this movement persists with in the Sec61-Ribosome complex.

Because of these questions it was interesting to observe the structure of Sec61 bound to the ribosome and translocating the secretory segment of the LepT construct.

When compared to the model for the idle translocon, the structure is in a broadly similar conformation. A slight opening in the lateral gate is visible, mostly due to shifts in TM2 and TM3. This opening is enough to move the aliphatic side-chains of amino acids that form the pore ring into positions where they cannot possibly participate in the

formation of the ring, indicating at least partial destabilization of the ion seal. The peptide chain probably acts to re-form the barrier to ion flow (Fig. 44).

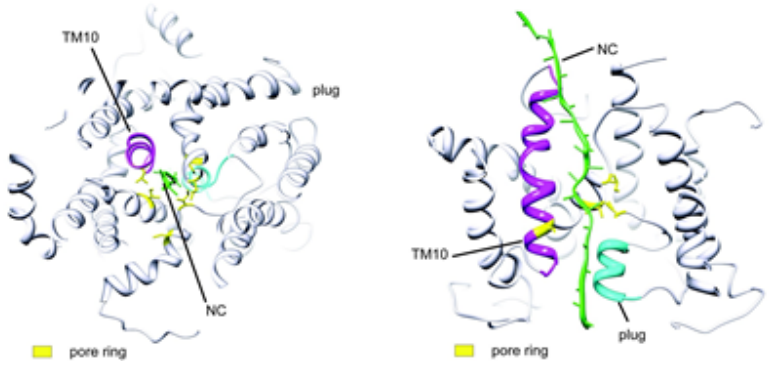

Figure 44: An extended peptide (green) can fit into the central channel of a LepT-engaged translocon. The conformational shift necessary to create this opening also arranges the segments carrying the pore ring residues (yellow) in such a way that they cannot form a complete pore ring. The plug helix (cyan) and TM10 (magenta) are arranged to provide ample space for a secreting polypeptide.

The plug helix is in roughly the same position as in the idle structure. This position is shifted slightly outward when compared to the crystal structure of the idle SecYEβ. The central channel is opened, however, by a shift in the lower part of TM10 (Fig. 45). This is consistent with genetic experiments localizing some of the prl mutants to TM10 (Osborne & Silhavy 1993; Lycklama A Nijeholt et al. 2010), as well as cross-linking and fluorescence results showing that the plug helix is not displaced significantly for secretion (Lycklama a Nijeholt et al. 2011). Despite the presence of a tRNA in the ribosomal P-site as well as an extra density in the ribosomal exit tunnel, all indicating the existence of a nascent chain in the ribosome, no chain was visible within the translocon. This might indicate that the peptide straddles the translocon as an extended chain that cannot be resolved at a 7-8 Å resolution.

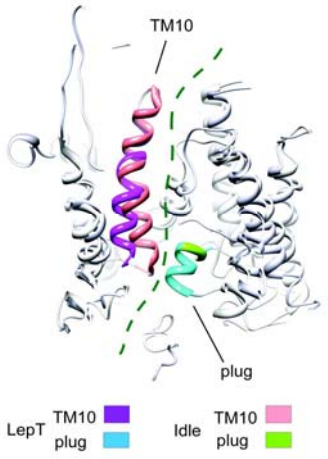

Figure 45: Side view comparison of the central channel in a LepT engaged and an idle translocon. The Plug is essentially unchanged while a shift in TM10 provides the opening. The color scheme for the plug and TM10 is provided in the lower part of the image. The dashed green line represents a possible pathway for the nascent peptide.

Taken together, my data are consistent with more recent fluorescence and cross-linking data indicating that the plug helix has to shift only slightly for translocation and that a small opening of the lateral gate happens. The observed shift in TM10 also explains the role of this helix in translocation.

Structure of the inserting translocon

Insertion of transmembrane domains into the lipid bi-layer is the second function of the translocon. From the available crystal structures, supported by biochemical and genetic results, a model for translocon catalyzed peptide insertion has been proposed (Van den Berg et al. 2004). According to this model, the lateral gate formed by TM2 and TM7 of the translocon has to open in order to facilitate lateral egress of the helix into the membrane. It was not clear whether the opening of the lateral gate requires movement of both TM2 and TM7 or only one of them and whether the movement is restricted to these two helices or requires shifts of the N-terminal or C-terminal half of the translocon.

The contribution of the plug helix to this process was also not completely clear until now. Investigation of plug behavior via fluorescence indicated that the plug does now move

into a more hydrophilic environment during insertion. But whether there is any movement within the translocon and to what extent was not known (Lycklama a Nijeholt et al. 2011).

In my structure of the Sec61 bound to a LepM translating ribosome, I could observe a clear conformational change in the translocon. Most strikingly, the lateral gate was opened by about 12 Å with an extra helix inserted in the middle. This movement was mostly due to shifts in TM2 and TM3 and did not span the whole N-terminal half of the translocon (Fig. 46). The C-terminal half of the molecule remained virtually unchanged when compared to the idle and LepT engaged Sec61.

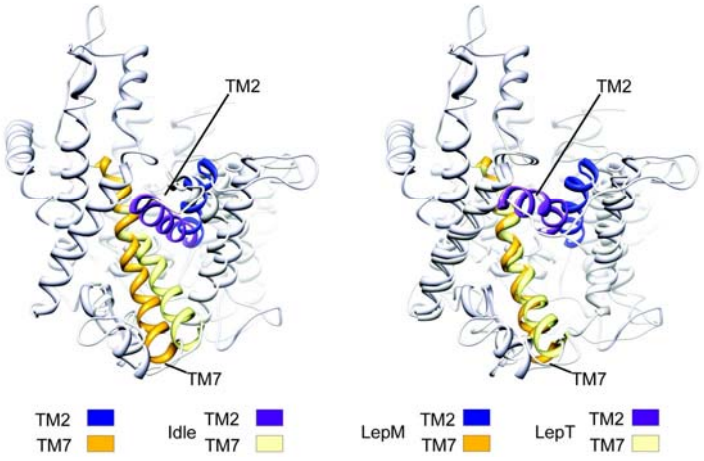

Figure 46: Conformational change in the lateral gate of LepM compared to the idle (left) and LepT-engaged (right) translocon.

While TM7 of LepM is in the same position as in LepT, the opening created by a shift in TM2 is much larger than in LepT.

This arrangement, in particular the extent of the opening of the lateral gate, bares striking resemblance to a crystal structure of SecYEβ from *Pyrococcus furiosus* where crystal packing interactions induced the opening of the lateral gate (Egea & Stroud 2010), (Fig. 47).

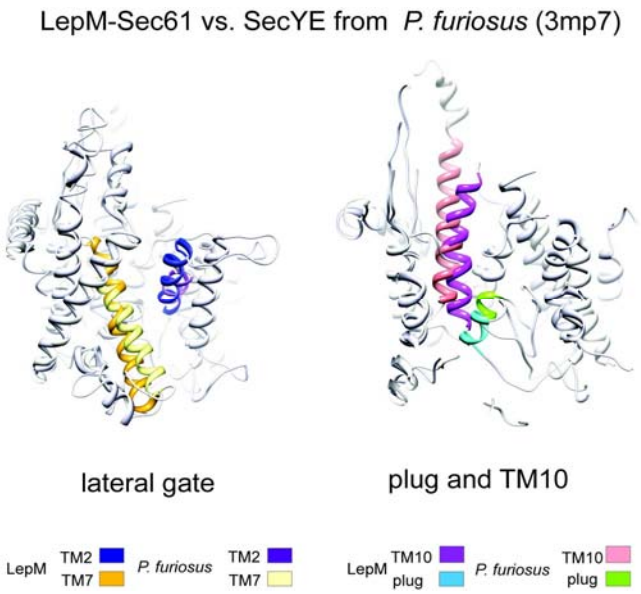

Figure 47: Comparison of the LepM structure with a crystal structure of a *P. furiosus* SecYEβ that was crystallized with a helical segment inserted into its lateral gate due to crystal packing. While the lateral gates of both translocons are in the same position necessary to accommodate a transmembrane helix (left), the positions of TM10 and the plug helix diverge (right). Color codes are given in the lower part of the figure.

The position of the plug helix is slightly different than in the idle or LepT translocating molecule in that it is shifted deeper into the center of the molecule. Together with the shift of the plug, the lower part of TM10 is shifted inwards, further blocking the central channel (Fig. 48). These movements might serve to prevent ion leakage through the central channel of the molecule as the pore ring is strongly destabilized by shifts in TM2 and TM10 and as there is no peptide chain in the center of the channel to replace it.

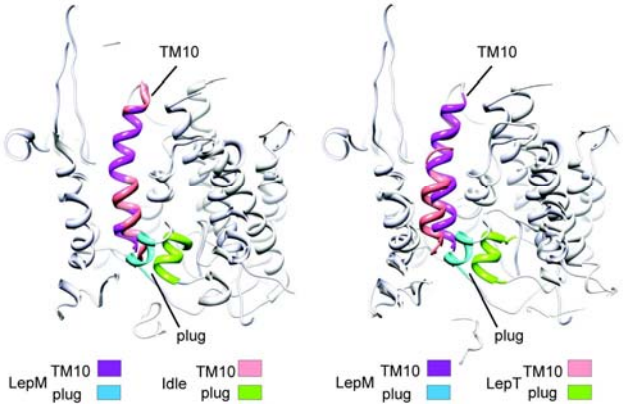

Figure 48: Side view comparison of the central channel in a LepM engaged translocon to that in an idle (left) and LepT (right) engaged translocon.

The TM10 is in the same position as in the idle translocon, closing the channel while the plug is shifted inwards with respect to both structures further strengthening the seal. The color scheme for the plug and TM10 is provided in the lower part of the image.

This structure is consistent with previous data pointing to the role of the lateral gate in helix insertion (Plath et al. 1998; du Plessis et al. 2009), as well as the limited role of the plug helix in this movement and shines further light on both conformational changes as well as pointing to the role of TM10 in helping to maintain the membrane seal for ion flow.

Overall model of translocon activity

The data that I obtained enabled me to confirm and elaborate on the previously proposed model for translocon activity.

Upon ribosome binding the translocon stays in a largely inactive state except for a small shift in the plug helix accompanied by movement of TM10.

When a secretory stretch needs to be translocated, a small opening in the lateral gate and an outward movement of TM10, both acting to destabilize the central pore ring of aliphatic amino-acid side chains are enough to accommodate the extended substrate chain. For substrate insertion into the membrane bilayer, the lateral gate opens by 12 Å with the plug, TM10 and the inserting TM-helix all acting to re-seal the gap in the central channel (Fig. 49).

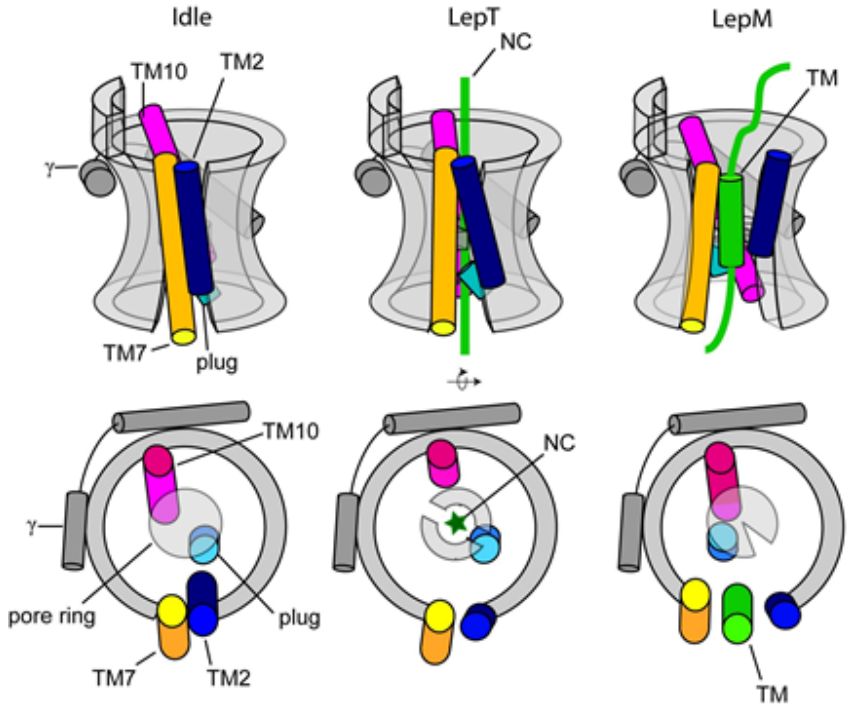

Figure 49: Overall model of translocon conformations in the idle state, when secreting a nascent chain (NC) and when handling an inserting transmembrane helix (LepT).
In short, in the idle state, both the lateral gate and the central channel are closed and the pore ring prevents ion leakage. Upon interaction with a secretory, extended nascent chain, the central channel opens by a shift in TM10. This movement also destabilizes the pore ring. Ion leakage is presumably prevented by the presence of the nascent chain. The lateral gate here is only slightly pried open but still quite similar to the closed state. Upon helix insertion, the lateral gate opens much wider and accommodates a helix between TM7 and TM2. Due to the opening of the gate, the pore ring is partially destabilized. This is compensated for by an inward shift in the plug helix, providing a seal to the channel.

Upon substrate release, the molecule returns to its inactive state. All these movements, with the notable exception of the lower part of TM10 seem to mostly affect the N-terminal part of the molecule. Only small differences could be noted between the ribosome contacting loops of the translocon inserting a substrate and the molecule in its secretory or inactive state, leaving the impact of substrate binding on ribosome-Sec61 interaction unexplained.

Sec61 binding to OST and TRAP

Although the Sec61-complex and the SRP receptor are necessary for protein translocation or membrane insertion there are several co-factors needed for efficient processing of proteins destined for the secretory pathway. How these interact with Sec61 is poorly known.

In order to elucidate the nature of OST and TRAP binding to the translocon, I solved a single particle Cryo-EM structure of the LepT RNC-Sec61-OST-TRAP complex. This data, accompanied by a Cryo-EM tomography and knock-down studies by collaborating groups enabled me to find out something more about the nature of this interaction.

Although the low resolution in the density corresponding to OST and TRAP as well as absence of crystal structures for the TRAP complex and for many of the subunits of the OST complex precluded building any models for the two complexes, the positioning of Sec61 as well as TRAP from previous studies (Menetret et al. 2000; Ménétret et al. 2008) enabled me to determine the location of OST with fair certainty (Fig. 50). Since I already knew the orientation of Sec61 bound to the translocon, I could determine that TRAP and OST bind the Sec61-complex primarily through its γ subunit.

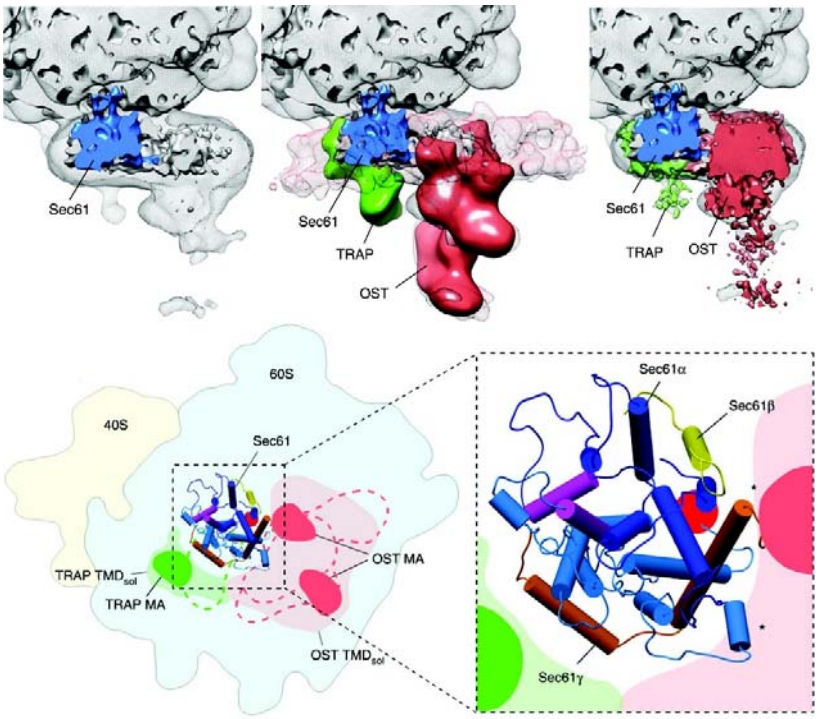

Figure 50: Placement of the model for Sec61 into Sec61-OST-TRAP density.
Upper left: Sec61 could be placed into the large density under the ribosome. Upper center: Based on previous single particle Cryo-EM, a part of the density could be ascribed to the TRAP complex. Data from Cryo-EM tomography in conjunction with knock-down experiments explained another part of the density as OST. Upper left: all of the density observed was thus explained as belonging to Sec61, TRAP, OST or the detergent micelle. Lower left: A model of Sec61αβγ could be built into the translocon density. From the positioning of the model it is clear that both OST and TRAP are located proximally to the γ-subunit of Sec61. Lower right: a close up of the model in context of OST and TRAP.

Electron density corresponding to the transmembrane area of TRAP is located near the N-terminal, amphipathic helix of Sec61γ, possibly also interacting with the C-terminal transmembrane helices 6, 8 and 9 of Sec61α. This position places TRAP next to the lateral gate and might explain its role in determining the topology of transmembrane helices.

The position of OST was previously suggested to be directly in front of the lateral gate of Sec61α (Chavan et al. 2005). In my work, I have observed density corresponding to OST on the opposite side of the molecule, positioned to interact with the C-terminal transmembrane helix of Sec61γ and possibly with transmembrane helices 1, 5 and 6 of Sec61α. This brings it into contact with the hinge area between the C- and N-terminal

halves of the translocon. In the absence of higher resolution data about the internal structure of OST as well as data on interactions of its individual subunits with the transmembrane areas of Sec61 it is hard to say what the biological significance of this positioning is.

Conclusions

The Sec61 translocon is a universally conserved, versatile protein capable of performing a dual function as a transmembrane channel for secretory polypeptide substrates as well as an insertase for transmembrane helices. In this capacity, the translocon has to not only discriminate between secretory and transmembrane substrates but also between different transmembrane helix orientations in determining the final topology of proteins in the secretory pathway. The Sec61 complex can act as a co-translational translocon, pairing with translating ribosomes or post-translationally, with the help of chaperons and other proteins.

In addition to these functions, the Sec61 translocon can form larger complexes, usually termed 'the holotranslocon', with, amongst other factors, OST, TRAP and TRAM and thus coordinate accessory functions such as glycosylation.

Crystal structures of archaeal and eubacterial homologues of the Sec61 complex have been solved, revealing it as a heterotrimer composed of a ten-transmembrane helical channel, Sec61α, bound to a single spanning transmembrane helix, Sec61β and a protein called Sec61γ, composed of a transmembrane and a cytoplasmic, amphipathic helix. An opening in Sec61α between its TM helices 2 and 7, facing the lipid bilayer has been proposed to be the site of peptide insertion into the membrane and has been termed 'the lateral gate' while a narrow, hydrophobic channel in the center of the molecule is believed to function in peptide secretion. The central channel is obstructed in the middle of the molecule by a small helix, TM2a, termed 'the plug'. This obstruction must somehow be removed in order for protein secretion to occur.

Despite a wealth of biochemical, genetic, biophysical and structural data on the translocon, a detailed picture of the nature of its interaction with its substrates as well as with accessory factors has thus far been lacking. In my work I have sought to investigate these states by solving Cryo-EM structures of the Sec61 translocon bound to idle 80S ribosomes as well as RNCs translating a secretory and a transmembrane substrate at a resolution allowing determination of the secondary structure. In addition, I solved a lower resolution structure of the Sec61, bound to a ribosome translating a secretory substrate, in complex with OST and TRAP.

From my structures, I propose a model for translocon activity.

According to my model, only small changes in the structure of Sec61 are necessary for secretion of an extended peptide. The plug helix, previously suggested to play a large role in protein secretion seems to shift already in response to binding an idle 80S ribosome and does not move significantly during secretion. Instead, the lower part of translocon TM10 shifts out, opening the central channel.

In contrast larger movements are needed for helix insertion into the membrane. Notably a large movement in the proposed lateral gate can be observed, mostly through a shift in TM2 and an extra density, presumably belonging to an inserting transmembrane helix is visible. The plug helix in this structure is shifted inwards, sealing the central channel of the molecule against ion flow.

From my structure of the RNC-Sec61-OST-TRAP complex, I determined that OST binds Sec61 dorsally to the lateral gate, proximally to the transmembrane helix of Sec61γ while TRAP binds proximally to the amphipathic helix of Sec61γ, close, but not at, the lateral gate, putting it in the position ideally suited for early interactions with transmembrane substrates.

Further Perspectives

Many questions remain unanswered about the structure and function of the translocon. Higher resolution structures, enabling study of positions of different side chains, are necessary to elucidate the nature of the strong binding of Sec61 to ribosomes as well as to determine how successful gating of the translocon results in stronger binding resistant to higher salt concentrations.

Furthermore, different substrates interact with the translocon in markedly different ways, meaning that just two substrates are still a far cry from the full repertoire of translocon states and conformations.

The translocon is a potential target for selective inhibitors that might be useful as anti-tumor and anti-viral drug candidates, making high resolution structures of Sec61 in complex with candidate drugs highly desirable.

Also, little is known about the internal composition of the OST and TRAP complexes as well as which of their subunits interact with the Sec61 complex. High-to-medium resolution Cryo-EM data in conjunction with cross-linking and sequence analysis might provide answers to these questions.

Bibliography

Adelman, M.R., Sabatini, D.D. & Blobel, G., 1973. Ribosome-membrane interaction. Nondestructive disassembly of rat liver rough microsomes into ribosomal and membranous components. *The Journal of cell biology*, 56(1), pp.206–29. Available at: http://www.pubmedcentral.nih.gov/articlerender.fcgi?artid=2108843&tool=pmcentrez&rendertype=abstract [Accessed December 11, 2014].

Armache, J.-P. et al., 2010. Cryo-EM structure and rRNA model of a translating eukaryotic 80S ribosome at 5.5-A resolution. *Proceedings of the National Academy of Sciences of the United States of America*, 107(46), pp.19748–53. Available at: http://www.pubmedcentral.nih.gov/articlerender.fcgi?artid=2993355&tool=pmcentrez&rendertype=abstract [Accessed December 11, 2014].

Audigier, Y., Friedlander, M. & Blobel, G., 1987. Multiple topogenic sequences in bovine opsin. *Proceedings of the National Academy of Sciences of the United States of America*, 84(16), pp.5783–7. Available at: http://www.pubmedcentral.nih.gov/articlerender.fcgi?artid=298947&tool=pmcentrez&rendertype=abstract [Accessed December 10, 2014].

Becker, T. et al., 2009. Structure of monomeric yeast and mammalian Sec61 complexes interacting with the translating ribosome. *Science (New York, N.Y.)*, 326(5958), pp.1369–73. Available at: http://www.pubmedcentral.nih.gov/articlerender.fcgi?artid=2920595&tool=pmcentrez&rendertype=abstract [Accessed November 16, 2014].

Beckmann, R. et al., 1997. Alignment of conduits for the nascent polypeptide chain in the ribosome-Sec61 complex. *Science (New York, N.Y.)*, 278(5346), pp.2123–6. Available at: http://www.ncbi.nlm.nih.gov/pubmed/9405348 [Accessed December 11, 2014].

Van den Berg, B. et al., 2004. X-ray structure of a protein-conducting channel. *Nature*, 427(6969), pp.36–44. Available at: http://www.ncbi.nlm.nih.gov/pubmed/14661030 [Accessed November 10, 2014].

Berg, J.M., Tymoczko, J.L. & Stryer, L., 2002. Biochemistry. *W H Freeman*, New York. , p.1. Available at: papers2://publication/uuid/7EB6183C-F1A3-4903-A72F-B1A659CECF68.

Bieker, K.L., Phillips, G.J. & Silhavy, T.J., 1990. The sec and prl genes of Escherichia coli. *Journal of bioenergetics and biomembranes*, 22(3), pp.291–310. Available at: http://www.ncbi.nlm.nih.gov/pubmed/2202721 [Accessed December 11, 2014].

Bonardi, F. et al., 2011. Probing the SecYEG translocation pore size with preproteins conjugated with sizable rigid spherical molecules. *Proceedings of the National Academy of Sciences of the United States of America*, 108(19), pp.7775–80. Available at: http://www.pubmedcentral.nih.gov/articlerender.fcgi?artid=3093497&tool=pmcentrez&rendertype=abstract [Accessed December 11, 2014].

Brundage, L. et al., 1990. The purified E. coli integral membrane protein SecY/E is sufficient for reconstitution of SecA-dependent precursor protein translocation. *Cell*, 62(4), pp.649–57. Available at: http://www.ncbi.nlm.nih.gov/pubmed/2167176 [Accessed December 11, 2014].

Chavan, M., Yan, A. & Lennarz, W.J., 2005. Subunits of the translocon interact with components of the oligosaccharyl transferase complex. *The Journal of biological chemistry*, 280(24), pp.22917–24. Available at: http://www.ncbi.nlm.nih.gov/pubmed/15831493 [Accessed December 11, 2014].

Cheng, Z. et al., 2005. Identification of cytoplasmic residues of Sec61p involved in ribosome binding and cotranslational translocation. *The Journal of cell biology*, 168(1), pp.67–77. Available at: http://www.pubmedcentral.nih.gov/articlerender.fcgi?artid=2171681&tool=pmcentrez&rendertype=abstract [Accessed December 11, 2014].

Cooper, G.M. & Hausman, R.E., 2007. *The Cell: A Molecular Approach 2nd Edition*,

Derman, A.I. et al., 1993. A signal sequence is not required for protein export in prlA mutants of Escherichia coli. *The EMBO journal*, 12(3), pp.879–88. Available at: http://www.pubmedcentral.nih.gov/articlerender.fcgi?artid=413286&tool=pmcentrez&rendertype=abstract [Accessed December 11, 2014].

Dumax-Vorzet, A., Roboti, P. & High, S., 2013. OST4 is a subunit of the mammalian oligosaccharyltransferase required for efficient N-glycosylation. *Journal of cell science*, 126(Pt 12), pp.2595–606. Available at: http://www.pubmedcentral.nih.gov/articlerender.fcgi?artid=3687696&tool=pmcentrez&rendertype=abstract [Accessed December 11, 2014].

Egea, P.F. & Stroud, R.M., 2010. Lateral opening of a translocon upon entry of protein suggests the mechanism of insertion into membranes. *Proceedings of the National Academy of Sciences of the United States of America*, 107(40), pp.17182–7. Available at: http://www.pubmedcentral.nih.gov/articlerender.fcgi?artid=2951439&tool=pmcentrez&rendertype=abstract [Accessed December 10, 2014].

Emr, S.D. & Bassford, P.J., 1982. Localization and processing of outer membrane and periplasmic proteins in Escherichia coli strains harboring export-specific suppressor

mutations. *The Journal of biological chemistry*, 257(10), pp.5852–60. Available at: http://www.ncbi.nlm.nih.gov/pubmed/7040375 [Accessed December 11, 2014].

Emr, S.D., Hanley-Way, S. & Silhavy, T.J., 1981. Suppressor mutations that restore export of a protein with a defective signal sequence. *Cell*, 23(1), pp.79–88. Available at: http://www.ncbi.nlm.nih.gov/pubmed/7011570 [Accessed December 11, 2014].

Emsley, P. et al., 2010. Features and development of Coot. *Acta crystallographica. Section D, Biological crystallography*, 66(Pt 4), pp.486–501. Available at: http://www.pubmedcentral.nih.gov/articlerender.fcgi?artid=2852313&tool=pmcentrez&rendertype=abstract [Accessed July 11, 2014].

Erickson, A.H. & Blobel, G., 1983. Cell-free translation of messenger RNA in a wheat germ system. *Methods in enzymology*, 96, pp.38–50. Available at: http://www.ncbi.nlm.nih.gov/pubmed/6656637 [Accessed December 10, 2014].

Flower, A.M., Osborne, R.S. & Silhavy, T.J., 1995. The allele-specific synthetic lethality of prlA-prlG double mutants predicts interactive domains of SecY and SecE. *The EMBO journal*, 14(5), pp.884–93. Available at: http://www.pubmedcentral.nih.gov/articlerender.fcgi?artid=398161&tool=pmcentrez&rendertype=abstract [Accessed December 11, 2014].

Frauenfeld, J. et al., 2011. Cryo-EM structure of the ribosome-SecYE complex in the membrane environment. *Nature structural & molecular biology*, 18(5), pp.614–21. Available at: http://www.pubmedcentral.nih.gov/articlerender.fcgi?artid=3412285&tool=pmcentrez&rendertype=abstract [Accessed December 11, 2014].

Gogala, M. et al., 2014. Structures of the Sec61 complex engaged in nascent peptide translocation or membrane insertion. *Nature*, 506(7486), pp.107–10. Available at: http://www.ncbi.nlm.nih.gov/pubmed/24499919 [Accessed October 29, 2014].

Goldman, B.M. & Blobel, G., 1981. In vitro biosynthesis, core glycosylation, and membrane integration of opsin. *The Journal of cell biology*, 90(1), pp.236–42. Available at: http://www.pubmedcentral.nih.gov/articlerender.fcgi?artid=2111824&tool=pmcentrez&rendertype=abstract [Accessed December 10, 2014].

Görlich, D. et al., 1992. A protein of the endoplasmic reticulum involved early in polypeptide translocation. *Nature*, 357(6373), pp.47–52. Available at: http://www.ncbi.nlm.nih.gov/pubmed/1315422 [Accessed December 11, 2014].

Görlich, D. & Rapoport, T.A., 1993. Protein translocation into proteoliposomes reconstituted from purified components of the endoplasmic reticulum membrane.

Cell, 75(4), pp.615–30. Available at: http://www.ncbi.nlm.nih.gov/pubmed/8242738 [Accessed December 11, 2014].

Grudnik, P., Bange, G. & Sinning, I., 2009. Protein targeting by the signal recognition particle. *Biological chemistry*, 390(8), pp.775–82. Available at: http://www.ncbi.nlm.nih.gov/pubmed/19558326 [Accessed December 5, 2014].

Halic, M. & Beckmann, R., 2005. The signal recognition particle and its interactions during protein targeting. *Current opinion in structural biology*, 15(1), pp.116–25. Available at: http://www.ncbi.nlm.nih.gov/pubmed/15718142 [Accessed December 11, 2014].

Hanein, D. et al., 1996. Oligomeric rings of the Sec61p complex induced by ligands required for protein translocation. *Cell*, 87(4), pp.721–32. Available at: http://www.ncbi.nlm.nih.gov/pubmed/8929540 [Accessed December 11, 2014].

Harris, C.R. & Silhavy, T.J., 1999. Mapping an interface of SecY (PrlA) and SecE (PrlG) by using synthetic phenotypes and in vivo cross-linking. *Journal of bacteriology*, 181(11), pp.3438–44. Available at: http://www.pubmedcentral.nih.gov/articlerender.fcgi?artid=93811&tool=pmcentrez&rendertype=abstract [Accessed December 11, 2014].

Hartmann, E. et al., 1993. A tetrameric complex of membrane proteins in the endoplasmic reticulum. *European journal of biochemistry / FEBS*, 214(2), pp.375–81. Available at: http://www.ncbi.nlm.nih.gov/pubmed/7916687 [Accessed December 11, 2014].

Von Heijne, G., 1985. Signal sequences. The limits of variation. *Journal of molecular biology*, 184(1), pp.99–105. Available at: http://www.ncbi.nlm.nih.gov/pubmed/4032478 [Accessed December 11, 2014].

Helmers, J. et al., 2003. The beta-subunit of the protein-conducting channel of the endoplasmic reticulum functions as the guanine nucleotide exchange factor for the beta-subunit of the signal recognition particle receptor. *The Journal of biological chemistry*, 278(26), pp.23686–90. Available at: http://www.ncbi.nlm.nih.gov/pubmed/12750387 [Accessed December 11, 2014].

Humphrey, W., Dalke, A. & Schulten, K., 1996. VMD: visual molecular dynamics. *Journal of molecular graphics*, 14(1), pp.33–8, 27–8. Available at: http://www.ncbi.nlm.nih.gov/pubmed/8744570 [Accessed November 3, 2014].

Jiang, Y. et al., 2008. An interaction between the SRP receptor and the translocon is critical during cotranslational protein translocation. *The Journal of cell biology*, 180(6), pp.1149–61. Available at: http://www.pubmedcentral.nih.gov/articlerender.fcgi?artid=2290843&tool=pmcentrez&rendertype=abstract [Accessed December 11, 2014].

Jungnickel, B. & Rapoport, T.A., 1995. A posttargeting signal sequence recognition event in the endoplasmic reticulum membrane. *Cell*, 82(2), pp.261–70. Available at: http://www.ncbi.nlm.nih.gov/pubmed/7628015 [Accessed December 11, 2014].

Junne, T. et al., 2006. The plug domain of yeast Sec61p is important for efficient protein translocation, but is not essential for cell viability. *Molecular biology of the cell*, 17(9), pp.4063–8. Available at: http://www.pubmedcentral.nih.gov/articlerender.fcgi?artid=1556385&tool=pmcentrez&rendertype=abstract [Accessed December 11, 2014].

Kalies, K.U., Görlich, D. & Rapoport, T.A., 1994. Binding of ribosomes to the rough endoplasmic reticulum mediated by the Sec61p-complex. *The Journal of cell biology*, 126(4), pp.925–34. Available at: http://www.pubmedcentral.nih.gov/articlerender.fcgi?artid=2120124&tool=pmcentrez&rendertype=abstract [Accessed December 11, 2014].

Kelkar, A. & Dobberstein, B., 2009. Sec61beta, a subunit of the Sec61 protein translocation channel at the endoplasmic reticulum, is involved in the transport of Gurken to the plasma membrane. *BMC cell biology*, 10, p.11. Available at: http://www.pubmedcentral.nih.gov/articlerender.fcgi?artid=2653466&tool=pmcentrez&rendertype=abstract [Accessed December 9, 2014].

Kelleher, D.J., Kreibich, G. & Gilmore, R., 1992. Oligosaccharyltransferase activity is associated with a protein complex composed of ribophorins I and II and a 48 kd protein. *Cell*, 69(1), pp.55–65. Available at: http://www.ncbi.nlm.nih.gov/pubmed/1555242 [Accessed December 11, 2014].

Kihara, A., Akiyama, Y. & Ito, K., 1995. FtsH is required for proteolytic elimination of uncomplexed forms of SecY, an essential protein translocase subunit. *Proceedings of the National Academy of Sciences of the United States of America*, 92(10), pp.4532–6. Available at: http://www.pubmedcentral.nih.gov/articlerender.fcgi?artid=41978&tool=pmcentrez&rendertype=abstract [Accessed December 11, 2014].

Kim, S.J. et al., 2002. Signal sequences control gating of the protein translocation channel in a substrate-specific manner. *Developmental cell*, 2(2), pp.207–17. Available at: http://www.ncbi.nlm.nih.gov/pubmed/11832246 [Accessed December 11, 2014].

Kinch, L.N., Saier, M.H. & Grishin, N. V, 2002. Sec61beta--a component of the archaeal protein secretory system. *Trends in biochemical sciences*, 27(4), pp.170–1. Available at: http://www.ncbi.nlm.nih.gov/pubmed/11943537 [Accessed December 11, 2014].

Kontinen, V.P. et al., 1996. Roles of the conserved cytoplasmic region and non-conserved carboxy-terminal region of SecE in Escherichia coli protein translocase.

Journal of biochemistry, 119(6), pp.1124–30. Available at: http://www.ncbi.nlm.nih.gov/pubmed/8827448 [Accessed December 11, 2014].

Leroux, A. & Rokeach, L.A., 2008. Inter-species complementation of the translocon beta subunit requires only its transmembrane domain. *PloS one*, 3(12), p.e3880. Available at: http://www.pubmedcentral.nih.gov/articlerender.fcgi?artid=2586087&tool=pmcentrez&rendertype=abstract [Accessed December 11, 2014].

Li, H. et al., 2008. Structure of the oligosaccharyl transferase complex at 12 A resolution. *Structure (London, England : 1993)*, 16(3), pp.432–40. Available at: http://www.ncbi.nlm.nih.gov/pubmed/18334218 [Accessed December 11, 2014].

Li, W. et al., 2007. The plug domain of the SecY protein stabilizes the closed state of the translocation channel and maintains a membrane seal. *Molecular cell*, 26(4), pp.511–21. Available at: http://www.ncbi.nlm.nih.gov/pubmed/17531810 [Accessed December 11, 2014].

Lipschutz, J.H., Lingappa, V.R. & Mostov, K.E., 2003. The exocyst affects protein synthesis by acting on the translocation machinery of the endoplasmic reticulum. *The Journal of biological chemistry*, 278(23), pp.20954–60. Available at: http://www.ncbi.nlm.nih.gov/pubmed/12665531 [Accessed December 11, 2014].

Lizak, C. et al., 2011. X-ray structure of a bacterial oligosaccharyltransferase. *Nature*, 474(7351), pp.350–5. Available at: http://www.ncbi.nlm.nih.gov/pubmed/21677752 [Accessed November 28, 2014].

Lycklama a Nijeholt, J.A. et al., 2013. Characterization of the supporting role of SecE in protein translocation. *FEBS letters*, 587(18), pp.3083–8. Available at: http://www.ncbi.nlm.nih.gov/pubmed/23954289 [Accessed November 29, 2014].

Lycklama A Nijeholt, J.A. et al., 2010. Immobilization of the plug domain inside the SecY channel allows unrestricted protein translocation. *The Journal of biological chemistry*, 285(31), pp.23747–54. Available at: http://www.pubmedcentral.nih.gov/articlerender.fcgi?artid=2911283&tool=pmcentrez&rendertype=abstract [Accessed December 11, 2014].

Lycklama a Nijeholt, J.A., Wu, Z.C. & Driessen, A.J.M., 2011. Conformational dynamics of the plug domain of the SecYEG protein-conducting channel. *The Journal of biological chemistry*, 286(51), pp.43881–90. Available at: http://www.pubmedcentral.nih.gov/articlerender.fcgi?artid=3243504&tool=pmcentrez&rendertype=abstract [Accessed December 11, 2014].

Maillard, A.P. et al., 2007. Deregulation of the SecYEG translocation channel upon removal of the plug domain. *The Journal of biological chemistry*, 282(2), pp.1281–

7. Available at: http://www.ncbi.nlm.nih.gov/pubmed/17092931 [Accessed December 11, 2014].

Maita, N. et al., 2010. Comparative structural biology of eubacterial and archaeal oligosaccharyltransferases. *The Journal of biological chemistry*, 285(7), pp.4941–50. Available at: http://www.pubmedcentral.nih.gov/articlerender.fcgi?artid=2836098&tool=pmcentrez&rendertype=abstract [Accessed December 7, 2014].

Matsumoto, S. et al., 2013. Crystal structures of an archaeal oligosaccharyltransferase provide insights into the catalytic cycle of N-linked protein glycosylation. *Proceedings of the National Academy of Sciences of the United States of America*, 110(44), pp.17868–73. Available at: http://www.pubmedcentral.nih.gov/articlerender.fcgi?artid=3816453&tool=pmcentrez&rendertype=abstract [Accessed December 1, 2014].

Menetret, J.F. et al., 2000. The structure of ribosome-channel complexes engaged in protein translocation. *Molecular cell*, 6(5), pp.1219–32. Available at: http://www.ncbi.nlm.nih.gov/pubmed/11106759 [Accessed December 11, 2014].

Ménétret, J.-F. et al., 2005. Architecture of the ribosome-channel complex derived from native membranes. *Journal of molecular biology*, 348(2), pp.445–57. Available at: http://www.ncbi.nlm.nih.gov/pubmed/15811380 [Accessed December 11, 2014].

Ménétret, J.-F. et al., 2007. Ribosome binding of a single copy of the SecY complex: implications for protein translocation. *Molecular cell*, 28(6), pp.1083–92. Available at: http://www.ncbi.nlm.nih.gov/pubmed/18158904 [Accessed December 11, 2014].

Ménétret, J.-F. et al., 2008. Single copies of Sec61 and TRAP associate with a nontranslating mammalian ribosome. *Structure (London, England : 1993)*, 16(7), pp.1126–37. Available at: http://www.pubmedcentral.nih.gov/articlerender.fcgi?artid=2527209&tool=pmcentrez&rendertype=abstract [Accessed December 11, 2014].

Mitra, K. et al., 2005. Structure of the E. coli protein-conducting channel bound to a translating ribosome. *Nature*, 438(7066), pp.318–24. Available at: http://www.pubmedcentral.nih.gov/articlerender.fcgi?artid=1351281&tool=pmcentrez&rendertype=abstract [Accessed November 28, 2014].

Mohorko, E. et al., 2014. Structural basis of substrate specificity of human oligosaccharyl transferase subunit N33/Tusc3 and its role in regulating protein N-glycosylation. *Structure (London, England : 1993)*, 22(4), pp.590–601. Available at: http://www.ncbi.nlm.nih.gov/pubmed/24685145 [Accessed December 11, 2014].

Mohorko, E., Glockshuber, R. & Aebi, M., 2011. Oligosaccharyltransferase: the central enzyme of N-linked protein glycosylation. *Journal of inherited metabolic disease*,

34(4), pp.869–78. Available at: http://www.ncbi.nlm.nih.gov/pubmed/21614585 [Accessed December 11, 2014].

Morgan, D.G. et al., 2002. Structure of the mammalian ribosome-channel complex at 17A resolution. *Journal of molecular biology*, 324(4), pp.871–86. Available at: http://www.ncbi.nlm.nih.gov/pubmed/12460584 [Accessed December 11, 2014].

Murphy, C.K. & Beckwith, J., 1994. Residues essential for the function of SecE, a membrane component of the Escherichia coli secretion apparatus, are located in a conserved cytoplasmic region. *Proceedings of the National Academy of Sciences of the United States of America*, 91(7), pp.2557–61. Available at: http://www.pubmedcentral.nih.gov/articlerender.fcgi?artid=43408&tool=pmcentrez&rendertype=abstract [Accessed December 11, 2014].

Nyathi, Y., Wilkinson, B.M. & Pool, M.R., 2013. Co-translational targeting and translocation of proteins to the endoplasmic reticulum. *Biochimica et biophysica acta*, 1833(11), pp.2392–402. Available at: http://www.ncbi.nlm.nih.gov/pubmed/23481039 [Accessed December 4, 2014].

Osborne, R.S. & Silhavy, T.J., 1993. PrlA suppressor mutations cluster in regions corresponding to three distinct topological domains. *The EMBO journal*, 12(9), pp.3391–8. Available at: http://www.pubmedcentral.nih.gov/articlerender.fcgi?artid=413613&tool=pmcentrez&rendertype=abstract [Accessed December 11, 2014].

Park, E. et al., 2014. Structure of the SecY channel during initiation of protein translocation. *Nature*, 506(7486), pp.102–6. Available at: http://www.pubmedcentral.nih.gov/articlerender.fcgi?artid=3948209&tool=pmcentrez&rendertype=abstract [Accessed December 10, 2014].

Park, E. & Rapoport, T.A., 2011. Preserving the membrane barrier for small molecules during bacterial protein translocation. *Nature*, 473(7346), pp.239–42. Available at: http://www.pubmedcentral.nih.gov/articlerender.fcgi?artid=3093665&tool=pmcentrez&rendertype=abstract [Accessed December 10, 2014].

Pettersen, E.F. et al., 2004. UCSF Chimera--a visualization system for exploratory research and analysis. *Journal of computational chemistry*, 25(13), pp.1605–12. Available at: http://www.ncbi.nlm.nih.gov/pubmed/15264254 [Accessed July 10, 2014].

Pfeffer, S. et al., 2014. Structure of the mammalian oligosaccharyl-transferase complex in the native ER protein translocon. *Nature communications*, 5, p.3072. Available at: http://www.ncbi.nlm.nih.gov/pubmed/24407213 [Accessed December 2, 2014].

Plath, K. et al., 1998. Signal sequence recognition in posttranslational protein transport across the yeast ER membrane. *Cell*, 94(6), pp.795–807. Available at: http://www.ncbi.nlm.nih.gov/pubmed/9753326 [Accessed December 11, 2014].

Du Plessis, D.J.F. et al., 2009. The lateral gate of SecYEG opens during protein translocation. *The Journal of biological chemistry*, 284(23), pp.15805–14. Available at: http://www.pubmedcentral.nih.gov/articlerender.fcgi?artid=2708877&tool=pmcentrez&rendertype=abstract [Accessed November 27, 2014].

Pohlschröder, M., Murphy, C. & Beckwith, J., 1996. In vivo analyses of interactions between SecE and SecY, core components of the Escherichia coli protein translocation machinery. *The Journal of biological chemistry*, 271(33), pp.19908–14. Available at: http://www.ncbi.nlm.nih.gov/pubmed/8702704 [Accessed December 11, 2014].

Raden, D. & Gilmore, R., 1998. Signal recognition particle-dependent targeting of ribosomes to the rough endoplasmic reticulum in the absence and presence of the nascent polypeptide-associated complex. *Molecular biology of the cell*, 9(1), pp.117–30. Available at: http://www.pubmedcentral.nih.gov/articlerender.fcgi?artid=25226&tool=pmcentrez&rendertype=abstract [Accessed December 11, 2014].

Raden, D., Song, W. & Gilmore, R., 2000. Role of the cytoplasmic segments of Sec61alpha in the ribosome-binding and translocation-promoting activities of the Sec61 complex. *The Journal of cell biology*, 150(1), pp.53–64. Available at: http://www.pubmedcentral.nih.gov/articlerender.fcgi?artid=2185549&tool=pmcentrez&rendertype=abstract [Accessed December 11, 2014].

Roberts, B.E. & Paterson, B.M., 1973. Efficient translation of tobacco mosaic virus RNA and rabbit globin 9S RNA in a cell-free system from commercial wheat germ. *Proceedings of the National Academy of Sciences of the United States of America*, 70(8), pp.2330–4. Available at: http://www.pubmedcentral.nih.gov/articlerender.fcgi?artid=433729&tool=pmcentrez&rendertype=abstract [Accessed December 10, 2014].

Ruiz-Canada, C., Kelleher, D.J. & Gilmore, R., 2009. Cotranslational and posttranslational N-glycosylation of polypeptides by distinct mammalian OST isoforms. *Cell*, 136(2), pp.272–83. Available at: http://www.pubmedcentral.nih.gov/articlerender.fcgi?artid=2859625&tool=pmcentrez&rendertype=abstract [Accessed December 1, 2014].

Sääf, A., Wallin, E. & von Heijne, G., 1998. Stop-transfer function of pseudo-random amino acid segments during translocation across prokaryotic and eukaryotic membranes. *European journal of biochemistry / FEBS*, 251(3), pp.821–9. Available at: http://www.ncbi.nlm.nih.gov/pubmed/9490057 [Accessed December 11, 2014].

Sali, A. & Blundell, T.L., 1993. Comparative protein modelling by satisfaction of spatial restraints. *Journal of molecular biology*, 234(3), pp.779–815. Available at: http://www.ncbi.nlm.nih.gov/pubmed/8254673 [Accessed July 9, 2014].

Schaletzky, J. & Rapoport, T.A., 2006. Ribosome binding to and dissociation from translocation sites of the endoplasmic reticulum membrane. *Molecular biology of the cell*, 17(9), pp.3860–9. Available at: http://www.pubmedcentral.nih.gov/articlerender.fcgi?artid=1593163&tool=pmcentrez&rendertype=abstract [Accessed December 11, 2014].

Schatz, P.J. et al., 1991. One of three transmembrane stretches is sufficient for the functioning of the SecE protein, a membrane component of the E. coli secretion machinery. *The EMBO journal*, 10(7), pp.1749–57. Available at: http://www.pubmedcentral.nih.gov/articlerender.fcgi?artid=452846&tool=pmcentrez&rendertype=abstract [Accessed December 11, 2014].

Schechter, I. et al., 1979. Messenger RNA of opsin from bovine retina: isolation and partial sequence of the in vitro translation product. *Proceedings of the National Academy of Sciences of the United States of America*, 76(6), pp.2654–8. Available at: http://www.pubmedcentral.nih.gov/articlerender.fcgi?artid=383666&tool=pmcentrez&rendertype=abstract [Accessed December 10, 2014].

Schwartz, T. & Blobel, G., 2003. Structural basis for the function of the beta subunit of the eukaryotic signal recognition particle receptor. *Cell*, 112(6), pp.793–803. Available at: http://www.ncbi.nlm.nih.gov/pubmed/12654246 [Accessed December 11, 2014].

Shan, S. & Walter, P., 2005. Co-translational protein targeting by the signal recognition particle. *FEBS letters*, 579(4), pp.921–6. Available at: http://www.ncbi.nlm.nih.gov/pubmed/15680975 [Accessed December 1, 2014].

Shimokawa, N., Mori, H. & Ito, K., 2003. Importance of transmembrane segments in Escherichia coli SecY. *Molecular genetics and genomics : MGG*, 269(2), pp.180–7. Available at: http://www.ncbi.nlm.nih.gov/pubmed/12756530 [Accessed December 11, 2014].

Sibbald, M.J.J.B. et al., 2010. Synthetic effects of secG and secY2 mutations on exoproteome biogenesis in Staphylococcus aureus. *Journal of bacteriology*, 192(14), pp.3788–800. Available at: http://www.pubmedcentral.nih.gov/articlerender.fcgi?artid=2897339&tool=pmcentrez&rendertype=abstract [Accessed December 11, 2014].

Simon, S.M. & Blobel, G., 1991. A protein-conducting channel in the endoplasmic reticulum. *Cell*, 65(3), pp.371–80. Available at: http://www.ncbi.nlm.nih.gov/pubmed/1902142 [Accessed December 10, 2014].

Smith, M.A. et al., 2005. Modeling the effects of prl mutations on the Escherichia coli SecY complex. *Journal of bacteriology*, 187(18), pp.6454–65. Available at: http://www.pubmedcentral.nih.gov/articlerender.fcgi?artid=1236629&tool=pmcentrez&rendertype=abstract [Accessed December 11, 2014].

Sommer, N. et al., 2013. TRAP assists membrane protein topogenesis at the mammalian ER membrane. *Biochimica et biophysica acta*, 1833(12), pp.3104–11. Available at: http://www.ncbi.nlm.nih.gov/pubmed/24013069 [Accessed December 11, 2014].

Song, W. et al., 2000. Role of Sec61alpha in the regulated transfer of the ribosome-nascent chain complex from the signal recognition particle to the translocation channel. *Cell*, 100(3), pp.333–43. Available at: http://www.ncbi.nlm.nih.gov/pubmed/10676815 [Accessed December 11, 2014].

Stojanovski, D. et al., 2008. The MIA system for protein import into the mitochondrial intermembrane space. *Biochimica et biophysica acta*, 1783(4), pp.610–7. Available at: http://www.ncbi.nlm.nih.gov/pubmed/17996737 [Accessed December 9, 2014].

Tam, P.C.K. et al., 2005. Investigating the SecY plug movement at the SecYEG translocation channel. *The EMBO journal*, 24(19), pp.3380–8. Available at: http://www.pubmedcentral.nih.gov/articlerender.fcgi?artid=1276166&tool=pmcentrez&rendertype=abstract [Accessed December 11, 2014].

Trabuco, L.G. et al., 2008. Flexible fitting of atomic structures into electron microscopy maps using molecular dynamics. *Structure (London, England : 1993)*, 16(5), pp.673–83. Available at: http://www.pubmedcentral.nih.gov/articlerender.fcgi?artid=2430731&tool=pmcentrez&rendertype=abstract [Accessed December 11, 2014].

Tsukazaki, T. et al., 2008. Conformational transition of Sec machinery inferred from bacterial SecYE structures. *Nature*, 455(7215), pp.988–91. Available at: http://www.pubmedcentral.nih.gov/articlerender.fcgi?artid=2590585&tool=pmcentrez&rendertype=abstract [Accessed December 11, 2014].

Valcárcel, R. et al., 1999. Sec61beta, a subunit of the protein translocation channel, is required during Drosophila development. *Journal of cell science*, 112 (Pt 2, pp.4389–96. Available at: http://www.ncbi.nlm.nih.gov/pubmed/10564656 [Accessed December 11, 2014].

Voorhees, R.M. et al., 2014. Structure of the mammalian ribosome-Sec61 complex to 3.4 Å resolution. *Cell*, 157(7), pp.1632–43. Available at: http://www.pubmedcentral.nih.gov/articlerender.fcgi?artid=4081569&tool=pmcentrez&rendertype=abstract [Accessed November 10, 2014].

Walter, P. & Blobel, G., 1983. Preparation of microsomal membranes for cotranslational protein translocation. *Methods in enzymology*, 96, pp.84–93. Available at: http://www.ncbi.nlm.nih.gov/pubmed/6656655 [Accessed December 10, 2014].

Wang, L. & Dobberstein, B., 1999. Oligomeric complexes involved in translocation of proteins across the membrane of the endoplasmic reticulum. *FEBS letters*, 457(3), pp.316–22. Available at: http://www.ncbi.nlm.nih.gov/pubmed/10471800 [Accessed December 11, 2014].

Wolin, S.L. & Walter, P., 1993. Discrete nascent chain lengths are required for the insertion of presecretory proteins into microsomal membranes. *The Journal of cell biology*, 121(6), pp.1211–9. Available at: http://www.pubmedcentral.nih.gov/articlerender.fcgi?artid=2119713&tool=pmcentrez&rendertype=abstract [Accessed December 11, 2014].

Zimmer, J., Nam, Y. & Rapoport, T.A., 2008. Structure of a complex of the ATPase SecA and the protein-translocation channel. *Nature*, 455(7215), pp.936–43. Available at: http://www.ncbi.nlm.nih.gov/pubmed/18923516 [Accessed October 30, 2014].

Acknowledgements

First of all, I would like to thank Prof. Dr. Roland Beckmann for being an amazing mentor and supervisor who not only made my project possible but also supported me further in many steps, not least during the publication process. Thank you Roland, it was a pleasure working with you!

I would also like to thank Dr. Thomas Becker whose project I basically took over and who shared his experience in working with the translocon.

I thank Dr. Birgitta Beatrix for providing me with several key biochemical protocols and helping me out during the labors of SRP purification.

I am also grateful to Dr. Jean-Paul Armache who helped me out with the computational processing of my datasets and who shared many of his scripts with me.

Many thanks also go to Clara Barrio-Garcia for helping me model the ribosomal subunits necessary for submissions of the PDB files from this work.

Also, thanks are due to Dr. Otto Berninghausen and Charlotte Ungewickell for preparing my cryo-EM grids for me and for collecting the datasets that resulted in this work.

I would also like to thank my collaborators, Dr. Friedrich Förster and Steffan Pfeffer for deep discussions and amazing results which came out of our work together.

I would like to thank the whole Beckmann group for friendship, support and useful advice.

During my time in the Gene Center people from other groups also provided their help and friendly support. This is especially true for the whole Halić lab. Thank you guys, hvala, grazie und ein großes Dankeschön!

Finally, I would like to thank my mom and dad for being amazing parents, my friends in need and for having fostered my interest in science. Hvala vam I voli vas vaš Dr. Sin!